A NEW POWER SIGNAL PROCESSOR FOR CONVERTER-INTERFACED DISTRIBUTED GENERATION SYSTEMS

by

Davood Yazdani

A thesis submitted to the Department of Electrical Engineering

In conformity with the requirements for

the degree of Doctor of Philosophy

Queen's University

Kingston, Ontario, Canada

(January, 2009)

ISBN:978-0-494-48233-9

Abstract

Environmentally friendly renewable energy technologies such as wind and solar energy systems are among the fleet of new generating technologies driving the demand for distributed generation of electricity. Power Electronics has initiated the next technological revolution and enables the connection of distributed generation (DG) systems to the grid. The challenge is to achieve system functionality without extensive custom engineering, yet still have high system reliability and generation placement flexibility. Nowadays, it is a general trend to increase the electricity production using DG systems. If these systems are not properly controlled, their connection to the utility network can generate problems on the grid side. Therefore, considerations about power generation, safe running and grid synchronization must be done before connecting these systems to the utility network.

This thesis introduces a new grid-synchronization, or more visibly a new "*power signal processor*" adaptive notch filtering (ANF) tool that can potentially stimulate much interest in the field and provide improvement solutions for grid-connected operation of DG systems. The processor is simple and offers high degree of immunity and insensitivity to power system disturbances, harmonics and other types of pollutions that exist in the grid signal. The processor is capable of decomposing three-phase quantities into symmetrical components, extracting harmonics, tracking the frequency variations, and providing means for voltage regulation and reactive power control. In addition, this simple and powerful synchronization tool will simplify the control issues currently challenging the integration of distributed energy technologies onto the electricity grid. All converter-interfaced equipments like FACTS (flexible ac transmission systems) and Custom Power Controllers will benefit from this technique. The theoretical analysis is presented, and simulation and experimental results confirm the validity of the analytical work.

Acknowledgements

First of all I would like to express my gratitude and appreciation to my thesis advisors, Dr. Alireza Bakhshai and Dr. Geza Joos. Their continuous advice, guidance, feedback and encouragement are much behind the realization of this work. Without their help this work would not have been possible.

I also owe a lot to my committee members, whose advice and feedback were a valuable contribution to this thesis. I would also like to thank Dr. Mohsen Mojiri for his eagerness to share his knowledge and time, which is very greatly appreciated.

Many thanks to the office staff of the ECE Department here at Queen's for their invaluable help in administrative matters during the tenure of my Ph.D. degree. I would also like to express special thanks to Mrs. Bernice Ison, the former graduate program assistant and Ms. Debie Fraser, the graduate secretary at the Department of Electrical and Computer Engineering at Queen's University for their great help with all the procedural and paper work throughout my time in the Ph.D. program at Queen's University.

I would like to thank all of my colleagues at the ePearl lab for lending me their generous support whenever needed. In particular I would like to thank Majid Pahlevaninezhad for sharing his time and valuable expertise in applied mathematics, and Suzan Eren and Joanne Hui for helping me with editing the thesis.

Last but not least I would like to thank my parents and siblings for their love and support without which I would not have been able to make it through the frustrations of the past few years.

Table of Contents

List of Figures

Glossary

ANF	Adaptive Notch Filter
APF	Active Power Filter
DFT	Discrete Fourier Transform
DG	Distributed Generation
DDSRF-PLL	Decoupled Double Synchronous Reference Frame-PLL
DSOGI-PLL	Double Second Order Generalized Integrator PLL
EPLL	Enhanced PLL
FACTS	Flexible AC Transmission Systems
FFT	Fast Fourier Transform
ISC	Instantaneous Symmetrical Components
LP	Loop Filter
LPF	Low Pass Filter
PD	Phase Detector
PLL	Phase Locked Loop
PSF-PLL	Positive Sequence Filter PLL
QPLL	Quadrature PLL
SRF-PLL	Synchronous Reference Frame PLL
SSI-PLL	Sinusoidal Signal Integrator PLL
STATCOMs	STATic COMpensators
UPFCs	Unified Power Flow Controllers
VCO	Voltage-Controlled Oscillator

Chapter 1

Introduction

1.1 Problem Definition

Distributed Generation (DG) systems such as wind farms, photovoltaics, fuel cells, and micro-turbines can solve environmental problems, cope with rising energy prices and power plant construction costs, and reduce world's dependence on fossil fuels.

A general structure for distributed systems is illustrated in Figure 1.1. The input power is transformed into electricity by means of a power conversion unit whose configuration is closely related to the input power nature [1]-[5]. The electricity produced can be delivered to the local loads or to the utility network, depending where the generation system is connected. One important part of a distributed system is its control [1],[6]. The control tasks can be divided into two major parts.

- Input-side controller, with the main property to extract the maximum power from the input source. Naturally, protection of the input-side converter is also considered in this controller.
- Grid-side power processor, which performs the following tasks: providing the required feedback variables to feed the overall control system unit for the control of the generated

active power; reactive power control transferred between the DG and the grid; dc-link voltage control; power quality control; and grid synchronization.

In addition, the grid operator might request services like local voltage and frequency regulation, voltage harmonic compensation, or active filtering [6]-[10].

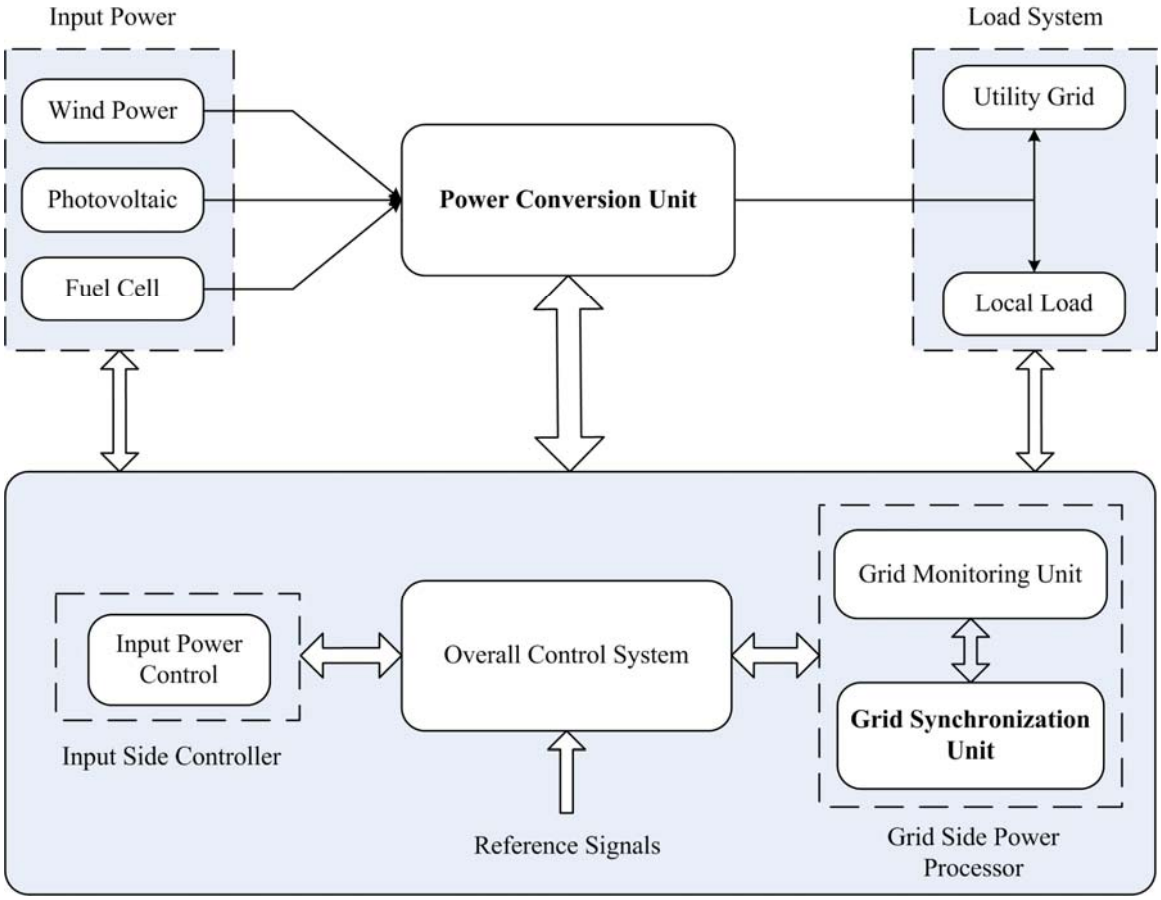

Figure 1.1 General structure for distributed power system [1].

One important part of the grid side power processor is the grid synchronization unit [1]. Converter-interfaced DG units must be synchronized with the utility system. Grid synchronization is a challenging task especially when the utility signal is polluted with harmonics

and disturbances, or is of a variable frequency. The phase angle of the utility voltage is a critical piece of information for this task. In fact, in all grid-connected converters such as the static VAR compensators, active power filters, and grid connected DG systems, a phase-detecting technique provides a reference phase signal synchronized with the grid voltage that is required to control and meet the power quality standards. This is particularly critical in converter-interfaced DG units where the synchronization scheme should provide a high degree of immunity and insensitivity to power system disturbances, harmonics, unbalance, voltage sags, and other types of pollutions that exist in the grid signal [1], [11]. Various phase angle detecting methods have already been developed and reported in [1], [11]-[43]. These techniques are briefly reviewed in chapter 2. Among these techniques the voltage zero-crossing is the simplest one and the phase-locked loop (PLL)-based techniques are the state-of-the-art techniques in detecting the phase angle of the grid voltages [1], [11]-[15]. In general, a good synchronization scheme must i) proficiently detect the phase angle of the utility signal, ii) smoothly track the phase and frequency variations, and iii) forcefully reject harmonics and disturbances. These factors, together with the implementation simplicity and the cost are all important when examining the credibility of a synchronization scheme.

Another important part of the grid side power processor is the grid monitoring unit which is our secondary interest in this thesis. This unit plays a vital task in power quality and protection of grid connected converters. Harmonics detection and active/reactive current (power) extraction of the load/grid are among the main duties of this unit. Advanced signal processing methods in both time- and frequency-domains have been developed to detect and extract the compensating signal for power quality control [44]-[63]. Frequency-domain approaches are the Fast Fourier Transform (FFT) and Discrete Fourier Transform (DFT) techniques. And important time-domain schemes

are the instantaneous "*p–q*", the synchronous *d–q*, notch filters, approximated band-pass resonant filters, and stationary frame filters.

To sum up, a powerful grid side power processor should contain an advanced synchronization scheme that in addition to detecting the grid phase angle can detect current harmonics and extract the active/reactive current component for power quality purposes.

1.2 Thesis Objectives

As mentioned earlier, a synchronization technique is essential in all grid-connected power converters. The synchronization scheme provides a reference phase signal synchronized with the grid voltage that is required to control and meet the power quality standards.

The main objective of this thesis is the development of a new "*power signal processor*" based on a new synchronization scheme that is simple, fast, and accurate. The new "*power signal processor*" can further be used for grid measuring, monitoring and processing of the grid signal. The proposed "*power signal processor*" can be employed as the grid side power processor in Fig 1.1. In more detail, the objectives of this thesis are:

1. Development of a grid synchronization technique to: i) proficiently detect the phase angle of the utility signal, ii) smoothly track the phase and frequency variations, iii) effectively outputs the useful signal information, and iv) forcefully reject harmonics and disturbances.
2. Development of an advanced grid synchronization technique to: i) proficiently detect current harmonics, ii) precisely extract the active/reactive component of the load/grid

current, and iii) forcefully reject harmonics and disturbances and extract the symmetrical components.

1.3 Thesis Contributions

This thesis presents a new synchronization method that demonstrates not only an advanced synchronization performance in corrupted grid environment; but also effectively handles the unbalance situations. The proposed synchronization device does not require a synchronizing tool like a PLL, and it is based on a newly developed adaptive notch filter (ANF) system. The prime application of the proposed synchronization method is found in distributed generation system, e.g., micro-grid systems, where grid synchronization is of certain concern in grid-connected operation mode. The proposed approach is adapted to meet special interests including the real-time extraction and measurement of harmonics and reactive components of a power signal of a time-varying characteristic. Adaptive nature of the proposed technique allows precise tracking of the frequency and amplitude variations. The structural simplicity of the algorithm makes it desirable from the standpoint of digital implementation in both software environment, e.g., a digital signal processor (DSP), and hardware environment, e.g., a field programmable gate array (FPGA) or application-specific integrated circuit (ASIC) environments. The theoretical analysis is presented, and simulation and experimental results confirm the validity of the analytical work.

The research on the proposed *"power signal processor"* has addressed the following outcomes and contributions:

1. An adaptive frequency tracker for single and multiple frequencies tracking/estimation
2. An adaptive, simple and powerful grid synchronization tool for grid-connected converters.

3. An advanced power signal processor to extract key power system information required especially in single-/three- phase converter-interfaced DG systems. This includes:
    a. accurate measuring of positive and negative sequences for unbalance system operation,
    b. real-time extraction of harmonics and reactive currents components,
    c. real-time extraction of selective harmonics.
4. Development of a three-phase adaptive, simple and powerful grid synchronization tool for grid-connected converters.
5. An advanced three-phase power signal processor to extract key power system information required especially in converter-interfaced DG systems for real-time extraction and decomposition of symmetrical components and harmonics.

This new processor with some modification can perfectly perform almost every single signal processing function that might be required for control and safety purposes in DG systems. In addition, the new processor employs mathematical tools that streamline the control formulation and thus the system implementation.

1.4 Thesis Organization

This thesis is organized as follows. Chapter 2 reviews the existing grid synchronization methods. The chapter summarizes the most important techniques and outlines their features and drawbacks. Chapter 3 introduces a new ANF-based frequency tracker, extends the frequency tracker for multiple frequency estimation, evaluates its performance experimentally, and compares simulation results obtained from the proposed technique with those of its main

competitor. Chapter 4 proposes a new single-phase based *"power signal processor"* for converter-interfaced DG systems, and extends the proposed method to extract the symmetrical components and harmonics/active/reactive current components for potential control and safety purposes. Chapter 5 introduces a new three-phase ANF-based frequency tracker, presents a brief stability analysis for it, extends the frequency tracker for multiple frequency estimation, and compares the proposed technique with its main competitor. Chapter 6 proposes a new three-phase *"power signal processor"* for converter-interfaced DG systems, and explores signal processing techniques for potential control and safety purposes to extract key power system information required especially in converter-interfaced DG systems. Chapter 7 concludes the thesis and outlines the future works.

Chapter 2
Literature Review

This chapter is dedicated to the existing grid synchronization methods. The chapter summarizes the most important techniques and outlines their features and drawbacks.

2.1 Grid-Synchronization Methods

2.1.1 Filtering Algorithms

Filtering the grid voltages in an *α-β* stationary reference frame, or in a *d-q* synchronous rotating reference frame is a simple way to detect the phase angle of the grid voltage. Figure 2.1 depicts one of such filtering approaches in α-β stationary reference frame.

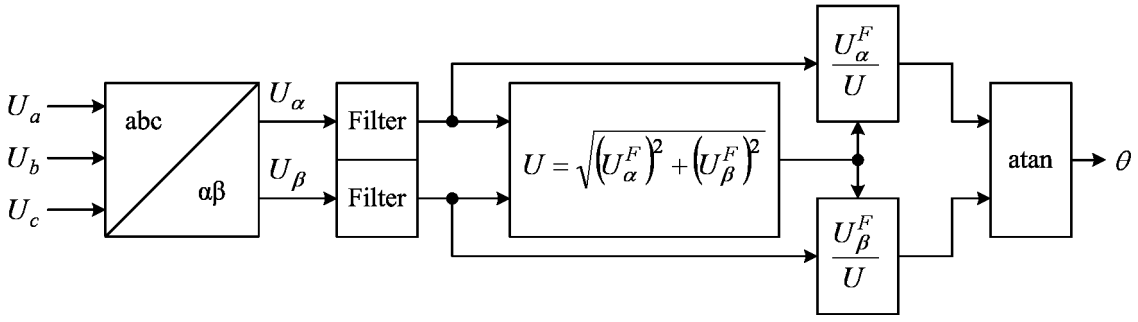

Figure 2.1 Synchronization method using filtering on αβ stationary frame [12].

Three phase voltages are transformed to the αβ reference frame, and filtering is applied to both α and β components of the grid voltage [16]. In [12], different filters such as low pass filter (LPF), notch filter, space vector filter, etc. are investigated and their effectiveness is discussed. It is a well-known fact that filtering causes delay, which is unacceptable especially for detecting the grid voltage angle; therefore care must be taken into consideration when designing such filters. When design the filters, a trade-off should be made between the robustness and the transient convergence speed. A smaller cut-off frequency results in less distortion in the estimated angle. However, this results in a slower rate of convergence. In [17]-[18], a good resonant band-pass filter that does not introduce a delay is proposed in the α-β plane. Filtering techniques in the d-q reference frame are easier to design, since voltage components are dc variables, Fig. 2.2. Various filtering techniques including notch filter, LPF, band-stop filter, etc. have been introduced in the rotating *dq* reference frame [17]. Major deficiencies of filtering methods include their bad performance in case of grid frequency deviations, or voltage unbalance situation [1], [11].

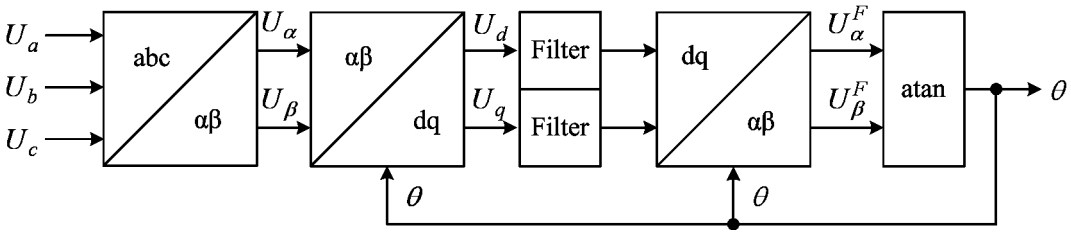

Figure 2.2 Synchronization method using filtering on *dq* synchronous reference frame [17].

2.1.2 PLL-based Methods

2.1.2.1 Single Phase Structures

The phase-locked loop (PLL) is a fundamental and conceptual tool that has been used in various disciplines of electrical technology [19]. The principal idea of phase locking is to generate a signal whose phase angle is adaptively tracking variations of the phase angle of a given signal. The conventional strategy for phase locking is to estimate the difference between phase angle of the input signal and that of a generated output signal and drive this value to zero by means of a control loop. A block diagram of a single-phase PLL is shown in Figure 2.3. The phase difference between the input and the output signals is measured using a phase detector (PD). The error signal is then passed through a loop filter (LF). The output of the filter drives a voltage-controlled oscillator (VCO), which generates the output signal.

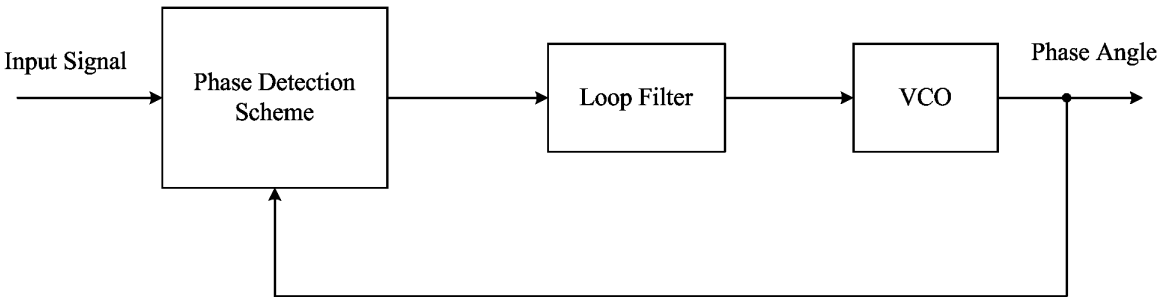

Figure 2.3 PLL structure.

Several works, mainly on the PD block, have been done using the PLL in Fig 2.3 [15], [19]-[28]. An intuitive structure for the PD block is a multiplier. Fig. 2.4 displays the single-phase power-based PLL (pPLL) where its PD is a single multiplier. The PD dynamics rely entirely on the filter structure. The main issue that has hampered the utilization of the single-phase PLL is that a single-phase design normally generates second-order harmonic, which has to be filtered

out. At first sight, the low pass filter (LPF) should have a low cutoff frequency, which degrades system speed response. Thus, a careful design of the LPF and compensator must be performed in order to provide good dynamic response and disturbance rejection [20].

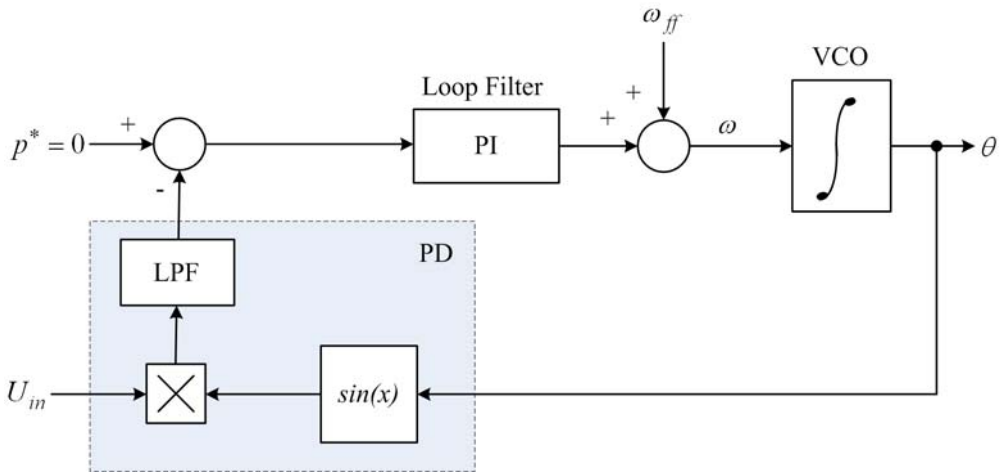

Figure 2.4 Single phase power PLL structure [15].

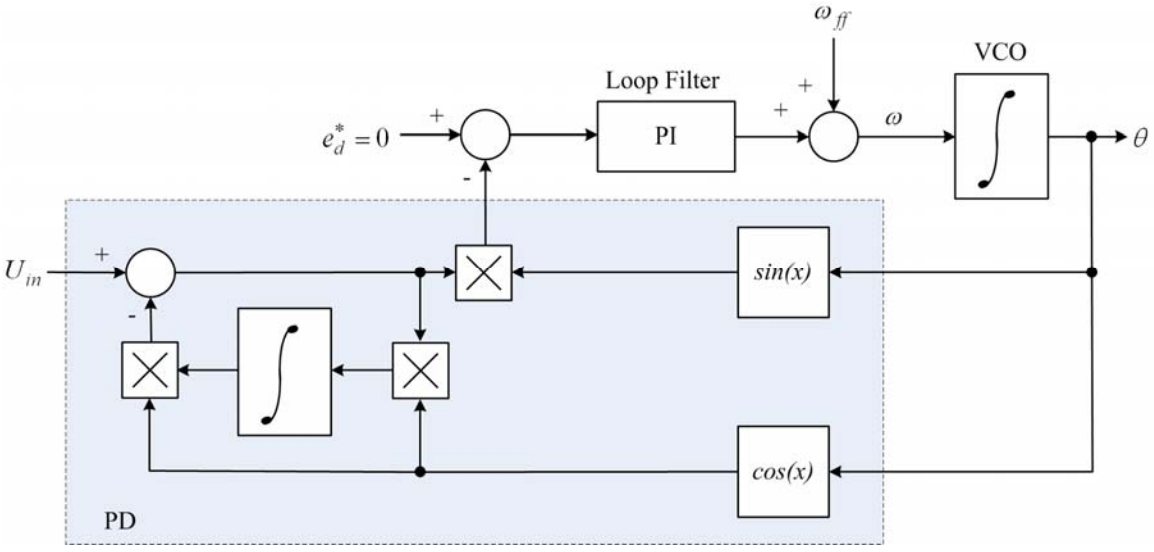

Figure 2.5 EPLL structure [21].

In [21], an enhanced PLL (EPLL) is introduced that is shown in Fig. 2.5. The major advantage of the EPLL system is its special PD mechanism. The conventional PD is replaced by a new mechanism that allows more flexibility and provides additional information such as the amplitude and the phase angle of the input signal. The governing equations of the EPLL are derived based on defining and minimizing an instantaneous cost function by means of the gradient-descent algorithm. Operation of the EPLL is based on estimating amplitude and phase angle of the fundamental component.

Another structure for the PLL, so-called the quadrature PLL (QPLL), is based on estimating in-phase and quadrature-phase amplitudes of the fundamental component of the input signal [22]. The process of phase detection in the QPLL is somehow similar to the EPLL. Amplitude and phase angle are not directly estimated by the QPLL. However, they can simply be calculated from available outputs. Thus, the QPLL is expected to have a superior performance over the conventional PLL, particularly, it is capable of following large and abrupt variations of the frequency [22].

Another structure for the single-phase PLL is the so called "inversed Park-based PLL method" [15]. In the inversed Park-based PLL method, Fig. 2.6, a two-phase signal is generated in an inner feedback loop and by means of an *αβ-dq* and a *dq-αβ* transformations. The first order filters output dc quantities of V_d and V_q. The filtered V_d is then fed back into the outer loop to generate the phase angle. Several works has been reported so far based on this concept. A generalized second-order integrator, a two-phase signal generator, and a sinusoidal signal generator are introduced for orthogonal system generation. The main differences among them is only in the way they generate a two-phase signal [23]-[28] and in all approaches, there is a tradeoff between the speed of the response and their capability in harmonic rejection.

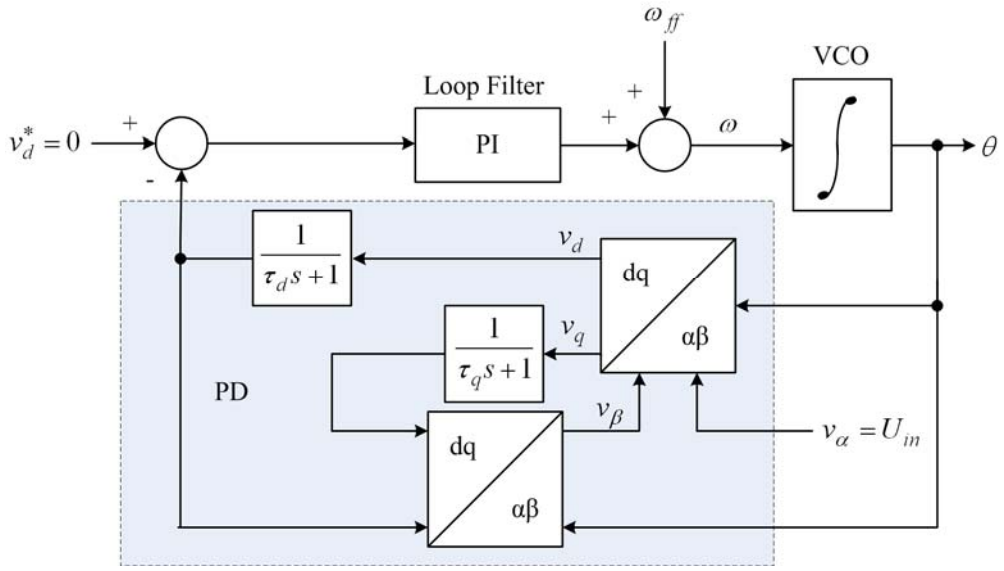

Figure 2.6 Single phase park-based PLL structure [15].

2.1.2.2 Three-Phase Structures

A common structure for grid synchronization in three-phase systems is a phase locked loop implemented in the d-q synchronous reference frame, as illustrated in Figure 2.7 [29]-[31]. This structure uses an *abc/dq* coordinate transformation and the lock is realized by setting the U_d^* to zero. A regulator, usually a PI regulator, regulates the error to zero. The VCO integrates the grid frequency and outputs the utility voltage angle that is fed back into the *α-β* to *d-q* transformation module.

This structure of PLL consists of two major parts, the transformation module and the PLL controller. The transformation module has no dynamics. In fact, the PLL controller determines the system dynamics. Therefore, the bandwidth of the loop filter determines the filter's filtering

performance and its time response. As a consequence, the loop filter parameters have a significant influence on the lock quality and the overall PLL dynamics.

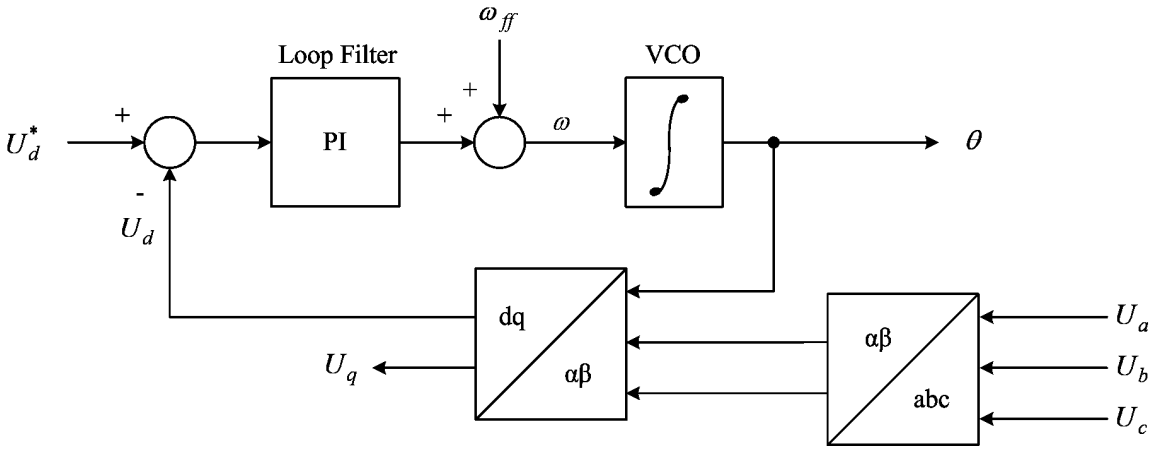

Figure 2.7 General structure of *dq* PLL method [29]-[31].

The method in Fig. 2.7 is also called the synchronous reference frame PLL (SRF–PLL) [1], [14]. Under ideal utility conditions, i.e., balanced system with no distortion, a loop filter of a wide band-width yields a fast and precise detection of the phase angle and the amplitude of the utility voltage vector. This method will not operate satisfactory if the utility voltage is unbalanced, distorted by harmonics or frequency variations.

Several works have been published based on the SRF-PLL of Fig 2.7 to improve its performance [14], [32]-[38]. In general, improved versions of the SRF-PLL use specific "filtering" techniques to deliver a non distorted signal to the conventional SRF-PLL structure. Synchronous reference frame PLL with positive sequence filter (PSF-PLL) [32], synchronous reference frame PLL with sinusoidal signal integrator (SSI-PLL) [33], and double second order generalized integrator PLL (DSOGI-PLL) [34]-[36], shown in Fig. 2.8, are among the newly

developed solutions to improve SRF-PLL performance. These techniques employ sinusoidal signal integrators (SSI) as a positive sequence filter to improve system's robustness against the utility voltage distortions and unbalances.

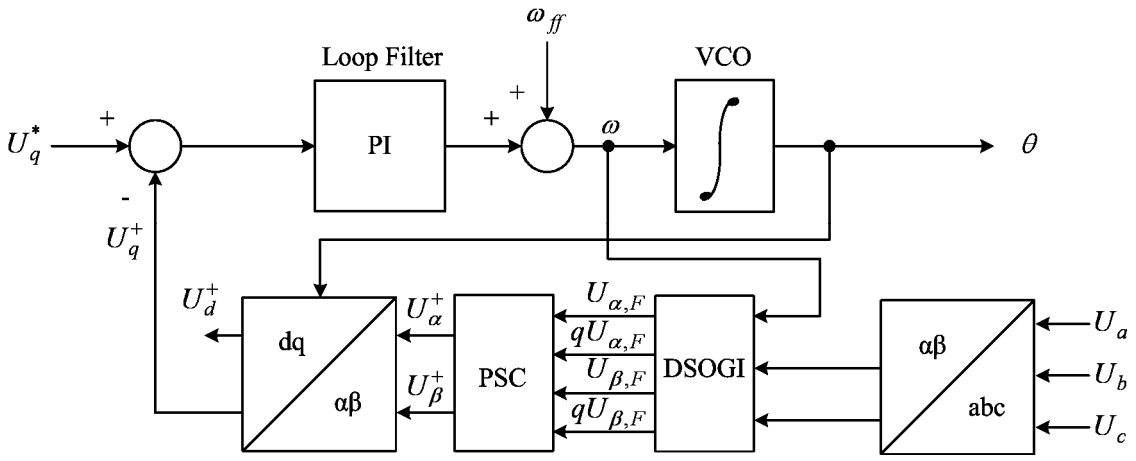

Figure 2.8 The structure of double second order generalized integrator PLL [34]-[36].

In [37], notch filters are added to the SRF-PLL structure to remove the double frequency ripple caused by input unbalance. To handle unbalance situations, a decoupled double synchronous reference frame PLL (DDSRF-PLL) was introduced in [38], Figure 2.9. In DDSRF-PLL, an unbalanced voltage vector, consisting of both positive- and negative-sequence components, is expressed into a double synchronous reference frame to detect the positive-sequence component [38]. This system when combined with a proper decoupling procedure enables a fast and accurate phase angle and amplitude detection of the utility voltage positive-sequence component under unbalanced utility conditions.

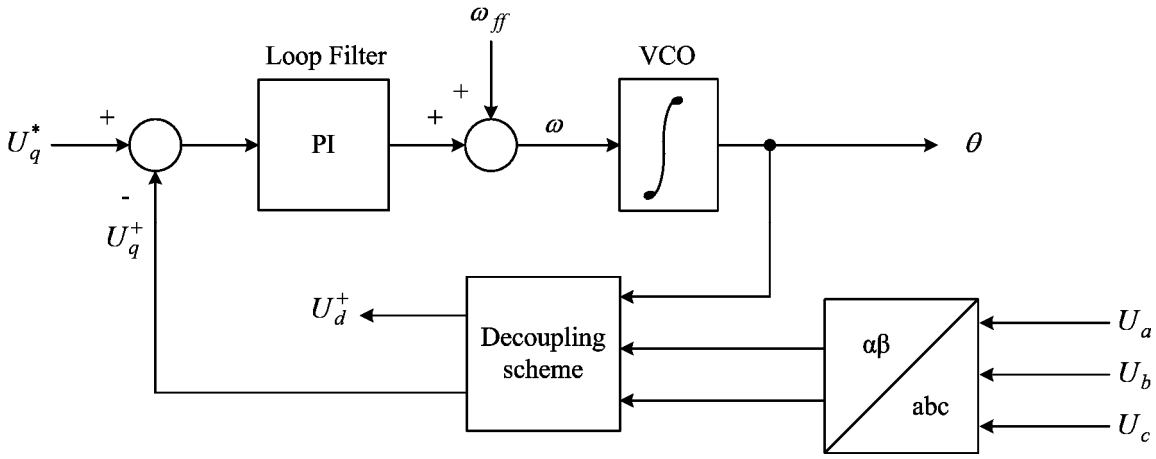

Figure 2.9 The Decoupled Double Synchronous Reference Frame-PLL(DDSRF-PLL) [38].

The results show that the performance of the method degrades when the input signal is distorted with harmonics. To attenuate the harmonics, the PLL bandwidth can be reduced at the expense of increasing its time response.

In general, many grid-connected converters use a three-phase PLL configuration that measures a three-phase signal (voltages or currents) and derives a single phase-reference signal. The distinct phase-references for individual phases are obtained by adding or subtracting $2\pi/3$ radians to the measured phase angle. Such a three-phase design has the advantage of triple harmonic cancellation, however, in case of unsymmetrical transients; the system is unable to correctly measure the phase angle of each individual phase. In fact, such a PLL will give an average phase angle over three phases that poorly represents the individual phase angles [39].

Another technique employs all-pass $90°$ phase-shifters for each phase, and uses in-phase and quadrature-phase waveforms for phase angle estimation [40]. The phase voltages and their $90°$ phase-shifted values can be used by the instantaneous symmetrical components (ISC) method to detect the positive-sequence voltages of the three-phase system [41]. The phase angle of the

extracted positive sequence is of interest especially in unbalance situations. All-pass filters are not frequency-adaptive, and thus can not make appropriate 90-degree phase shift when the frequency deviates from its nominal value. In addition, all-pass filters do not block harmonics and distortions. Therefore, the performance of the phase detection scheme is compromised to some degree. A low-pass filter is recommended to be used after component extraction to reduce the impact of harmonics [42].

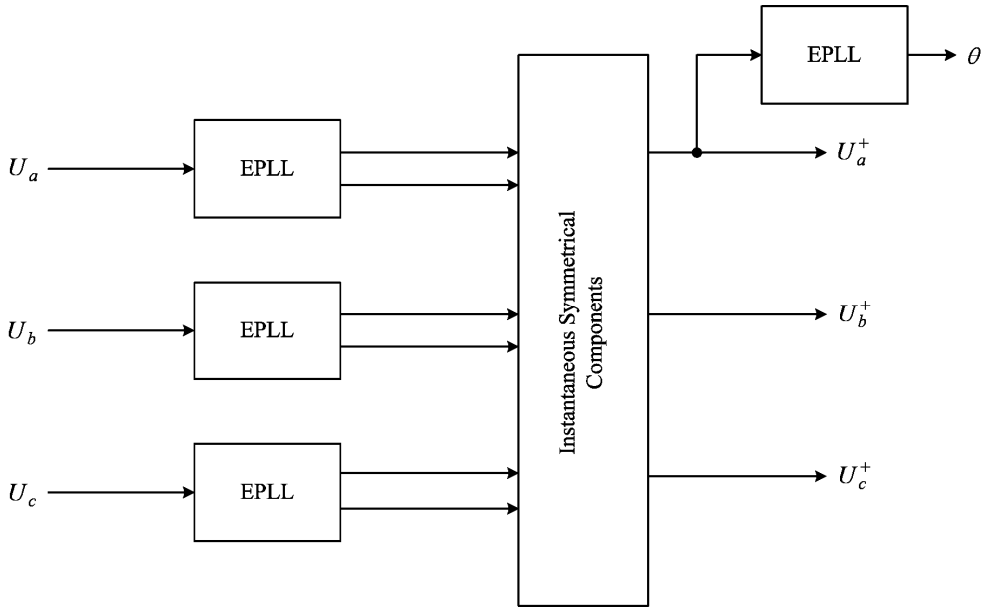

Figure 2.10 Positive sequence extractor based on EPLL [42].

In [42], the all-pass filters are replaced with EPLLs. The EPLLs adaptively extract the fundamental components of the system voltages and their 90-degree phase-shifted versions, Figure 2.10. The ISC block receives the fundamental and its corresponding 90-degree phase-shifted component and calculates the positive sequence component of the utility voltages. In fact, the EPLL is an adaptive notch filter whose frequency moves with the grid frequency. This removes the method's sensitivity to frequency variations, which is a major deficiency of the

method in [42]. Moreover, since the EPLL is a band-pass filter, the extracted positive sequence is almost distortion-free. Indeed, the input signal undergoes two filtering stages: once in the positive sequence extraction stage and again in the phase estimation stage. This improved version of the ISC approach uses an additional single-phase PLL to estimate the phase-angle of the detected positive-sequence voltage. This four-independent single-phase PLL-based technique offers good results in the estimation of the positive-sequence component under unbalanced conditions [13].

2.1.3 Other Methods

Other techniques have also been introduced to perform grid synchronization. One of the simplest methods detects the zero crossing of the utility voltages [1]. However, the zero crossing points occur only at every half cycle of the utility voltage; thus the dynamic performance of this technique is quite low. In addition, disturbances in the input signal, such as voltage sags and harmonics, influence the accuracy of this technique. Hence, further discussion on the zero crossing schemes seems to be less relevant for this overview.

The Extended Kalman Filter (EKF)-Based methods estimate the amplitude, frequency, and phase angle vectors of the input voltage. The EKF can estimate these vectors provided that the state-space model of the system sufficiently model actual variations of the state vectors. However, it is not a trivial task to develop such adequate model that can follow vector variations due to mostly indeterminist changes in the utility voltages [12]. In addition, the EKF-based method is not able to cope with unbalanced input conditions.

The recursive weighted least-squares estimation (WLSE) algorithm [43] rejects the impact of negative-sequence and accommodates variations in the frequency. However, this method has

three shortcomings: 1) long convergence time in detecting frequency changes; 2) computational dilemmas associated with the LS methods, and 3) weak performance in noisy environments.

The Space Vector Filter (SVF)-Based method was developed based on mutual dependency of the α-β components of the grid voltage. A SVF-based method can be tuned to provide highly distortion-free estimation. Major drawback of this method is its sensitivity to the input frequency variations and imbalance. Attempts have been made to modify the SVF-based method to accommodate frequency deviations [12]. Investigations show that the modified SVF-based method is not fully capable of exhibiting the desired performance. Difficulty in precise adjustment in the presence of noise and harmonics are additional drawbacks of this method [13].

2.2 Conclusion

This chapter provides a quick overview of the existing techniques for grid synchronization. The chapter addresses important existing grid synchronization techniques and highlights both the merits and shortcomings of each. Among all these techniques, the PLL-based algorithms show a better performance. However, PLL-based algorithms also suffer from situations such as grid voltage unbalance.

In the next chapter, a synchronization scheme based on an adaptive notch filtering approach is presented. The proposed scheme is simpler than the PLL-based approaches, and overcomes some shortcomings of the PLL systems.

Chapter 3
Proposed Grid Synchronization Unit

A synchronization scheme based on an adaptive notch filtering approach is presented in this chapter. In addition to the phase angle, the proposed synchronization technique outputs very useful signal information such as the fundamental component, its 90 degrees phase-shift, its amplitude, its frequency, *sin*/*cos* functions of its phase angle, and harmonics. Having access to the additional signal information enables the user to synchronize the on/off times of the switching devices, calculate active/reactive power, and transform the feedback variables to a frame suitable for control purposes. The proposed scheme is simpler than the PLL-based approaches, and overcomes some shortcomings of the PLL systems.

3.1 Proposed Grid-Synchronization Unit

3.1.1 Problem Definition

As mentioned in chapter 1, the grid synchronization unit is the important part of the grid side power processor in converter-interfaced DG units. Utility signals are usually polluted with harmonics and disturbances, and in some cases are of a variable frequency.

In grid-connected converters, the input signal to the synchronization tool is usually a periodic signal and is in the form defined in (3.1).

$$u(t) = \sum_{i=1}^{n} A_i \sin\phi_i \qquad \text{where} \qquad \phi_i = \omega_i t + \varphi_i \tag{3.1}$$

Nonzero amplitudes A_i, the nonzero frequencies ω_i, $i = 1,2,....n$, and the phases φ_i, $i = 1,2,....n$, are typically unknown parameters. Estimating unknown parameters, especially unknown frequencies, is a required task in many applications, and is a fundamental issue in systems theory and signal processing. Fast and precise detection of the phase angle of such a polluted grid signal is the main task that a good synchronization technique must provide. Existing synchronization schemes, as mentioned in chapter 2, have some advantages and disadvantages. Looking for a different synchronization scheme that is simpler than existing schemes and overcomes the drawbacks of them is the main goal of this chapter.

3.1.2 The Adaptive Notch Filter (ANF) Dynamic and Structure

ANF is a basic adaptive structure that can be used to extract the desired sinusoidal component of a given periodic signal by tracking its frequency variations [64]-[70]. The dynamic behavior of the newly modified ANF [64]-[70], which is of our interest, is characterized by the following set of differential equations:

$$\begin{aligned} &\ddot{x} + \theta^2 x = 2\zeta\,\theta\, e(t) \\ &\dot{\theta} = -\gamma\, x\, \theta\, e(t) \\ &e(t) = u(t) - \dot{x} \end{aligned} \tag{3.2}$$

θ is the estimated frequency and ζ and γ are adjustable real positive parameters that determining the estimation accuracy and the convergence speed of the ANF. For a single sinusoid input signal (n=1), $u(t) = A_1 \sin(\omega_1 t + \varphi_1)$, this ANF has a unique periodic orbit located at:

$$o = \begin{pmatrix} x \\ \dot{x} \\ \theta \end{pmatrix} = \begin{pmatrix} -\frac{A_1}{\omega_1} cos(\omega_1 t + \varphi_1) \\ A_1 \, sin(\omega_1 t + \varphi_1) \\ \omega_1 \end{pmatrix} \tag{3.3}$$

The third entry of *O* is the estimated frequency, which is identical to its correct value, ω_1.

3.1.3 ANF as the Building Block of a Grid-Synchronization Unit

3.1.3.1 Single Frequency Estimation

The ANF in Section 3.1.2 can be employed to develop a new grid synchronization scheme, or more visibly a new "power signal processor". Figure 3.1 shows the schematic structure of the proposed grid-synchronization unit, where the ANF in Section 3.1.2 is functioning as the main cell. The input is a distorted sinusoidal signal or in general a periodic signal. The power of the proposed synchronization structure is that it outputs useful signal information such as the fundamental component, its 90 degrees phase-shift, its amplitude, its frequency, sin/cos functions of its phase angle, and harmonics.

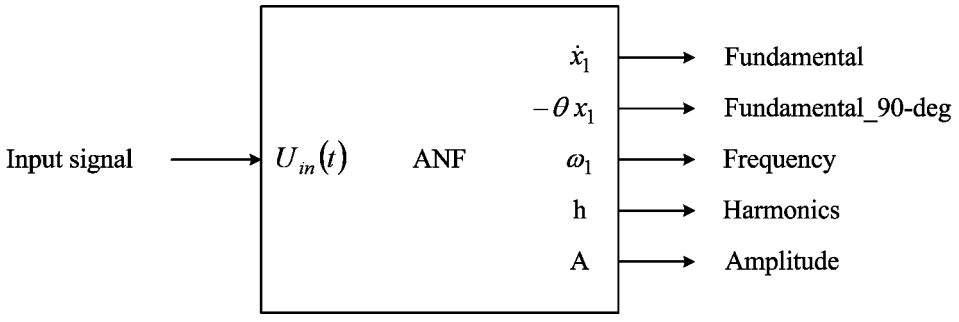

Figure 3.1 Proposed Signal Processing Unit [68].

As mentioned in Chapter 2, the state-of-the art technology in grid-connected converters is the use of a PLL device to find the phase angle of the grid voltage. We will show that in the proposed approach there is no need for a synchronizing tool like a PLL. In addition, having access to additional signal information enables the user to synchronize the on/off times of the switching devices, calculate active/reactive power, and transform the feedback variables to a frame suitable for control purposes [68]-[69].

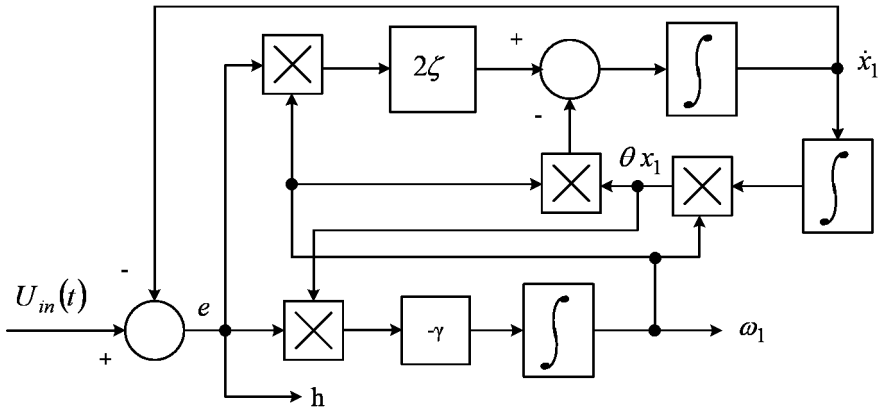

Figure 3.2 Detailed implementation of the proposed structure [68].

Getting back to the ANF dynamical equations, a close observation at (3.2) and (3.3) reveals that the fundamental component and its 90-degree phase-shift are essentially $\dot{\bar{x}}$ and $-\bar{\theta}\,\bar{x}$, respectively. Therefore, the amplitude of the fundamental component is easily determined from $A_1 = \left(\theta^2 {x_1}^2 + \dot{x}_1^2\right)^{1/2}$. A detailed implementation diagram of the proposed synchronization scheme is shown in Figure 3.2. The ANF is composed of simple adders, multipliers, and integrators. The output θ provides the fundamental frequency of the input signal, ω_1, and the

amplitude of the fundamental component is calculated using two additional multipliers, a summer, and a square-root function. The sin/cos functions of the phase angle are simply obtained by dividing the fundamental component and its 90 degrees phase-shift by the amplitude the fundamental component.

3.1.3.2 Multiple Frequency Estimation

In some applications it is desirable to estimate more than one frequency [44]. Examples are found in active power filters (APFs), where the removal of a selected number of harmonics, especially low order harmonics, is desirable. In this section it will be shown how an extended structure of our filter can simply extract multiple frequencies [73].

Consider the ANF equations of (3.2) with the periodic orbit of (3.3). The filter dynamics in (3.2) is identical to a resonator, $\ddot{x}+\theta^2 x=0$, that is forced with the error signal $e(t)$. The error signal incorporates the signal $x(t)$ in the update law in (3.2). The term θ in both equations is for scaling. In addition, the second component of the periodic orbit of (3.3), $\dot{\bar{x}}=A_1 sin(\omega_1 t+\varphi_1)$, is equal to the fundamental component of the input signal. These key ideas are used to propose a new structure composed of *n* parallel adaptive sub-filters to directly estimate frequencies of an input signal $u(t)$ given by (3.1). In such a structure, the *i*th sub-filter is formulated by [65]

$$\begin{aligned}
&\ddot{x}_i+i^2\theta^2 x_i=2\zeta_i\,\theta\,e(t)\\
&\dot{\theta}=-\gamma\,x_1\,\theta\,e(t)\\
&e(t)=u(t)-\sum_{l=1}^{n}\dot{x}_l
\end{aligned}\qquad (3.4)$$

Similarly, in (3.4), ζ_i and γ determine the behavior of the *i*th sub-filter in terms of accuracy and convergence speed, are real positive numbers.

The proposed method for multiple frequencies estimation, based on the concept of ANF, is shown in Figure 3.3. This figure shows a schematic structure of the proposed multiple frequencies estimator that extracts the fundamental component and the 5th and 7th order harmonics of the input signal. The input signal in this figure contains the fundamental (the 1st order harmonic) and only harmonics of the order of $(6k \pm 1)$, $k = 1,2,\ldots$.

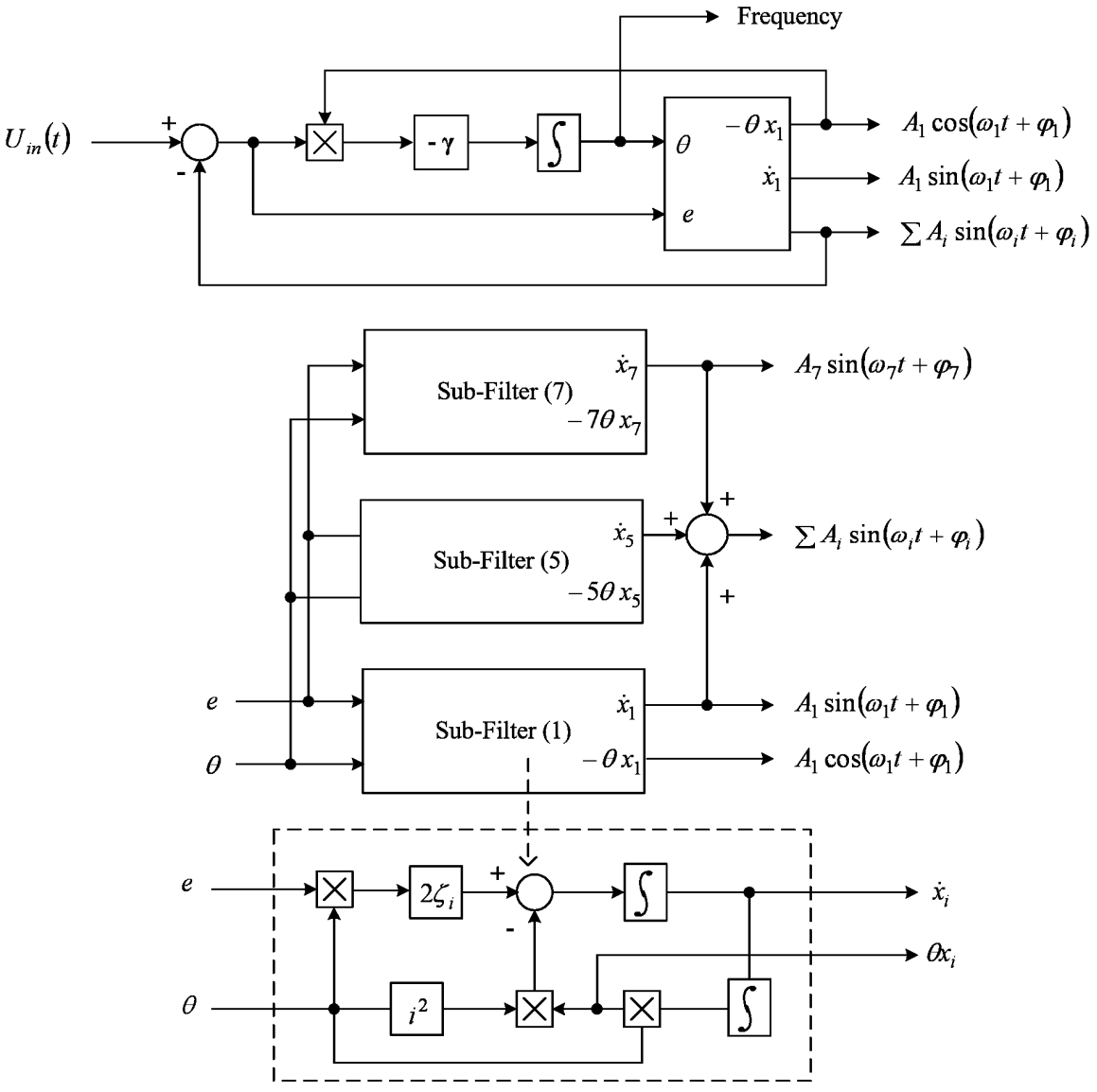

Figure 3.3 Proposed structure for selective harmonics extraction.

The proposed multi frequencies estimator consists of i) a master ANF that estimates the fundamental component of the input signal and its frequency; and ii) a multiplicity of slave ANFs that use these information and extract a number of harmonic components and their frequencies The master and slave ANFs are linked to each others in a parallel structure, and operational frequencies of the slave ANFs are dictated by the frequency estimation loop embedded in the master ANF.

The operating principles of this multi frequencies estimator can be explained as follows. At steady-state, $\dot{\bar{x}}_i = A_i \sin\phi_i(t)$ (the i^{th} component of the input signal) appears at the output of the corresponding slave filter. In other words, for instance, the 2nd filter in the proposed algorithm finds the instantaneous frequency of the 5^{th} harmonic of the input signal, $\dot{\bar{x}}_5$, and depicts it at its output. Simultaneously, the master ANF outputs the fundamental frequency, $\theta = \omega_1$. In addition, at steady-state we can write $A_i = \left(i^2\theta^2 x_i^2 + \dot{x}_i^2\right)^{1/2}$, that is the amplitude of the i^{th} harmonic component of the input signal. This means the proposed algorithm can be further furnished to estimate the amplitudes of the harmonics using arithmetic units that compute the right-hand side of A_i. Note the $i^2\bar{\theta}^2\bar{x}_i^2$ is available, therefore, the computation load of right-hand side of A_i is low. Particularly, this computation needs two multiplications, a sum and square-root computations.

3.1.4 Stability Analysis

The ANF dynamic in (3.2) is stable, which means that the proposed ANF is stable. This was mathematically proved in [65]. However, we proceed with a brief discussion on the stability of

the proposed ANF. Using the first equation of (3.2), the right side term of the θ update law can be rewritten as:

$$\dot{\theta} = -\frac{\gamma}{2\zeta} x\left(\ddot{x} + \theta^2 x\right) \tag{3.5}$$

Close to the periodic orbit O, where $\overline{\theta} = \omega_1$ and $\ddot{\overline{x}} = -\omega_1^2 \overline{x}$, we have

$$\dot{\theta} \approx -\frac{\gamma}{2\zeta} x^2\left(\theta^2 - \omega_1^2\right) \tag{3.6}$$

The above derivation shows that close to the desired orbit, the adaptation process is slow and the search in parameter space of θ will go to the correct direction (i.e., $\left\{\theta > \omega_1 \Rightarrow \dot{\theta} < 0\right\}$, and vice versa).

3.1.5 Filter Parameters and Initial Conditions

The basic structure of Figure 3.2 has two independent design parameters, γ and ζ. The parameter γ determines the adaptation speed, hence, the capability of the proposed algorithm in tracking the signal characteristics variations. Particularly, the convergence rate of the estimated frequency is proportional to γ. The parameter ζ determines the depth of the notch, hence, the noise sensitivity of the filter. A trade-off between the (steady-state) accuracy and (transient) convergence speed can be carried out by adjusting the design parameters, ζ and γ. By increasing γ one can achieve faster convergence speed, however, at the same time ζ should be increased to avoid oscillatory behaviors [69]. The proposed ANF structure has three integrators. The initial condition for the one that outputs the frequency, ω_1, is set to the nominal power system frequency. In other words, the initial condition for this integrator is set to 2π50 or 2π60 rad/sec

(similar to the center frequency of VCO in PLL schemes). The initial conditions for all other integrators are set to zero.

3.2 Performance Evaluation

Performance of the ANF-based power signal processor (grid synchronization) technique is evaluated experimentally through the use of dSPACE. The dSPACE 1103 DSP board was used to implement the proposed structure. The input signal, produced by a programmable voltage source, is fed into the ANF-based power signal processor implemented in dSPACE. The parameters of the ANF are set to γ=18000 and ζ=0.6. The initial condition for the integrator that outputs the frequency, ω_1, is set to $2\pi 60$ rad/sec (the nominal power system frequency). The initial conditions for all other integrators are set to zero.

3.2.1 Single-Frequency Estimator

The adaptability of the proposed power signal processing unit with respect to the frequency and amplitude variations, a common practice in actual distribution systems or grid-connected converters, is demonstrated here. For instance, the new grid codes for wind turbines are demanding a functionality of the turbine for a frequency deviation of ±3 Hz [75]. Thus, it is important for DG systems to have a synchronization algorithm which is able to run on such frequency band in addition to the amplitude variations.

Fig. 3.4 demonstrates the speed of the response and the accuracy of the proposed method, when a step change occurs in the frequency of the input signal. The input signal frequency jumps

from 60 Hz to 63 Hz. The frequency and the phase angle of the input signal are extracted and depicted in Fig. 3.4. Fig. 3.4 also shows the extracted and the actual frequency. It is noticeable that the proposed method precisely tracks the variations in the frequency within one cycle. The fast response and accurate performance of the proposed method are revealed under variation in frequency.

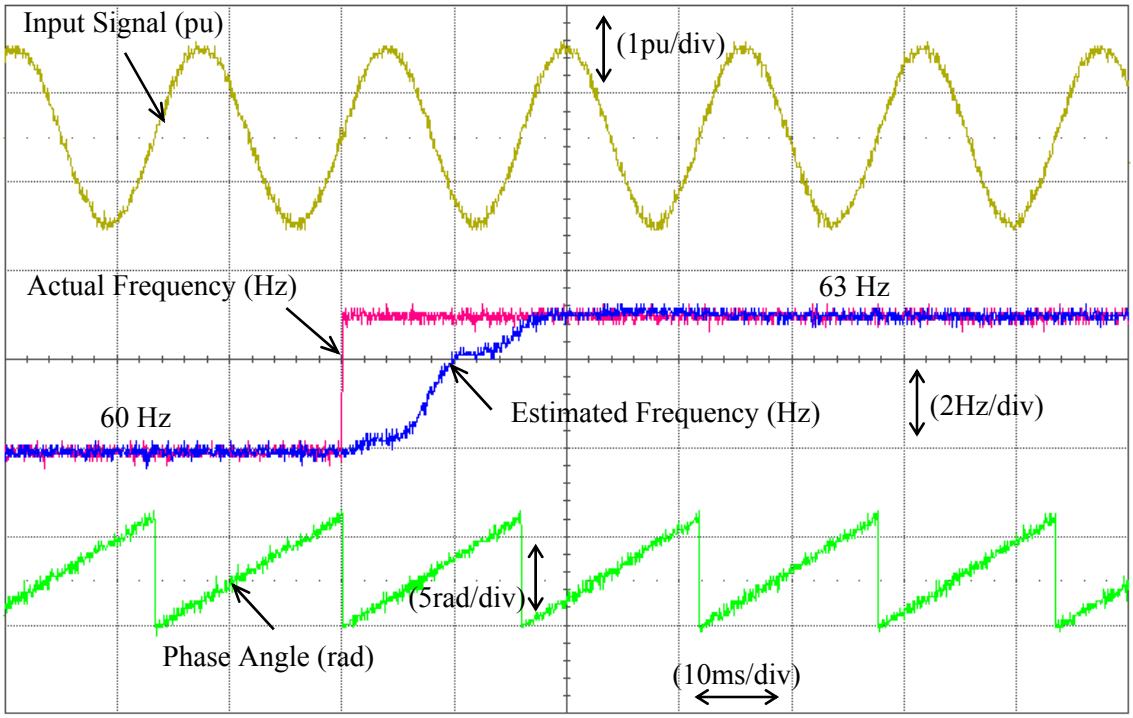

Figure 3.4 Response of the ANF-based method to a step change in the frequency of the input signal.

In another test, the input signal (in Fig. 3.5) consists of 0.8 p.u. fundamental component at 60 Hz, 1 p.u. fifth harmonic at 300 Hz (a low order harmonic), and 0.5 p.u. fiftieth harmonic at 3 kHz (a harmonic at switching frequency). A 40% reduction in the amplitudes of the input signal,

as shown in Fig. 3.5, does not affect the capability of the power signal processor in extracting the amplitude and the phase-angle of the fundamental component.

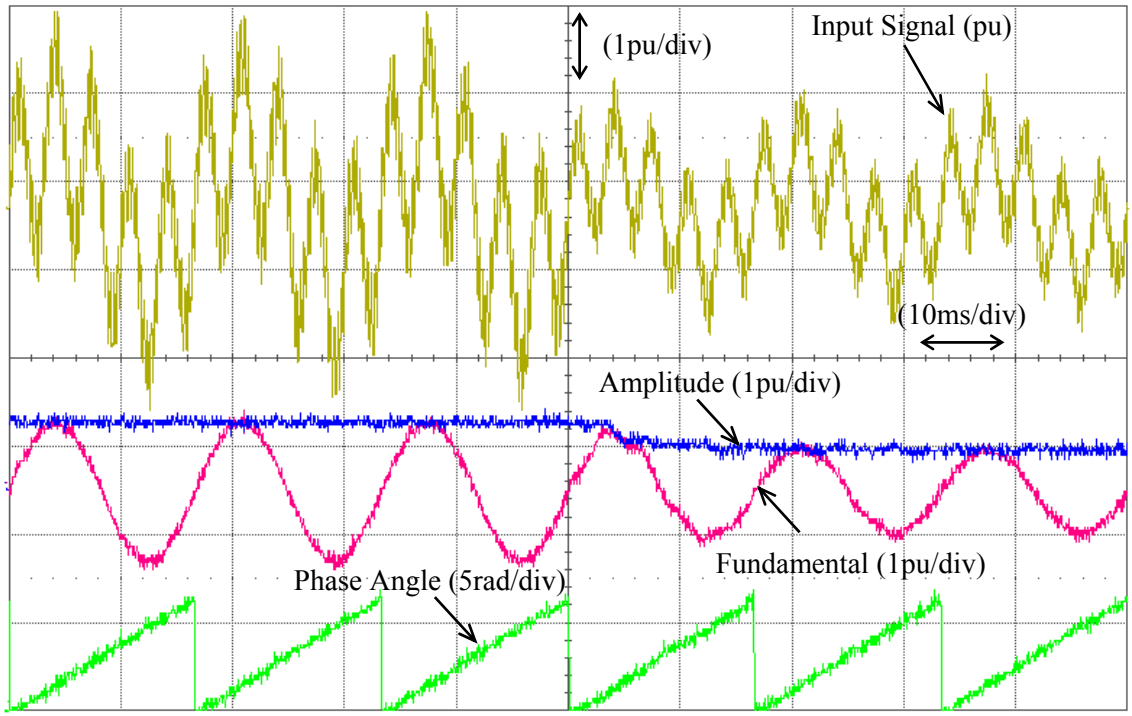

Figure 3.5 Response of the ANF-based method to a step change in the amplitude of the input signal.

3.2.2 Harmonic Extraction Capability

Accurate tracking and harmonic extraction feature of the proposed method is investigated in this section. The input signal is composed of a fundamental (1 p.u.), a fifth harmonic (0.3 p.u.), and a seventh harmonic (0.2 p.u.) components. Simultaneous step-changes in the fundamental component (from 1 p.u. to 0.8 p.u.), the fifth harmonic (from 0.3 p.u. to 0.1 p.u.), and the seventh harmonic (from 0.2 p.u. to 0.4 p.u.) are applied and the system response is recorded. Fig. 3.6

shows the input signal, the phase angle of fundamental, the 5th harmonic, and the 7th harmonic components.

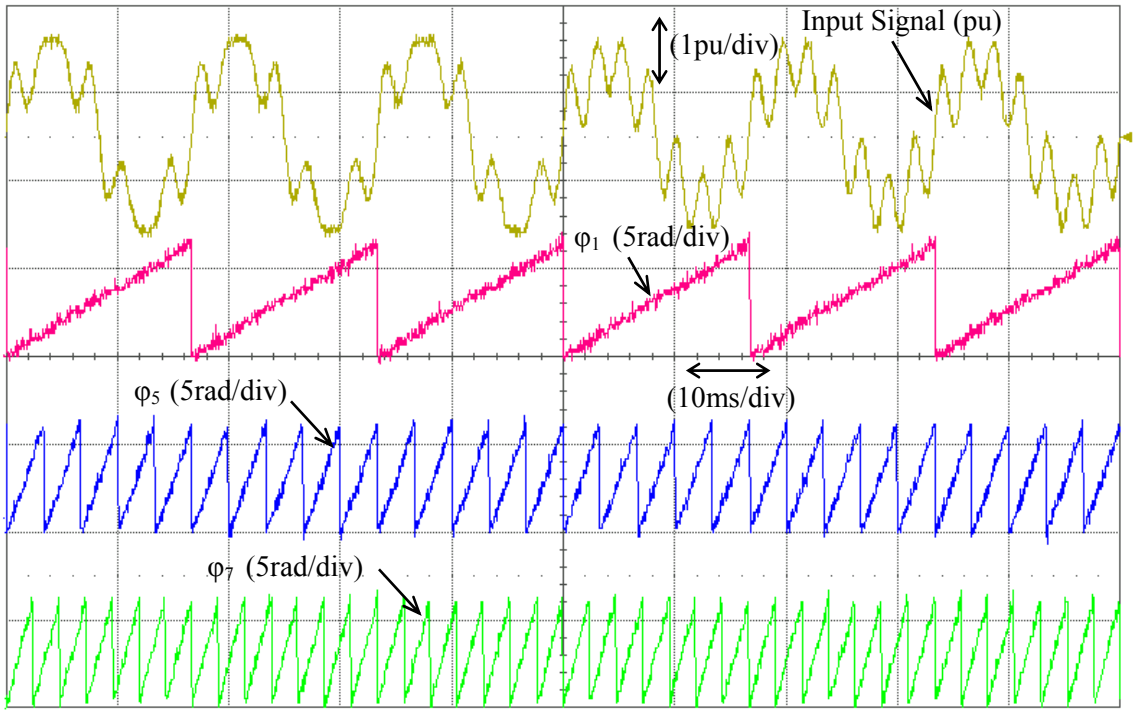

Figure 3.6 Response of the proposed method to simultaneous step changes in the amplitude of the fundamental, the fifth, and the seventh harmonic components: input signal, phase-angle of the fundamental component, the 5th and the 7th harmonics are shown.

The extracted fifth and seventh harmonic components and their corresponding amplitudes, shown in Fig. 3.7, confirm that the proposed scheme successfully tracks step-changes in less than two cycles of the fundamental component. This method can be used for selective harmonics elimination purposes.

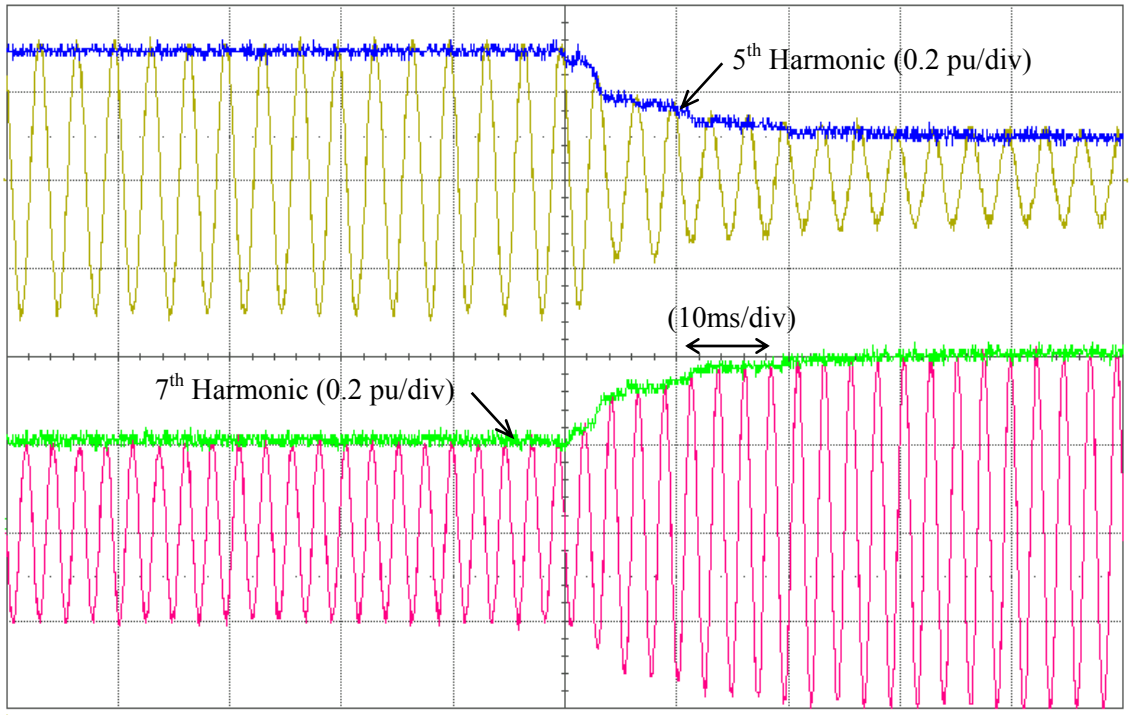

Figure 3.7 Response of the proposed method to simultaneous step changes in the amplitude of the fundamental, the fifth, and the seventh harmonic components: the 5th harmonic and its amplitude, the 7th harmonic and its amplitude are shown.

3.3 Informative Comparison and Conclusion

This section provides a brief comparison between the proposed and the existing techniques. As discussed in Chapter 2, the accuracy of the synchronization method based-on the voltage zero-crossing is influenced by disturbances, such as voltage sags and harmonics. Filtering techniques in different reference frames such as *d-q* or *α-β*, encounter difficulties in detecting the phase angle when unexpected variations in the grid voltage occur due to the appearance of faults or disturbances in the utility network. Although the PLL-based algorithms can successfully reject

harmonics, voltage sags, notches and other kind of disturbances; conventional PLL-based techniques fail to handle grid voltages unbalance situation. Experimental results obtained in this chapter show that the proposed synchronization technique successfully rejects harmonics, voltage sags, and other kind of disturbances. The interesting advantage of the proposed technique when compared to other techniques listed above is that it can simply be extended for extracting the individual harmonics' information, shown in section 3.2.2.

Fig. 3.8 provides a brief comparison between the ANF-based method and the techniques introduced in chapter 2. To compare the tracking capability of these methods, a step change has been applied to the input signal frequency from 60 Hz to 63 Hz at t=0.3 s. In this test, the input signal is pure sinusoidal. Fig. 3.8 (a) shows that orthogonal system generation (OSG) based technique is not able to track the frequency precisely. The reason for this is that the two phase signal generator used for the OSG is not frequency adaptive. Therefore, the generated two phase signal is not balanced in amplitude which leads to the double frequency in the estimated frequency when a step change occurs in the frequency of the input signal. Other methods such as the EPLL and Park-based PLL are able to track the frequency change quickly provided that the filters and PI controllers are designed properly. However, if these methods are designed to achieve a faster response, the estimated frequency will be sensitive to the harmonics of the input signal. To compare the tracking capability of these methods in the presence of harmonics in the input signal, a step change has been applied to the input signal frequency from 60 Hz to 63 Hz at t=0.3 s. In this test, at t=0.3 s, the input signal is composed of a fundamental (1 p.u.), a third harmonic (0.1 p.u.), and a fifth harmonic (0.1 p.u.) component. Fig. 3.8 (b) shows that the modified ANF method (multi-block ANF) gives a faster response while rejecting harmonics, compared to the other methods. Since the sub-filters in the modified ANF are notch filters, their dynamics only appear around their notch frequency (harmonic frequencies), and they do not

affect the dynamic of the main filter which is a notch filter centered at the fundamental frequency. However, to remove the low-order harmonics in the other methods, the bandwidth of the filter must be decreased, which is what makes them so slow.

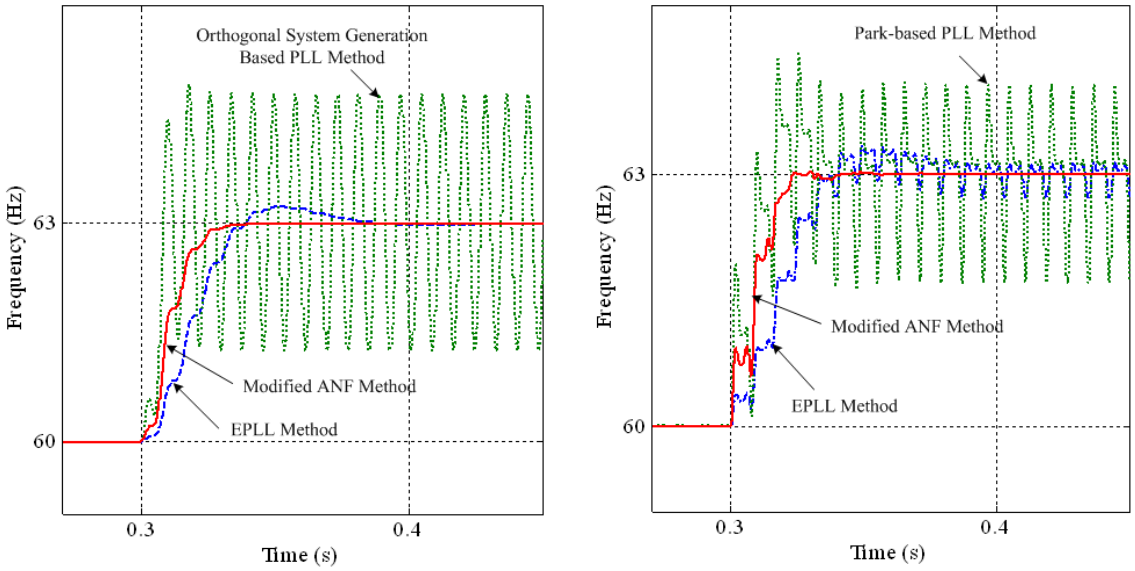

Figure 3.8 Response of the ANF-based, OSG-based PLL, Park-based PLL and EPLL-based methods to a step change in the frequency of the input signal; (a) no harmonics, (b) low order harmonics at t=0.3 s.

When compared to the PLL-based method, 1) the ANF-based scheme, since it does not require a voltage-controlled oscillator (VCO), is structurally simpler, 2) contrary to PLL-based methods, the ANF-based structure guarantees a fast and precise extraction of the frequency when the distorted input signal contains low order harmonics.

The proposed ANF-based algorithm outputs the important grid signal's information required for grid synchronization including the grid's voltage frequency, amplitude, and phase angle. The proposed technique naturally, without any additional component, outputs the *sin* and *cos*

functions of the phase angles of currents and voltages that are very useful in controlling all grid-connected converters. The existing methods need additional components and demand modifications to output all these information. In addition, the non-linear structure of the proposed algorithm allows direct estimation of the signal's frequency and its multiples with no use of linearization processes or other simplifying assumptions. Moreover, the proposed method can successfully detect and track the variations in the frequency of the signal and extract the time-varying harmonics. Comparison showed that the ANF-based structure guarantees a fast and precise extraction of the frequency when the distorted input signal contains low order harmonics.

Unique and multi-purpose features of the ANF-based technique, as discussed in Chapter 4, can be used for grid synchronization, sequence components decomposition, harmonic compensation and active power filtering, reactive power control, power flow control, voltage regulation, etc. All these, nominate the technique as a simple and powerful "power signal processor". The operating principles of such a power signal analyzer are presented in the next chapter.

Chapter 4
A New Single-Phase Based Power Signal Processor for Three-Phase Applications

Nowadays, it is a general trend to increase the electricity production using DG systems. If these systems are not properly controlled, their connection to the utility network can generate problems on the grid side [75]-[77]. Therefore, considerations about power generation, safe running and grid synchronization must be done before connecting these systems to the utility network.

Most of low power DG systems are single-phase. Grid-synchronization techniques developed for single-phase applications differ in many aspects from those developed for only three-phase systems. The strengths of the single-phase based synchronization technique presented in chapter 3 are that it successfully rejects disturbances and harmonics, causes no double frequency ripple, and is accurate, simple and straightforward. In addition, these simple synchronization units, which have a simple structure and a small number of interconnected arithmetic units, can be connected in a modular structure to form three-phase or even multi-phase synchronization modules.

It is shown in the previous chapter that useful grid information required for grid synchronization are extracted from the grid voltages by the proposed single-phase ANF algorithm in a simple and straightforward manner and with no need for a PLL system. This chapter, as

mentioned above, employs three single-phase based synchronization modules to form a three-phase synchronization scheme. Such a three-phase synchronization scheme is in fact an advanced "*power signal processor"* developed to extract key power system information that are required especially in converter-interfaced DG systems. This new processor with some modification can perfectly perform almost every single signal processing function that might be required for control and safety purposes in DG systems. The chapter highlights a number of power signal processing methods that use the input signal information extracted by the proposed grid synchronization scheme in chapter 3, and provides key power system processing scheme such as sequence decomposition, reactive current extraction, and harmonic extraction and rejection. A new three-phase-based synchronization scheme is also developed and presented in chapter 5.

4.1 Applications in Three-Phase Systems

In three-phase systems, a synchronization algorithm can be implemented in *abc* frame and by means of three aforementioned single-phase ANF systems [68], [73]. As explained in Chapter 3, grid information required for grid synchronization are simply extracted by the three ANFs without using a PLL system. One advantage of this implementation is that it provides distinctive information about the amplitude, frequency and phase angle of each phase voltage. This distinguishing feature as it provides additional information is very beneficial for grid monitoring. In addition, the use of a PLL block and/or a *dq-abc* transformation module is unnecessary in all control functions that employ the proposed ANF-based processor.

4.1.1 Sequence Component Decomposition for Transient and Unbalanced System Operation.

The availability of the fundamental and its 90-degree phase-shift components of the current or voltage is ideal for sequence components decomposition under transient and unbalanced system operations [68], [73]. This aspect is very beneficial in three-phase distributed power generation systems, where the ride-through capability of the synchronization tool under system unbalance situation and its capability for disturbance rejection are of great importance.

The concept of symmetrical components that was originally defined for phasors, can be extended to the signals as functions of time by replacing the complex phasor $\alpha = e^{j120^o}$ with a 120^o phase-shift operator in time domain [78]-[81].

$$\begin{pmatrix} v_a(t) \\ v_b(t) \\ v_c(t) \end{pmatrix} = \frac{1}{3}\begin{pmatrix} 1 & 1 & 1 \\ 1 & \alpha^2 & \alpha \\ 1 & \alpha & \alpha^2 \end{pmatrix}\begin{pmatrix} v_a^0(t) \\ v_a^+(t) \\ v_a^-(t) \end{pmatrix} \tag{4.1}$$

Based on (4.1), a three-phase signal, $v(t)$, can be decomposed to $v(t) = v^+(t) + v^-(t) + v^0(t)$, where, $v^+(t)$, $v^-(t)$ and, $v^0(t)$ are positive-, negative- and zero-sequence components, respectively. Sequence components in terms of a 90-degree phase-shift operator, which is much easier to implement are determined from,

$$\begin{aligned} v^+(t) &= T_2 X_1(t) + T_1 X_2(t) \\ v^-(t) &= T_2 X_1(t) - T_1 X_2(t) \\ v^0(t) &= (I - 2T_2) X_1(t) \end{aligned} \tag{4.2}$$

where $X_1(t)$ and $X_2(t)$ stand for the fundamental component of the input signal and its 90° phase-shift, receptively. T_1 and T_2 are 3 × 3 matrices given by $X_1(t)$ and $X_2(t)$

$$T_1 = \frac{1}{2\sqrt{3}}\begin{pmatrix} 0 & 1 & -1 \\ -1 & 0 & 1 \\ 1 & -1 & 0 \end{pmatrix} \tag{4.3}$$

$$T_2 = \frac{1}{3}\begin{pmatrix} 1 & -0.5 & -0.5 \\ -0.5 & 1 & -0.5 \\ -0.5 & -0.5 & 1 \end{pmatrix} \tag{4.4}$$

and I is a 3 × 3 identity matrix.

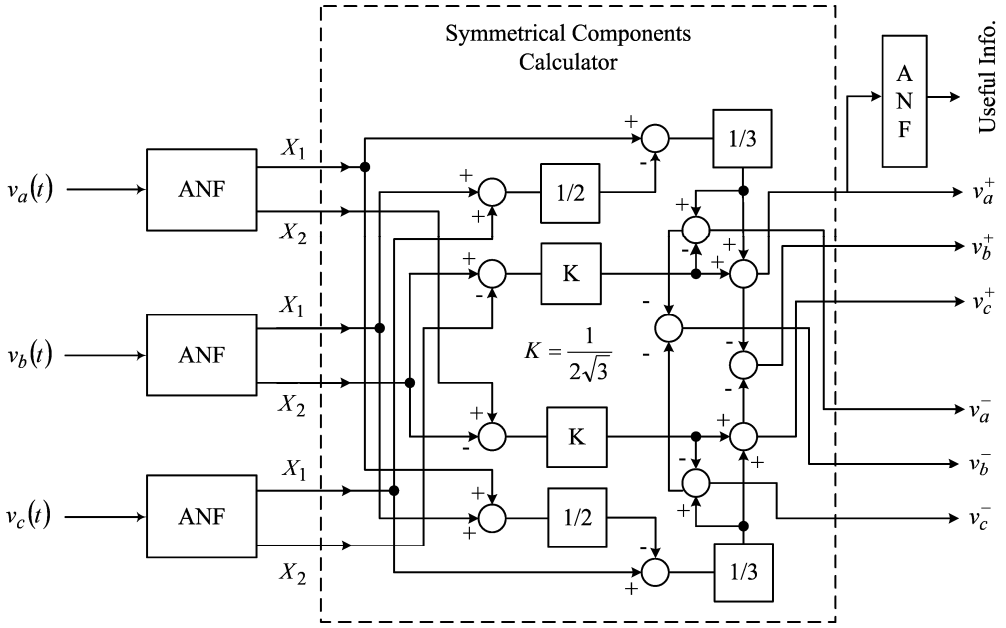

Figure 4.1 Proposed structure for three-phase systems [68].

The positive- and negative sequence extractor unit, shown in Fig. 4.1, is comprised of three ANFs and simple arithmetic operators. ANFs adaptively extract the fundamental voltages and their 90-degree phase-shift. The reminder system receives these components and calculates the positive- and negative-sequence voltages based on (4.2), (4.3), and (4.4). The extracted positive sequence component is then passed to another ANF that outputs useful information for grid

synchronization or other control purposes.

The symmetrical components can be employed in a variety of power system applications, such as protection, fault analysis, reactive power compensation, unbalance mitigation, system modeling and identification. Recently, the symmetrical components are used to synchronize the converter-interfaced DG units with the utility systems and keep generation up during the grid faults [1].

4.1.2 Active, Reactive and Harmonic Current Extraction

Detection and precise extraction of the compensating signal is the most important part of a grid-connected converter's control [44]-[63]. Advanced signal processing methods in both the time- and frequency-domains have been developed to detect and extract the compensating signal [44], [50]. Frequency-domain approaches are the fast Fourier transform (FFT) and discrete Fourier transform techniques. And important time-domain schemes are the instantaneous "*p*–*q*", the synchronous *d*–*q*, notch filters, approximated band-pass resonant filters, and stationary frame filters. More advanced control and signal processing techniques including fuzzy logic control, neural network theory, sliding mode control, and adaptive signal processing have also been applied [44]. Most of these algorithms are quite accurate and, of course, have a much better dynamic response than the FFT, but these algorithms require a large amount of calculation and none is reported to demonstrate good performance in frequency-varying environments. In case of frequency variations, the ideal solution is an adaptive approach capable of tracking the frequency variations of the power signal, hence tracking time-varying harmonics [44], [61]. An adaptive method of harmonic and reactive components detection is introduced in [61]. Shortcomings of the method presented in [62], as a harmonic detector, are its low convergence speed and lack of

robustness with respect to input frequency variations. Moreover, it is sensitive to voltage pollutions when it is used as reactive current detector. In [63], the filter structure is modified to overcome the first two drawbacks. However, it is only suitable for harmonic detection and is not able to extract the reactive current component.

This section introduces a new ANF-based approach for extraction of active/reactive/harmonics current components of the grid signal, which is of great importance in many applications in power systems such as power quality and control. The proposed method is based on the ANF introduced in the previous chapter which provides fast and accurate estimation of the signal's information in the presence of frequency and amplitude variations. In this section, the power signal processor in Fig. 3.2 is used to develop a novel and simple mechanism for extracting the harmonic and reactive current components of a signal. The approach, although is intended to extract harmonic and reactive current components, outputs useful information such as amplitude, *sin* and *cos* of the phase angle and frequency of the fundamental component, and with more modifications outputs the Total Harmonic Distortion (THD), and power factor.

For power quality purposes, all grid connected converters require an advanced phase-detecting scheme that might further be employed to detect current harmonics and extract the reactive current components [71]. Let's assume:

$$v(t) = V \sin\phi_v \tag{4.5}$$

$$i(t) = \sum_{h=1}^{\infty} I_h \sin\phi_{ih} \tag{4.6}$$

Only the fundamental component of the current contributes in power transfer (real power transfer). The right side of (4.6) can be decomposed into the fundamental and harmonic current components, as shown in (4.7).

$$i(t) = I_1 \sin\phi_{i1} + \sum_{h=2}^{\infty} I_h \sin\phi_{ih} \tag{4.7}$$

For the given input voltage, the active, i_a , and reactive components, i_r , of the current are given by (refer to Fig. 4.2):

$$i_a = I_1 \cos(\phi_{i1} - \phi_v) \sin\phi_v \tag{4.8}$$

$$i_r = I_1 \sin(\phi_{i1} - \phi_v) \cos\phi_v + \sum_{h=2}^{\infty} I_h \sin\phi_{ih} \tag{4.9}$$

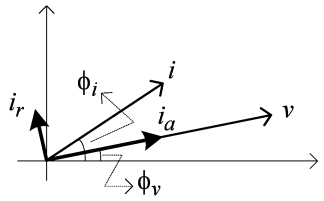

Figure 4.2 Proposed structure for harmonic/reactive extraction.

In general, when the input voltage/current are distorted:

$$v(t) = \sum_{h=1}^{\infty} V_h \sin\phi_{vh} \tag{4.10}$$

$$i(t) = \sum_{h=1}^{\infty} I_h \sin\phi_{ih} \tag{4.11}$$

The active and reactive components are calculated by:

$$i_a = \sum_{h=1}^{\infty} I_h \cos(\phi_{ih} - \phi_{vh}) \sin\phi_{vh} \tag{4.12}$$

$$i_r = i - i_a = \sum_{h=1}^{\infty} I_h \sin(\phi_{ih} - \phi_{vh}) \cos\phi_{vh} \tag{4.13}$$

Note that the calculation of the *sin* and *cos* functions of the phase angle difference between the voltage and current can be simply performed by:

$$cos(\phi_i - \phi_v) = cos(\phi_i)cos(\phi_v) + sin(\phi_i)sin(\phi_v) \quad (4.14)$$

$$sin(\phi_i - \phi_v) = sin(\phi_i)cos(\phi_v) - cos(\phi_i)sin(\phi_v) \quad (4.15)$$

The objective is to find an algorithm that receives the voltage/current and extracts: (i) the amplitude, phase angle and frequency of the fundamental component, (ii) sin and cos functions of phase angles of the voltage/ current which are used to calculate the phase angle difference between the phase voltage and phase current by (4.14 and 4.15), (iii) the harmonic content of the input signal, and (iv) the amplitude, and *sin* and *cos* functions of phase angles of the individual harmonics of the voltage/ current.

The proposed structure in Fig. 3.2 is used to develop a simple mechanism for extracting the harmonic and reactive current components of a measured signal. Fig. 4.3 shows the single-phase diagram of the harmonic/reactive-current component extractor.

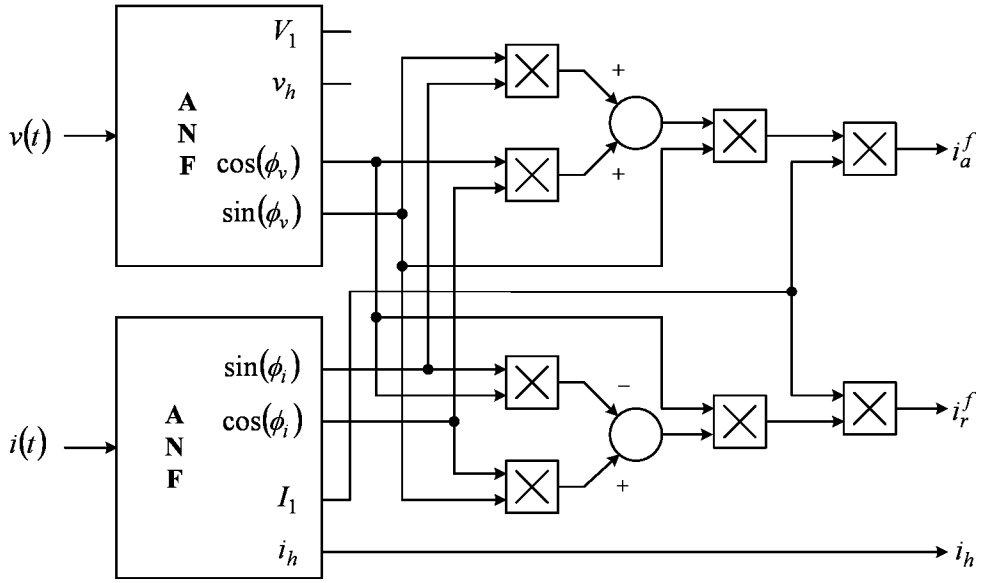

Figure 4.3 Proposed structure for harmonic/reactive extraction [68].

The two identical ANF units are to extract voltage and current information such as their harmonic contents, peak fundamental components, frequencies, and *sin* and *cos* functions of phase angles. Since I_1, $cos\phi_i$, $sin\phi_i$, $cos\phi_v$, and $sin\phi_v$ are all available at the output of the two ANFs, the phase angle difference between the phase voltage and phase current is simply obtained by (4.14 and 4.15) and thus active and reactive current components can be simply obtained based on (4.8 and 4.9). The approach, although intended to extract harmonic and reactive current components and useful signal information, can output the total harmonic distortion and power factor with more modifications.

4.2 Performance Evaluation

4.2.1 Simulation Results

Performance of the ANF-based method of synchronization is evaluated by means of simulations. The proposed ANF-based systems are simulated using MATLAB/Simulink. The parameters of the ANF are set to γ=18000 and ζ=0.6. The initial condition for the integrator that outputs the frequency, ω_1 , is set to 2π60 rad/sec (the nominal power system frequency). The initial conditions for all other integrators are set to zero.

4.2.1.1 Sequence Component Decomposition

The performance of the proposed three-phase structure on a simple distribution system, Figure 4.4, is evaluated in this section. The test case was aimed toward testing the sequence components extractor unit in tracking symmetrical components of the current signals polluted

with harmonic distortion. A simple test distributions network loaded with a static dc converter and operating under unbalance operations is shown in Fig. 4.4.

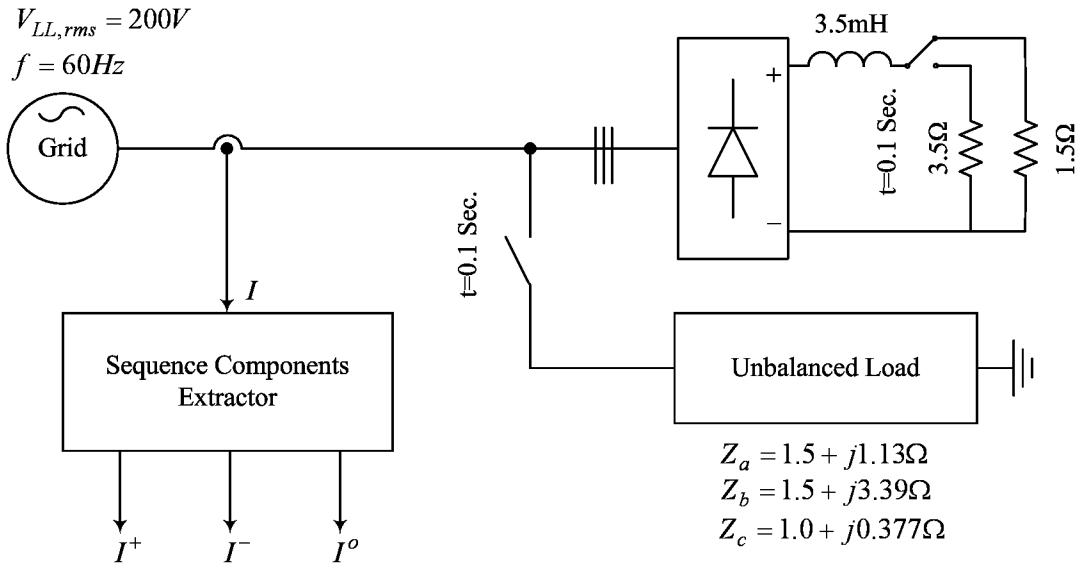

Figure 4.4 Simple distribution system configuration.

At t=0.1s, the unbalanced load is switched to the network and a sudden change occurs in the static dc converter's load. Fig. 4.5 shows the three-phase currents, which feed both nonlinear and three-phase unbalanced loads. These currents are measured and fed to the proposed processing unit. The unbalanced load is switched on at t=0.1s. The estimated fundamental components by the three independent ANFs at the first stage of the processing unit, and extracted positive and the negative sequence components are shown in Fig. 4.5. Before t=0.1s, the system was balanced, thus there is no negative sequence component. Switching the unbalanced load at t=0.1s makes the currents unbalance, and therefore negative sequence currents exist.

The fast response and accurate performance of the proposed processing unit in tracking symmetrical components are revealed even under dynamic load changing. Results show that the

proposed system needs less than one cycle to detect the fault and therefore symmetrical components.

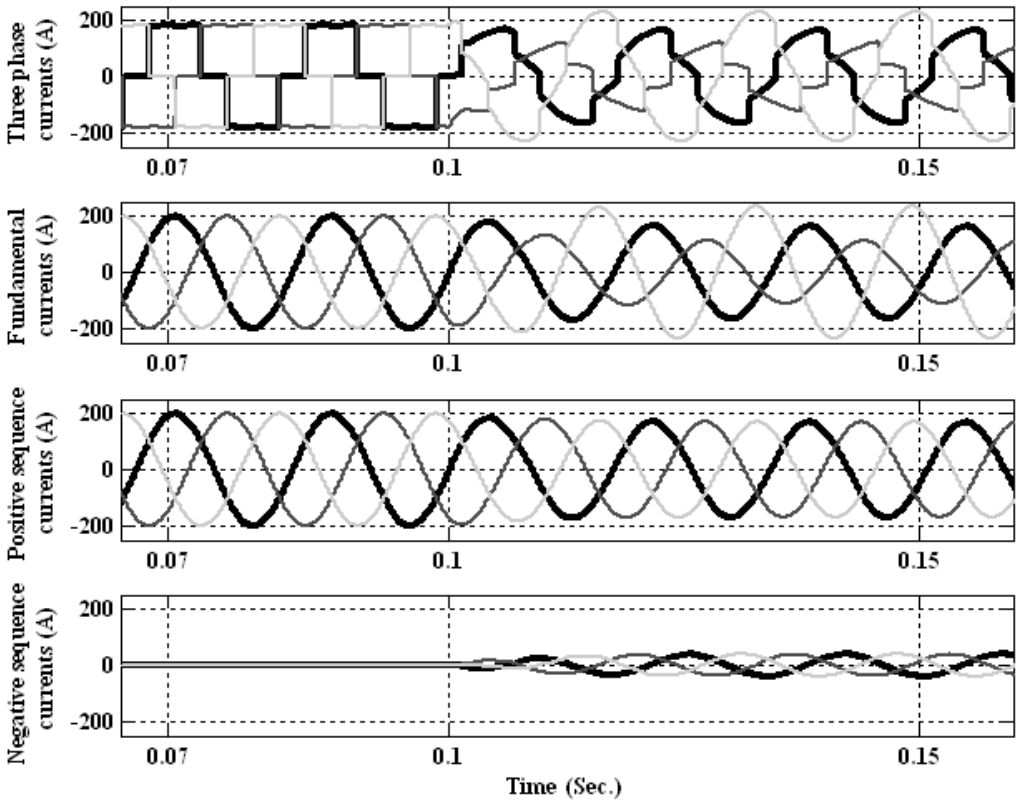

Figure 4.5 Extracted the grid currents' sequence components by the proposed technique.

4.2.1.2 Harmonic and Reactive Current Component

The capability of the proposed method in extracting the harmonic and reactive current components is evaluated on a typical nonlinear load. A typical nonlinear load (a three-phase thyristor rectifier) is selected for this set of evaluation, Fig. 4.6. Such a phase-controlled rectifier

is a well-known load and its power factor drops dramatically with the delay angle (firing angle) of thyristors.

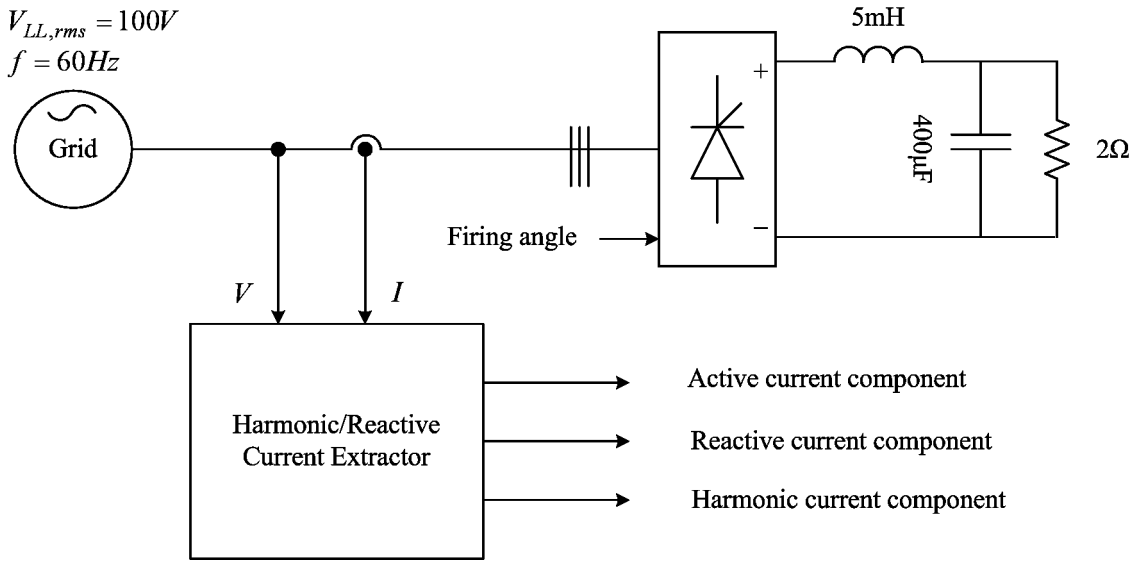

Figure 4.6 Simple three-phase thyristor rectifier as a non-linear load.

Initially, the firing angle was zero, and the fundamental current is in phase with the voltage, as expected. A step change in the firing angle was occurred at t=0.2 s. Fig. 4.7 shows that the current and the voltage are in phase (no reactive current component) before t=0.2 s. At t=0.2 s, the load current is phase-shifted because of the step change of 18^o in the firing angle of the three-phase thyristor rectifier. Fig. 4.7 shows that the scheme successfully extracts the active and reactive components of the load current, and the load harmonic current within one cycle of the system voltage. These extracted components are used to generate reference currents in the control system of various applications.

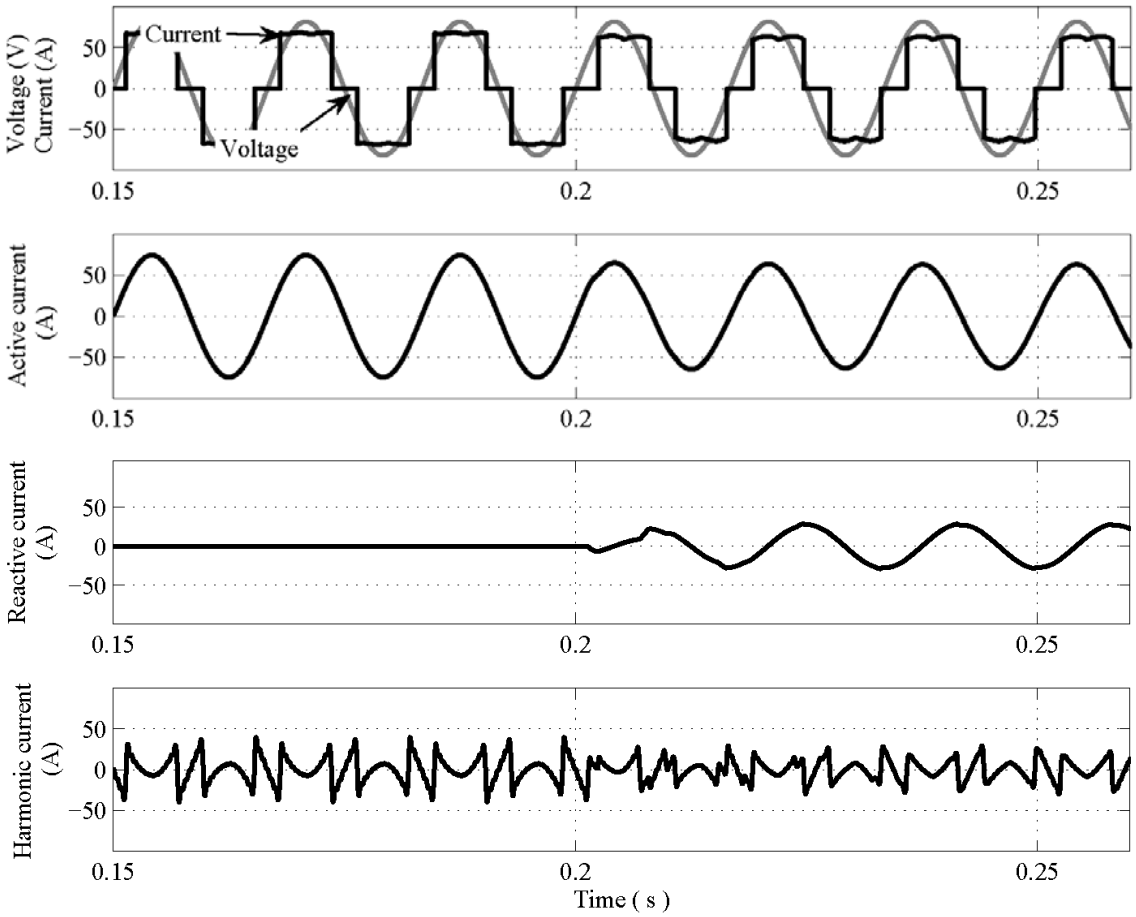

Figure 4.7 Response of the proposed technique to 18^{o} step change in the firing angle of the non-linear load current.

4.2.2 Experimental Results

4.2.2.1 Sequence Component Decomposition

The performance of the proposed three-phase sequence components decomposition unit is evaluated in this section. A three-phase programmable voltage source is used to produce step variations in the positive-, negative- and zero-sequence voltages. For the sake of simplicity,

voltages are assumed to be sinusoidal. The impact of harmonics has already been addressed in the previous chapter.

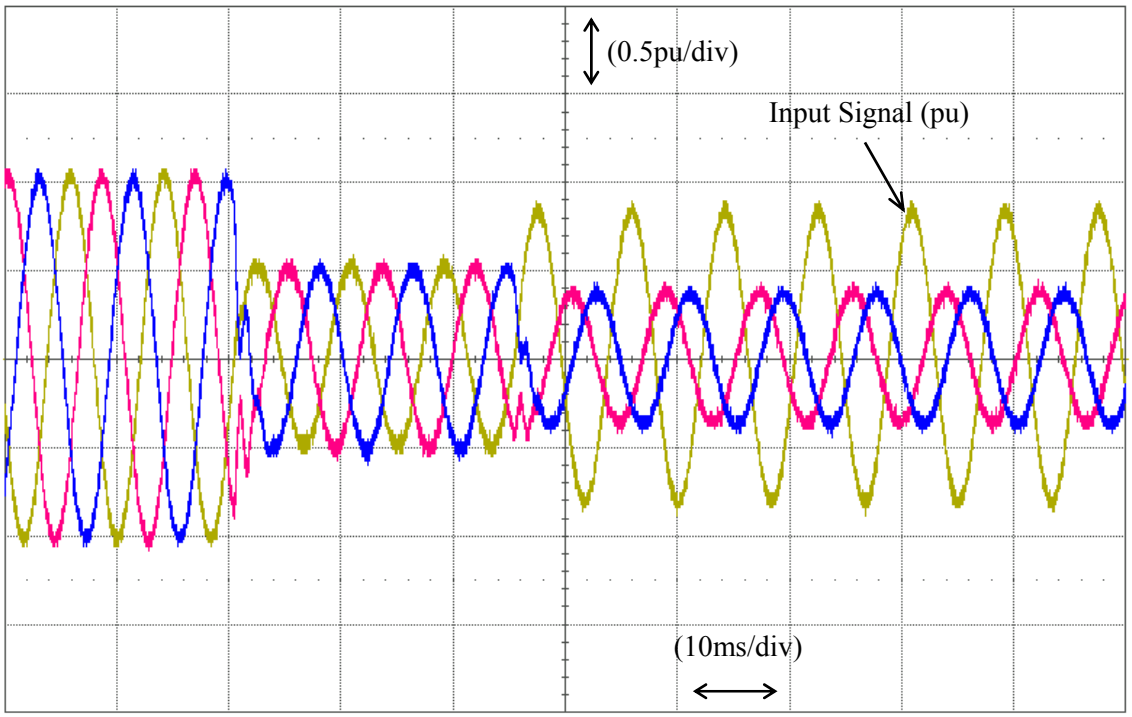

Figure 4.8 The three-phase test signal.

Under normal conditions, the input to the system is a set of balanced three-phase sinusoidal voltages of 1.0 p.u. amplitude. Since the system is balanced, no negative- or zero-sequence components exist. A frequently happening three-phase voltage sag is tested first. A step change (-0.5 p.u.) in the amplitudes of all three-phase voltages is applied. As expected, during this voltage sag, grid voltages remain balanced and no negative-sequence voltage exists. Experimentally obtained results in Fig. 4.8 and Fig. 4.9 validate this. Then, 0.2 p.u. negative-sequence and 0.1 p.u. zero-sequence voltages are added to the input signal, Fig. 4.8. Fig. 4.9 shows that the

proposed structure tracks all these variations and successfully extracts positive-, negative- and zero-sequence components.

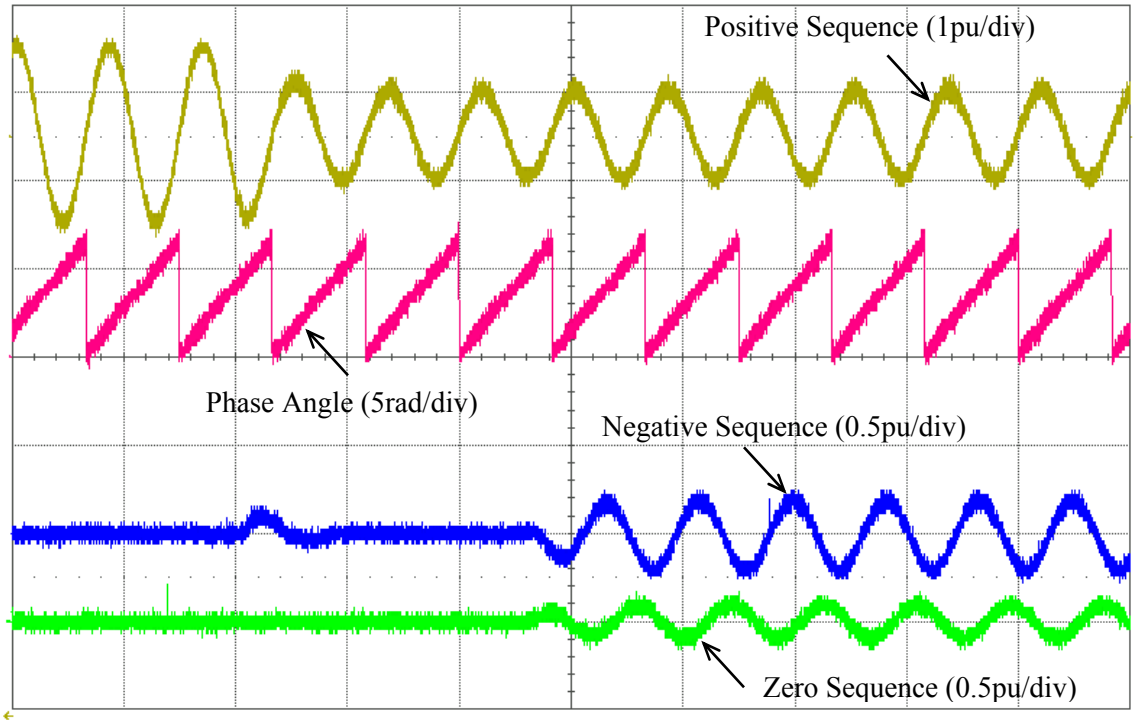

Figure 4.9 Extracted sequence components of input signal in Fig 4.8: Positive sequence of phase B and its phase-angle, negative sequence of phase B, and zero sequence.

Without loss of generality, the positive- and negative-sequence components of phase B is shown here. In addition, the extracted phase-angle of the positive-sequence component can be used for synchronization. Results show that the proposed system needs less than one cycle to detect the fault and decompose symmetrical components. This is fast enough for DG applications, according to the grid codes for wind turbines given in [1]. As mentioned earlier, the fast and accurate detection of the positive-sequence component of the utility voltage is required in order to synchronize the converter-interfaced DG units with the utility systems and keep generation up during the grid faults. The proposed method detects a voltage-dip or any other faults in the utility

network and extracts the positive sequence of the grid voltage, and therefore tracks the new phase angle of the grid voltage.

4.2.2.2 Harmonic and Reactive Current Component

The capability of the synchronization method in extracting the harmonic and reactive current components is evaluated on a nonlinear load. A typical highly distorted nonlinear current waveform (a square wave) is selected for this set of experimental evaluation, Fig 4.10. Initially, the current and the voltage are in phase (no reactive current component). As shown in Fig 4.10, the extracted phase angle of the current and the voltage are the same. The extracted active current is positive and the extracted reactive current is zero. The load current is then phase-shifted by 36-degrees and reduced by 40%.

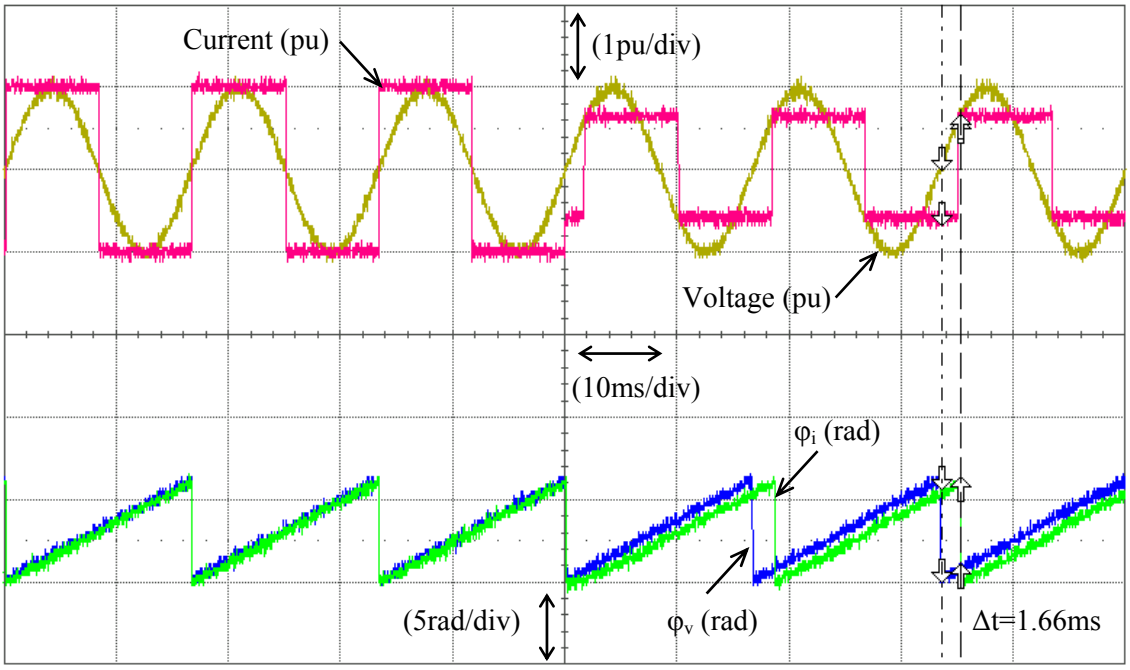

Figure 4.10 Response of the proposed system: input voltage and its extracted phase angle, input current and its extracted phase angle.

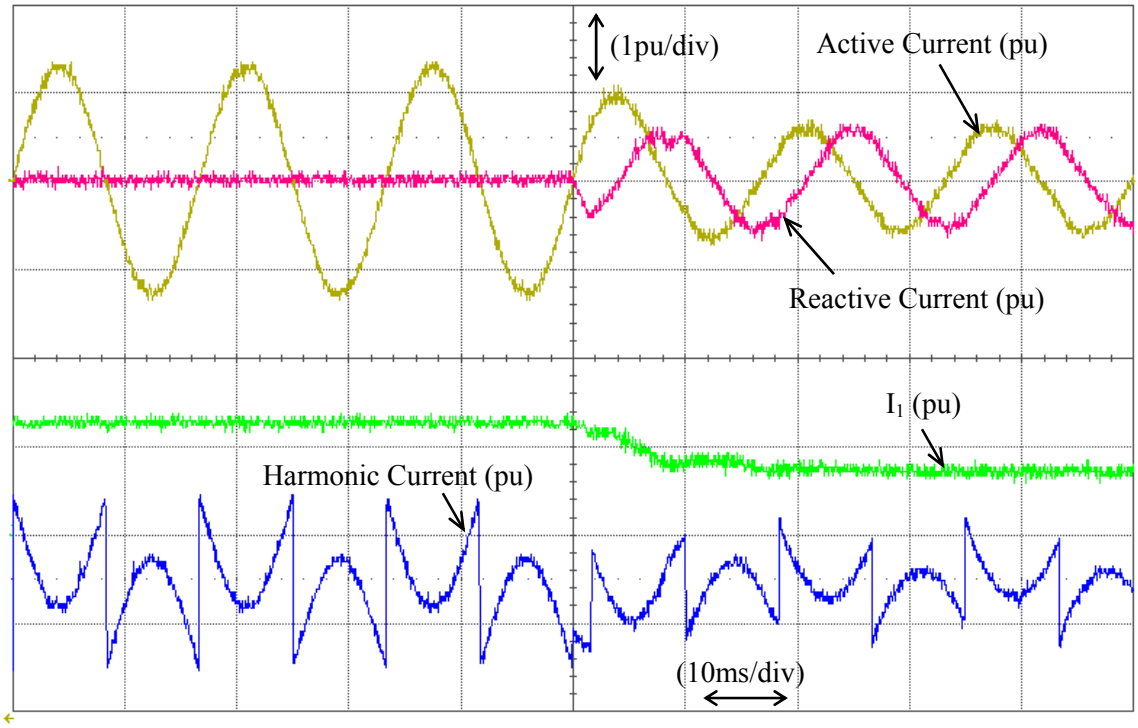

Figure 4.11 Response of the proposed system: extracted active current, reactive current, harmonic components, and amplitude of the fundamental component of the input current.

Fig. 4.11 shows that the scheme can effectively extract the active and reactive components of the load current, and the load harmonic current within one cycle of the system voltage. These extracted components are traditionally used to generate reference currents for the control system in various applications, especially for power quality purposes.

4.3 Conclusion

This chapter introduced an advanced power signal processor based on the proposed ANF-based synchronization method in Chapter 3. This new processor with some modification can

perfectly perform almost every single signal processing function that might be required for control and safety purposes in DG systems. In addition, the new processor employs mathematical tools that streamline the control formulation and thus the system implementation.

The proposed power signal processor has applications in a wide range of system equipments such as converter-interfaced distributed generation (DG) units, e.g. wind and photovoltaic, and in FACTS and Custom Power Controllers, e.g. Active Power Filters (APFs), Unified Power Flow Controllers (UPFCs) and STATic COMpensators (STATCOMs). The capability of the proposed technique to accurately measuring positive and negative sequences in unbalanced three-phase systems is a great solution for unbalance system operation. This advantage is very beneficial in three-phase distributed power generation systems, where ride through capability of the synchronization tool under system unbalance situation and its capability for disturbance rejection are of great importance. In addition, this chapter introduced a new ANF-based approach for extraction of harmonic and reactive current components. The main function of this method is to provide synchronized harmonic and reactive current components for the control purposes. Both proposed algorithms adaptively and simultaneously extracts and measures required components of a power signal with a time-varying characteristic. It also extracts all useful information embedded in the signal such as frequency, amplitude, and the phase angle.

Chapter 5
A New Three-Phase Based Synchronization Technique

This chapter introduces a new three-phase based approach for extraction of frequency, phase angle and amplitude of the grid signal. Unlike the method proposed in chapter4, which was based on three single-phase frequency estimation systems, the proposed method in this chapter is based on a three-phase ANF approach. Mathematical derivations of the proposed technique are presented to describe the principles of operation and experimental results confirm the validity of the analytical work.

5.1 Proposed Three-Phase Synchronization Method

In three-phase systems, a synchronization algorithm can be implemented in *abc* frame and by means of three single-phase ANF systems introduced in chapter 3, as shown in chapter 4. Each single-phase ANF is a third-order dynamic system (Equation 3.2), hence the three-phase system in chapter 4 has a dynamic of order nine. This makes the overall system complex for hardware implementation and demands high volume of calculations for software implementation. Additional order might also cause delays and reduce the speed of convergence. A new three-phase ANF-based synchronization for three-phase systems is proposed in this chapter. The three-phase based method introduced in this chapter uses a seven order dynamical ANF system and

provides fast and accurate estimation of the input signal's information in the presence of frequency and amplitude variations. In addition, the simplicity of the structure makes the method suitable for both software and hardware implementations. This section covers the mathematical structure and the features of the proposed algorithm devised to estimate the useful information of a three-phase signal.

5.1.1 Proposed Three-Phase Frequency Estimator

For three-phase applications, three single-phase ANFs can be employed to provide the fundamental component, its 90° phase-shift, it's phase angle, and its frequency for each $u_a(t)$, $u_b(t)$ and, $u_c(t)$. Each ANF is a third-order dynamic system (Equation 3.2), hence the three-phase system in has a dynamic of order nine [68].

However, the three-phase signals have a common frequency, ω_o, and therefore there is no need to estimate the frequency of each phase independently. Therefore, a common frequency estimation law based on the output information of all three ANFs is proposed here [74]. Consider three identical ANFs:

$$\ddot{x}_\alpha = -\theta^2 x_\alpha + 2\zeta_\alpha \theta e_\alpha(t), \quad \alpha = a,b,c$$

$$e_\alpha(t) = u_\alpha(t) - \dot{x}_\alpha \tag{5.1}$$

where θ is an estimate for ω_o. To derive an equation for estimating ω_o, we note that i) ω_o is the common frequency of three-phase signals, therefore, information of all three sub-filters must be incorporated into the update law for frequency estimation, and ii) the regressor signal $x(t)$ and the error signal $e(t)$ incorporate into the θ update law in (5-2). The term θ is for scaling.

Therefore, the update law for frequency estimation is proposed to be the following,

$$\dot{\theta} = -\gamma\,\theta \sum_{\alpha=a,b,c} x_\alpha\, e_\alpha(t) \tag{5.2}$$

For a three-phase sinusoidal signal $u(t)$ given by

$$u(t) = \begin{pmatrix} u_a(t) \\ u_b(t) \\ u_c(t) \end{pmatrix} = \begin{pmatrix} k_a\, sin(\omega_o t + \delta_a) \\ k_b\, sin(\omega_o t + \delta_b) \\ k_c\, sin(\omega_o t + \delta_c) \end{pmatrix} \tag{5.3}$$

the dynamical system given by (5-1) and (5-2) has a unique periodic orbit located at

$$P(t) = \begin{pmatrix} P_a(t) \\ P_b(t) \\ P_c(t) \\ \bar{\theta} \end{pmatrix} \tag{5.4}$$

where, $P_\alpha(t)$ is given by,

$$P_\alpha(t) = \begin{pmatrix} \bar{x}_\alpha \\ \dot{\bar{x}}_\alpha \end{pmatrix} = \begin{pmatrix} -\dfrac{A_\alpha}{\omega_o} cos(\omega_o t + \delta_\alpha) \\ A_\alpha\, sin(\omega_o t + \delta_\alpha) \end{pmatrix} \tag{5.5}$$

and $\bar{\theta} = \omega_o$. For the ANFα in the steady state, the defined outputs $\dot{x}_\alpha$ and θx_α are

$$\dot{\bar{x}}_\alpha = A_\alpha\, sin(\omega_o t + \delta_\alpha)$$

$$-\bar{\theta}\bar{x}_\alpha = A_\alpha\, cos(\omega_o t + \delta_\alpha) \tag{5.6}$$

which are equal to $u_\alpha(t)$ and $S_{90^\circ} u_\alpha(t)$. This means that the αth component of the input signal and its 90◦ phase shift are made available by ANFα at its outputs, $\dot{x}_\alpha$ and $-\theta x_\alpha$.

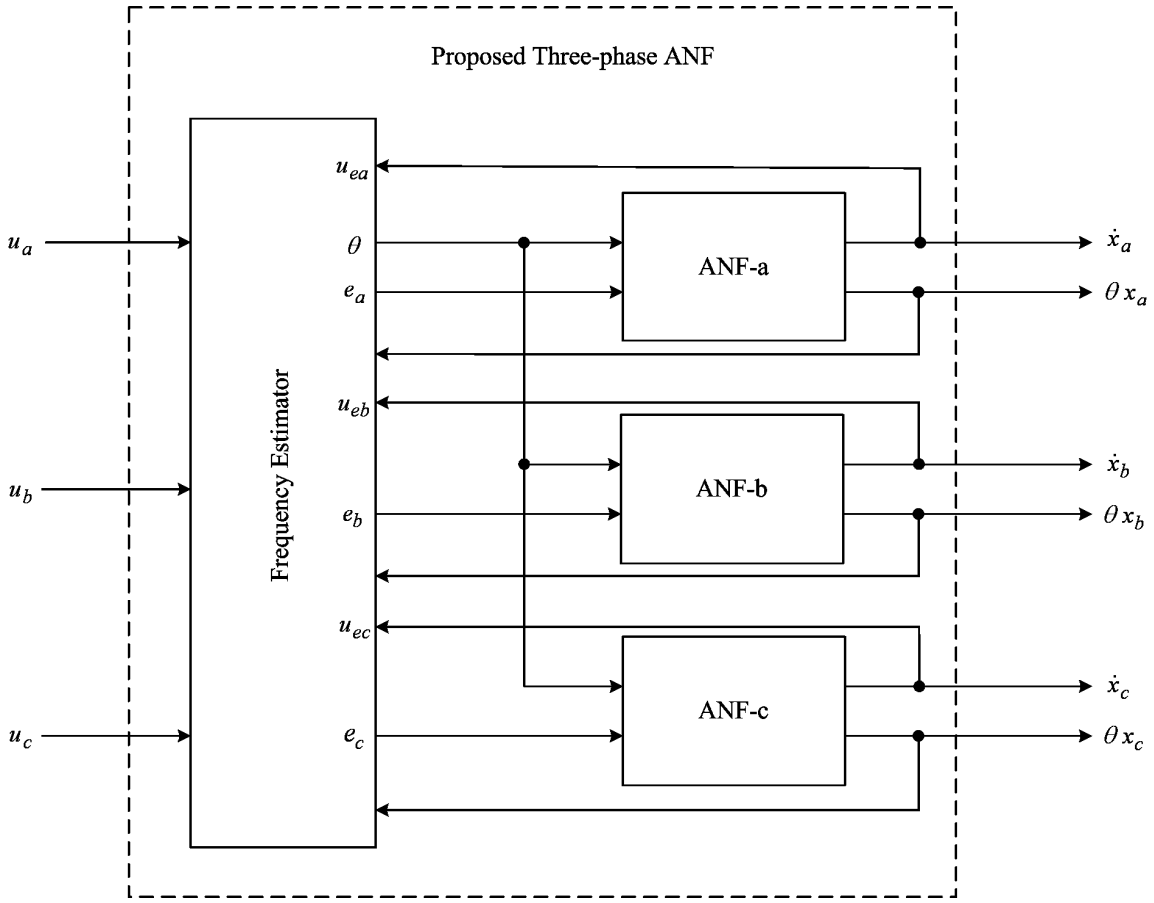

Figure 5.1 Proposed structure for three-phase systems.

A structural block diagram of the first stage of the proposed algorithm is shown in Fig. 5.1. Detailed implementation block diagram of the frequency estimator and the αth sub-filter (ANFα) are shown in Figs. 5.2 and 5.3. The basic structure of the proposed system has two independent design parameters, γ and ζ_α. Similar to the ANF in chapter 3, the same logic for setting the proposed ANF parameters is valid here. The initial condition for the integrator in the frequency estimator block is set to the nominal power system frequency and the initial conditions for all other integrators are set to zero.

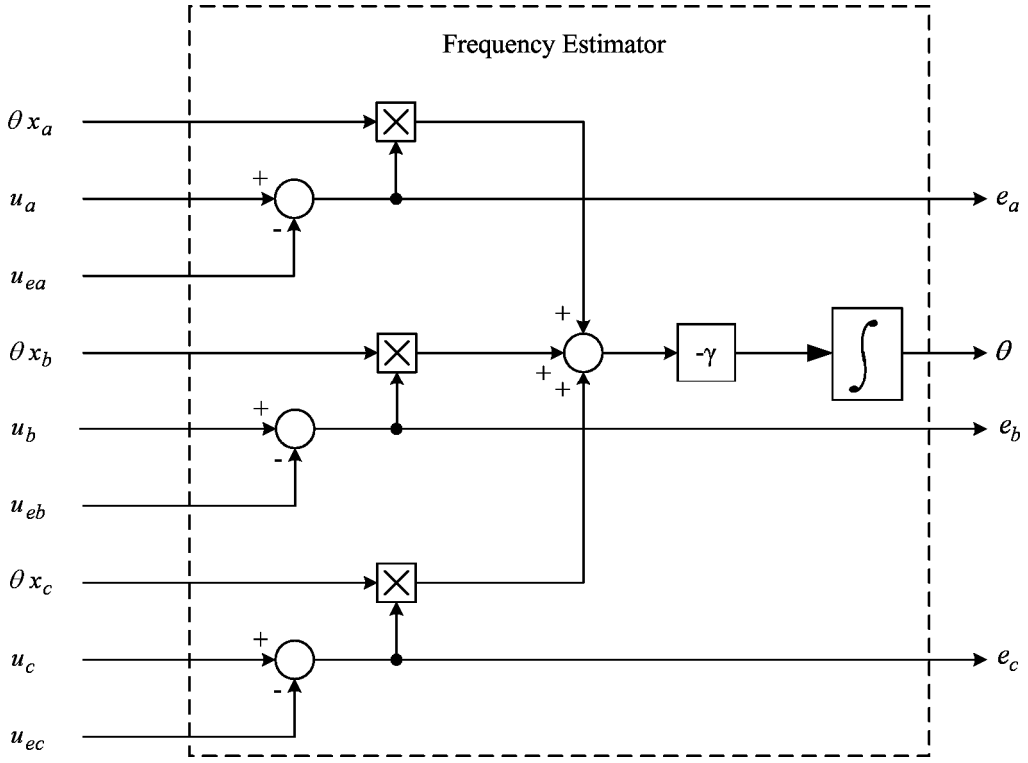

Figure 5.2 The structure of the frequency estimator unit.

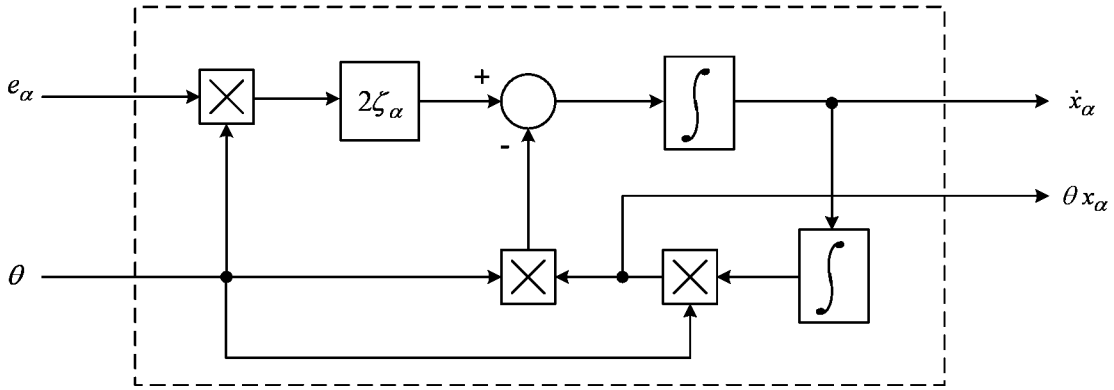

Figure 5.3 The structure of the α^{th} sub-filter.

This structure receives the three-phase input signals and outputs the fundamental component and its useful information associated to each phase. Contrary to the single-phase based method

proposed in chapter 4, which uses 3 frequency estimation laws for three-phase system, this configuration just needs one common frequency estimation law. This makes the overall system much simpler in terms of implementation. In the next section, the three-phase based method is extended to estimate more than one frequency. This has several applications in a variety of power electronics equipments, where the removal of a selected number of harmonics, especially low order harmonics, is desirable.

5.1.2 Three-Phase Multiple Frequency Estimator

To extract a selective order of harmonics, the structure of the sub-filter in Fig. 5.3 is modified and replaced by the multi-block ANF, as shown in Fig. 5.4, , which has a similar structure to the sub-filters of Fig. 3.3. In this configuration the inputs $e_\alpha\,(\alpha = a,b,c)$ and θ are coming from the frequency estimator and the outputs $u_{e\alpha}\,(\alpha = a,b,c)$ and $\theta x_\alpha\,(\alpha = a,b,c)$ are fed back to the frequency estimator of Fig. 5.1.

The operating principles of these sub-filters have already been explained in subsection 3.1.3.2. When the three-phase input signal contains harmonics, the first sub-filter outputs the fundamental component of the input signal and *ith* sub-filter outputs the *ith* harmonic components of the input signal for each phase. Note, $A_\alpha = \left(\theta^2 {x_\alpha}^2 + {\dot{x}_\alpha}^2\right)^{1/2}$ is the amplitude of the fundamental component of the α^{th} phase of the input signal. In other words, the algorithm can further be equipped to estimate the amplitudes of the each phase using arithmetic units that compute the right-hand side of A_α. Since $\overline{\theta x}_\alpha$ is available, the right-hand side of A_α can be calculated simply by performing two multiplications, a sum and a square-root computation.

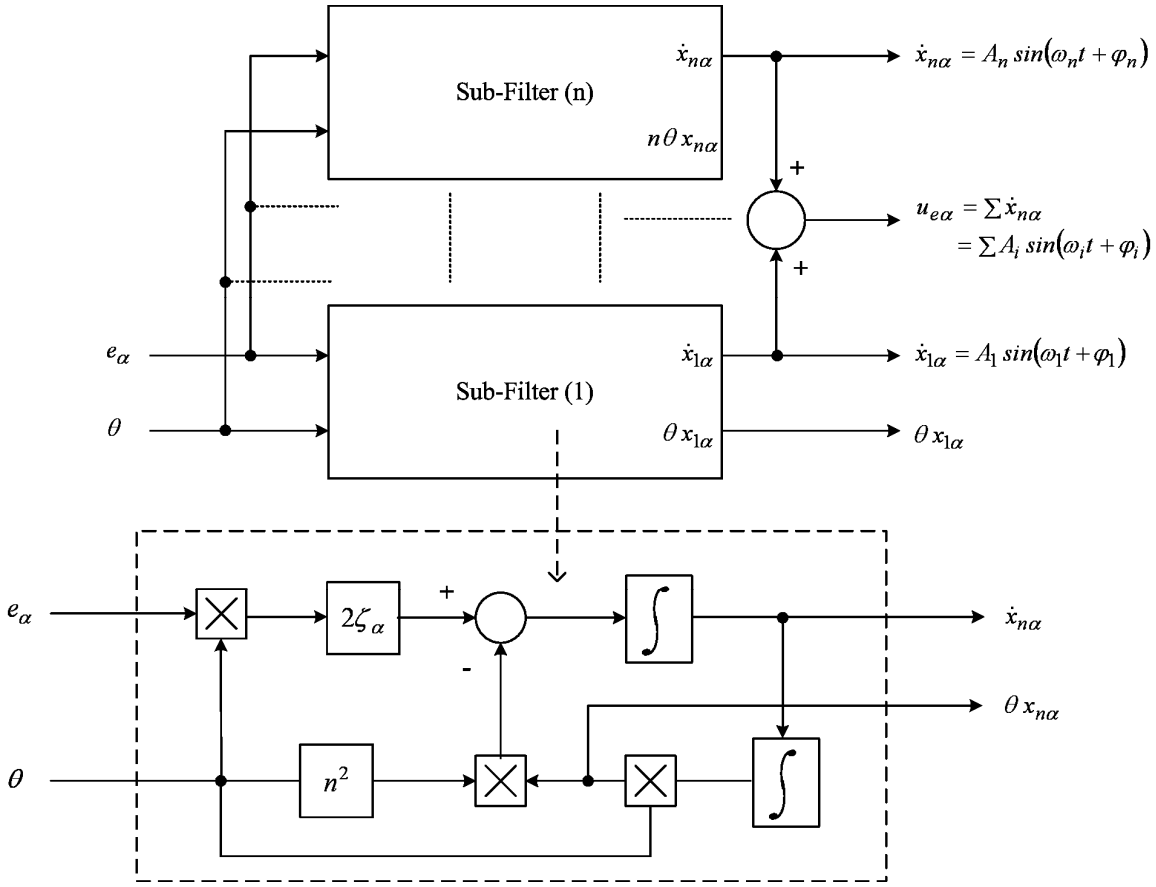

Figure 5.4 The structure of the α^{th} sub-filter; modified structure for faster time response.

Similarly, $A_i = \left(i^2\theta^2 x_i^2 + \dot{x}_i^2\right)^{1/2}$ is the amplitude of the i^{th} harmonic component of the input signal. Thus, the algorithm estimate the amplitudes of the harmonics using arithmetic units that compute the right-hand side of A_i. Note, since $i\theta x_i$ is available, the right-hand side of A_i can simply be calculated by two multiplications, a sum and a square-root computation.

This configuration guarantees a fast (one cycle) and precise extraction of the individual harmonics which can be employed for further harmonic analysis or elimination purposes.

5.1.3 Stability Analysis

A detailed stability analysis is provided in Appendix A. However, a quick sense on the stability analysis of the proposed algorithm can be given as follows. Using the first equation of (5.1), the θ update law can be rewritten as

$$\dot{\theta} = -\gamma \sum_{\alpha=a,b,c} \frac{1}{2\zeta_\alpha} x_\alpha \left(\ddot{x}_\alpha + \theta^2 x_\alpha \right) \tag{5.7}$$

close to the periodic orbit of $P(t)$ where $\bar{\theta} = \omega_o$ and $\ddot{\bar{x}}_\alpha = -\omega_o^2 \bar{x}_\alpha$ we have

$$\dot{\theta} \approx -\gamma \left(\theta^2 - \omega_o^2 \right) \sum_{\alpha=a,b,c} \frac{1}{2\zeta_\alpha} \bar{x}_\alpha^2 \tag{5.8}$$

The previous derivation shows that close to the periodic orbit of $P(t)$ the adaptation process is slow and the search in the θ space will go in the correct direction (i.e. $\theta > \omega_o \Rightarrow \dot{\theta} < 0$ and $\theta < \omega_o \Rightarrow \dot{\theta} > 0$).

5.2 Performance Evaluation

This section evaluates the performance of the proposed three-phase frequency estimator. Initiatory performance and tracking features of the proposed system are studied. The parameters of the ANF are set to γ=18000 and ζ_α=0.707. For sub-section 5.2.1, the input signal is an artificially constructed signal which is found by summing different known characteristic harmonics to the fundamental frequency via a programmable voltage source. Thus, the proposed method was tested under different signal conditions. In subsection 5.2.2, the performance of the proposed three-phase method in extracting signal's information and individual harmonic is evaluated on a grid connected nonlinear load.

5.2.1 Tracking Capability

The adaptability of the proposed unit with respect to the frequency and amplitude variations, a common requirement in actual distribution systems or grid-connected converters, is experimentally verified in this section. In the first test, the input signal (in Fig. 5.5) consists of a 1 p.u. fundamental component at 60 Hz, a 0.2 p.u. fifth harmonic at 300 Hz (a low order harmonic), a 0.3 p.u. seventh harmonic at 420 Hz (a low order harmonic), and a 0.3 p.u. fiftieth harmonic at 3 kHz (a harmonic at the switching frequency).

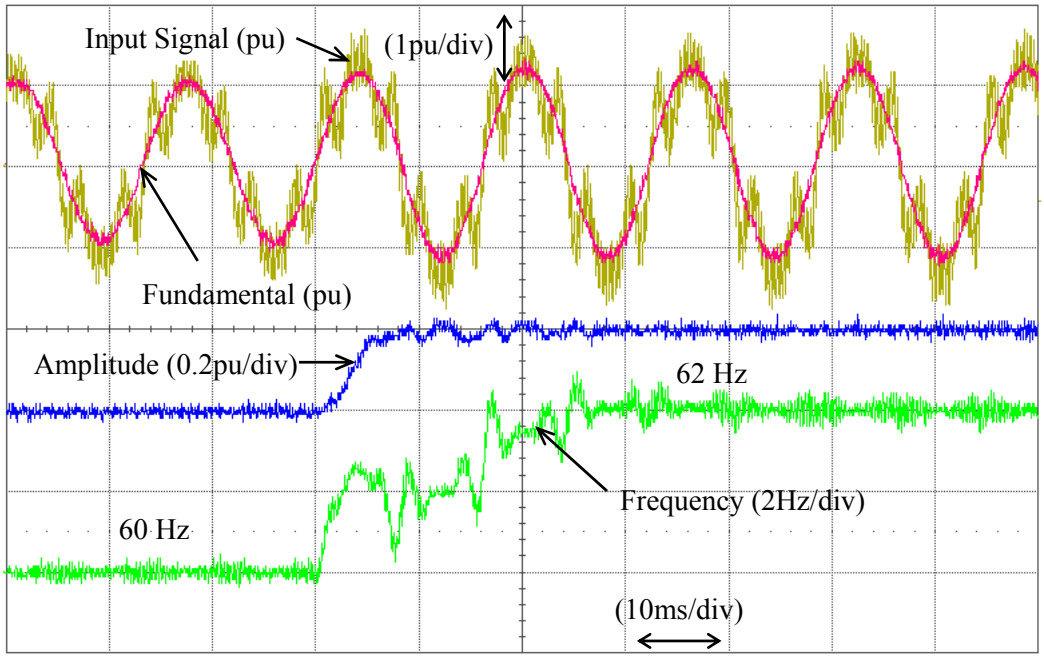

Figure 5.5 Experimental results; Response of the proposed system to the step changes in the amplitude and frequency: input signal and its extracted fundamental, amplitude and frequency.

A step change of 0.2pu in the fundamental component and 2Hz in the fundamental frequency, as shown in Fig. 5.5, does not affect the capability of the proposed method in extracting the

amplitude and the frequency of the fundamental component. The accurate tracking and harmonic extraction features of the proposed method are investigated by another test shown in Fig. 5.6. The input signal is composed of a fundamental component (1 p.u.), a fifth harmonic component (0.2 p.u.), a seventh harmonic (0.6 p.u.) component, and a fiftieth harmonic at 3 kHz (0.3 p.u.). Simultaneous step-changes in the fundamental component (from 1 p.u. to 0.8 p.u.), the fifth harmonic component (from 0.2 p.u. to 0.5 p.u.), and the seventh harmonic component (from 0.6 p.u. to 0.3 p.u.) are applied and the system response is recorded. Fig. 5.6 shows the input signal, the phase angle of the fundamental, the 5th harmonic, and the 7th harmonic components.

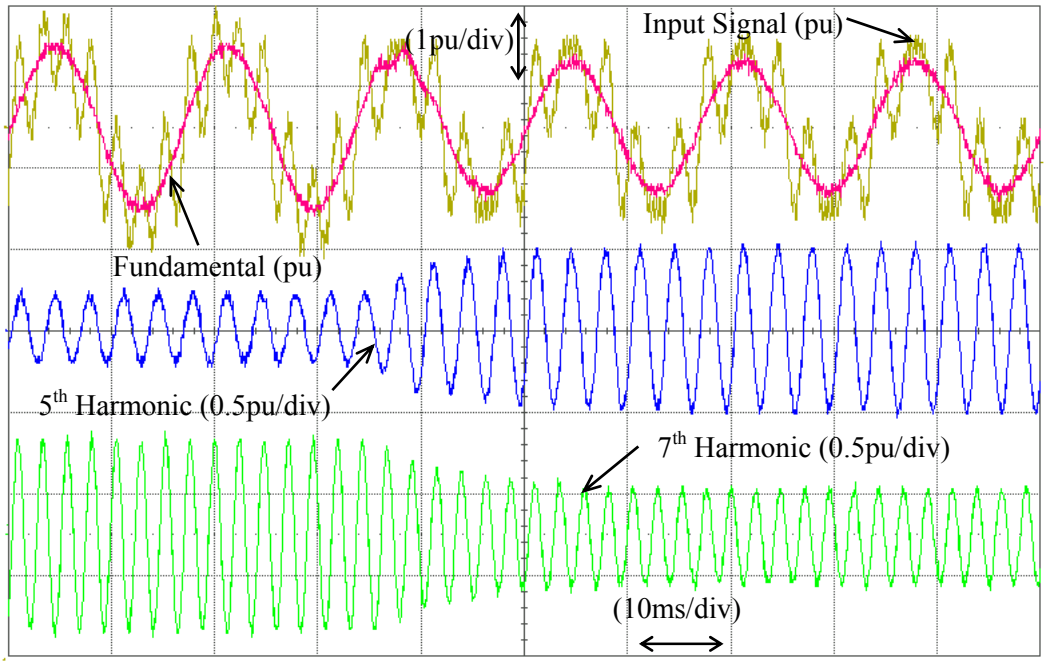

Figure 5.6 Experimental results; Response of the proposed method to the step changes in the amplitude of the fundamental and individual harmonics: input signal, extracted fundamental, 5th harmonic and 7th harmonic components.

Fig. 5.6 shows that the proposed three-phase ANF successfully extracts the fundamental, the fifth and the seventh harmonic components. This method can be used in some applications, such as active power filters (APFs), where the removal of a selected number of harmonics, especially low order harmonics, is desirable.

5.2.2 Harmonics Decomposition of a Grid-Connected Nonlinear Load

The performance of the proposed three-phase structure on a simple distribution system is evaluated in Figs. 5.7 to 5.11. A simple distribution network loaded with a static dc converter is shown in Fig. 5.7. The time response of the proposed method is evaluated by adding a step change to the static dc converter's load.

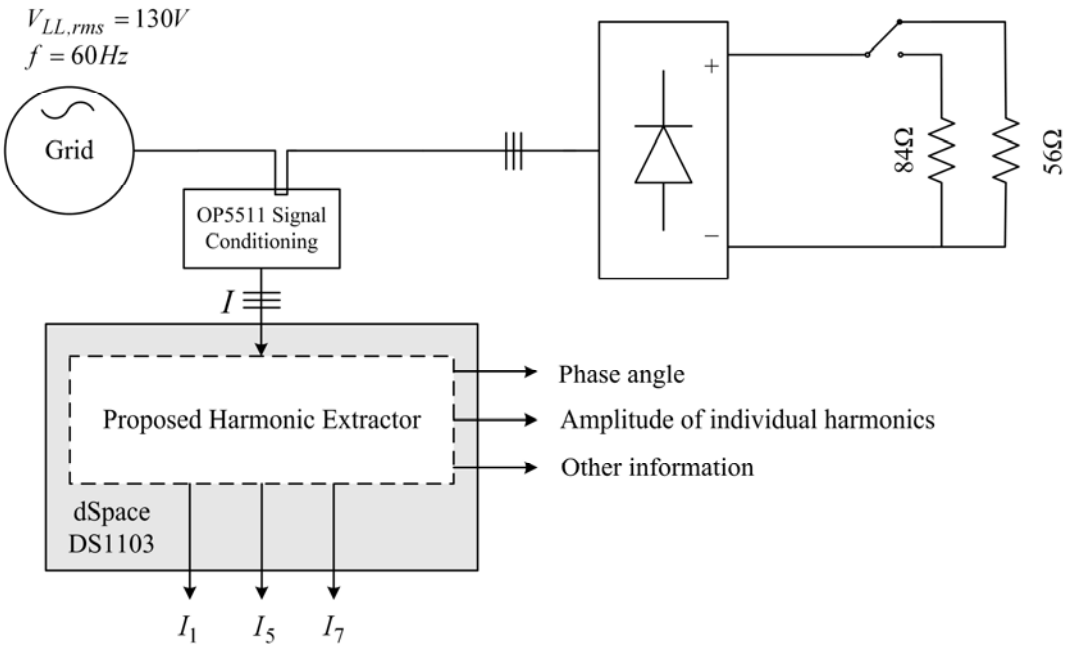

Figure 5.7 Simple distribution system configuration.

Figs. 5.8 to 5.11 show the phase A of the three-phase currents. The current is measured and fed to the proposed processing unit implemented in the dSPACE 1103 board. The extracted fundamental component and its phase angle, total current harmonics, and the 5^{th} harmonic component and its amplitude are shown in Figs. 5.8 to 5.11.

Results show that during this step change in the signal, the proposed scheme successfully tracks step-changes within one cycle of the fundamental component and extracts the desired information. The experimental results are in agreement with the theoretical discussion.

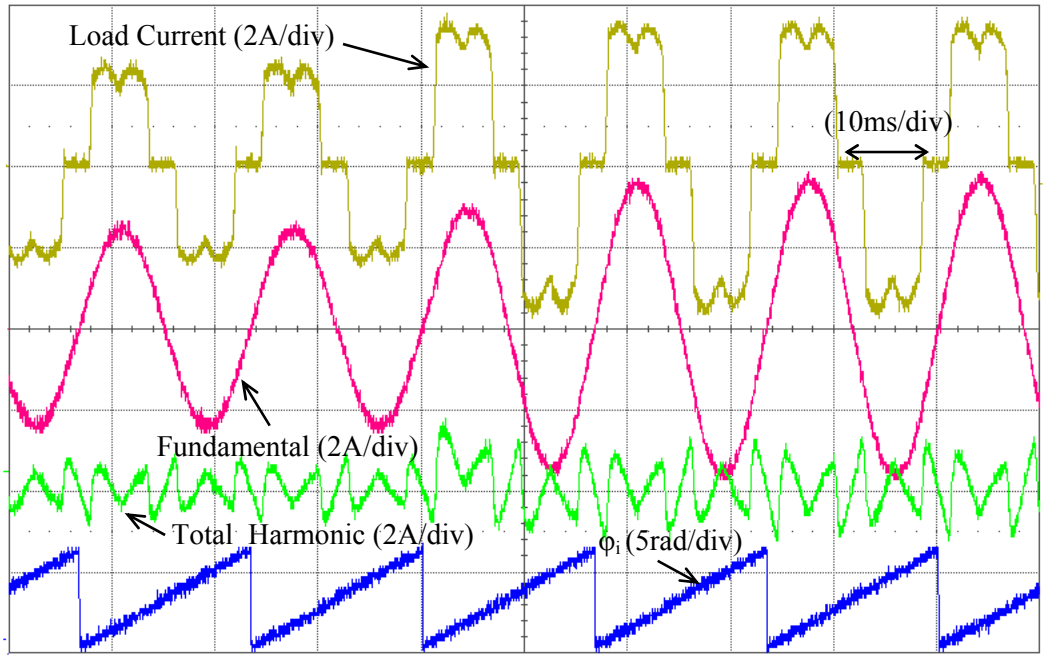

Figure 5.8 Response of the proposed system to a step change in the load current: load current, extracted fundamental component, its phase angle, total harmonics.

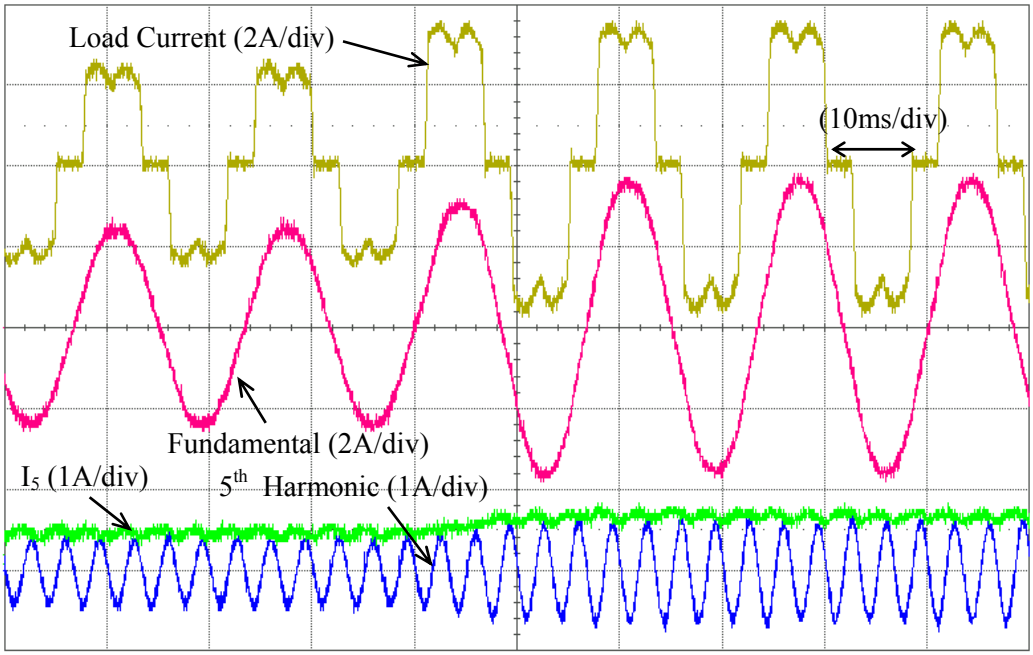

Figure 5.9 Response of the proposed system to a step change in the load current: load current, extracted fundamental component, 5^{th} harmonic component and its amplitude.

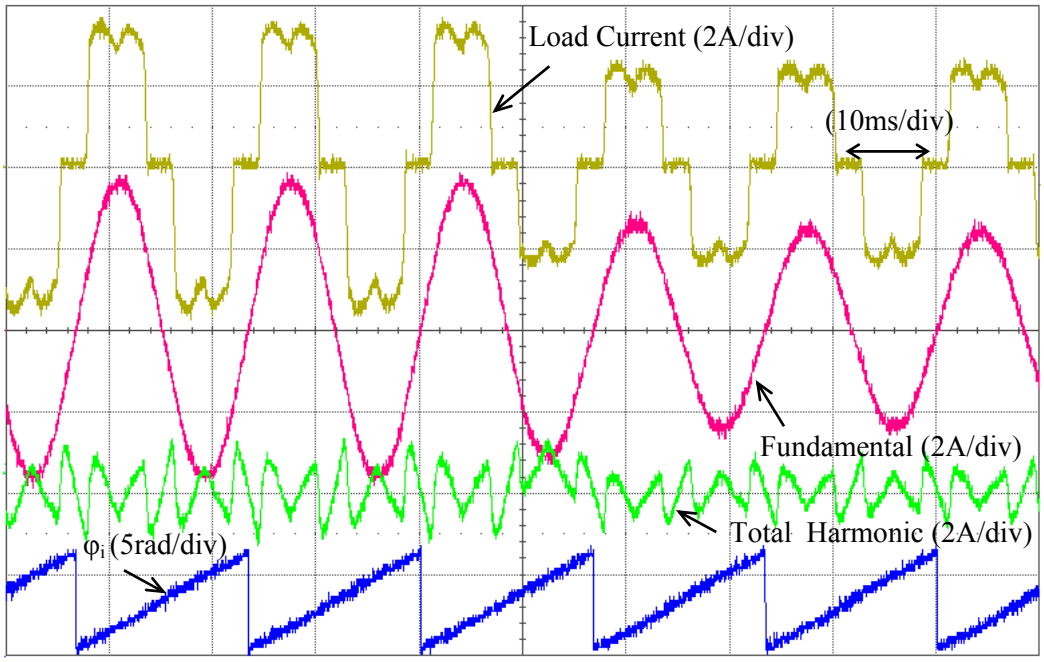

Figure 5.10 Response of the proposed system to a step change in the load current: load current, extracted fundamental component, its phase angle, total harmonics.

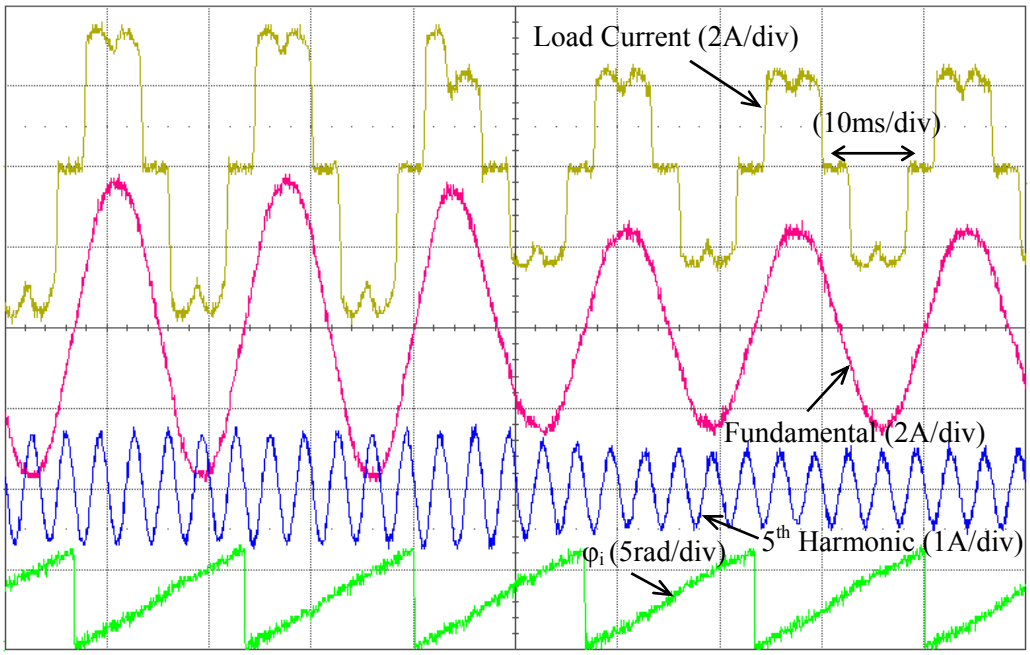

Figure 5.11 Response of the proposed system to a step change in the load current: load current, extracted fundamental component, its phase angle, and 5th harmonic component.

5.3 Conclusion

This chapter introduced a three-phase synchronization technique for extraction of frequency, phase angle and amplitude of the grid signal, which has several applications in power systems such as monitoring, synchronization, power quality and protection. The three-phase ANF based approach is extended for the extraction of individual harmonics of a load current and was experimentally evaluated for various load conditions. This chapter also verified the capability of the three-phase ANF in simultaneous extraction of individual harmonics and all useful information of a measured signal such as frequency, amplitude, and phase angle. Since the order of the three-phase ANF is lower than the one introduced in chapter 4, the three-phase ANF has a

simpler structure. Its simple structure leads to easy implementations in software/hardware environments. Mathematical derivations are presented to describe the principles of operation and experimental results are obtained to confirm the validity of the analytical work.

Chapter 6
A New Three-Phase Based Power Signal Processor

This chapter proposes a new three-phase based power signal processor which has the three-phase synchronization scheme proposed in Chapter 5 as the main cell. The *"three-phase power signal processor"* is developed to extract key power system information that are required especially in converter-interfaced DG systems. Similar to the single-phase based method in chapter4, this new processor with some modification can perfectly perform almost every single signal processing function that might be required for control and safety purposes in DG systems. This chapter addresses one of these important signal processing functions.

6.1 Symmetrical Component Decomposition

This section introduces a three-phase based approach for extraction of symmetrical components of the grid signal. As mentioned earlier, sequence components decomposition is of great importance in many applications in power systems such as power quality and protection. The proposed method is based on the three-phase ANF introduced in chapter 5, which provides fast and accurate estimation of the signal's information in the presence of frequency and amplitude variations.

Consider the three-phase set of signals

$$u(t)=\begin{pmatrix} u_a(t) \\ u_b(t) \\ u_c(t) \end{pmatrix}=\begin{pmatrix} k_a\, sin(\omega_o t+\delta_a) \\ k_b\, sin(\omega_o t+\delta_b) \\ k_c\, sin(\omega_o t+\delta_c) \end{pmatrix} \tag{6.1}$$

associated with a three-phase set of measurements. $u(t)$ can be decomposed to $u(t)=u_p(t)+u_n(t)+u_z(t)$, where, $u_p(t)$, $u_n(t)$ and, $u_z(t)$ are positive-, negative- and zero-sequence components, respectively and are related to the input signal $u(t)$ by the equations

$$\begin{aligned} u_p(t) &= T_2 u(t)+T_1 S_{90^\circ} u(t) \\ u_n(t) &= T_2 u(t)-T_1 S_{90^\circ} u(t) \\ u_z(t) &= (I-2T_2)u(t) \end{aligned} \tag{6.2}$$

where S_{90° stands for a 90° phase-shift operator in the time-domain. T_1 and T_2 are 3 × 3 matrices given in (4.3) and (4.4) and I is a 3 × 3 identity matrix. Fig. 6.1 shows the structure of the linear transformation to estimate symmetrical components.

The objective is to find an algorithm that receives the three-phase input signal $u(t)$ and estimates the three phase input signal's fundamentals and their 90° phase shifted versions, then linear transformation of (6.2) can be used to extract the symmetrical components. The on-line 90° phase-shift is a troublesome task. The characteristics of the input signal may be time varying, and a desirable algorithm must faithfully track such variations. Also, a desirable algorithm must be practical and implement-able using available software/hardware platforms. Structural and performance robustness are further desired features of the algorithm. The three phase ANF introduced in the previous section receives the three phase signals $u_a(t)$, $u_b(t)$ and, $u_c(t)$. Each sub-filter provides the fundamental component of each phase, its 90° phase-shift and its frequency. Then, all these information can be used to calculate the symmetrical components.

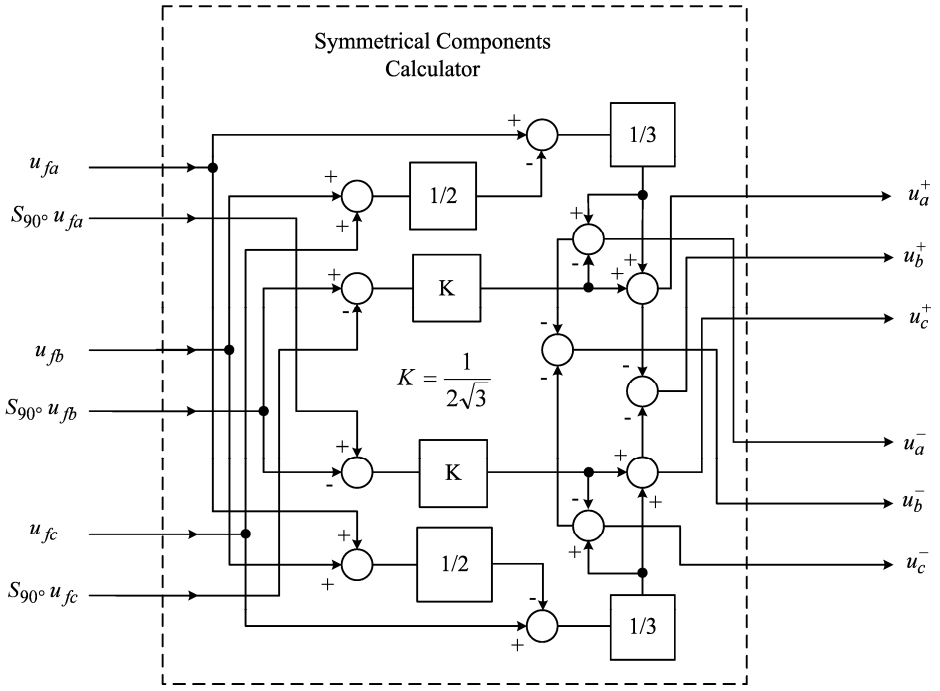

Figure 6.1 Linear transformation for symmetrical components calculator.

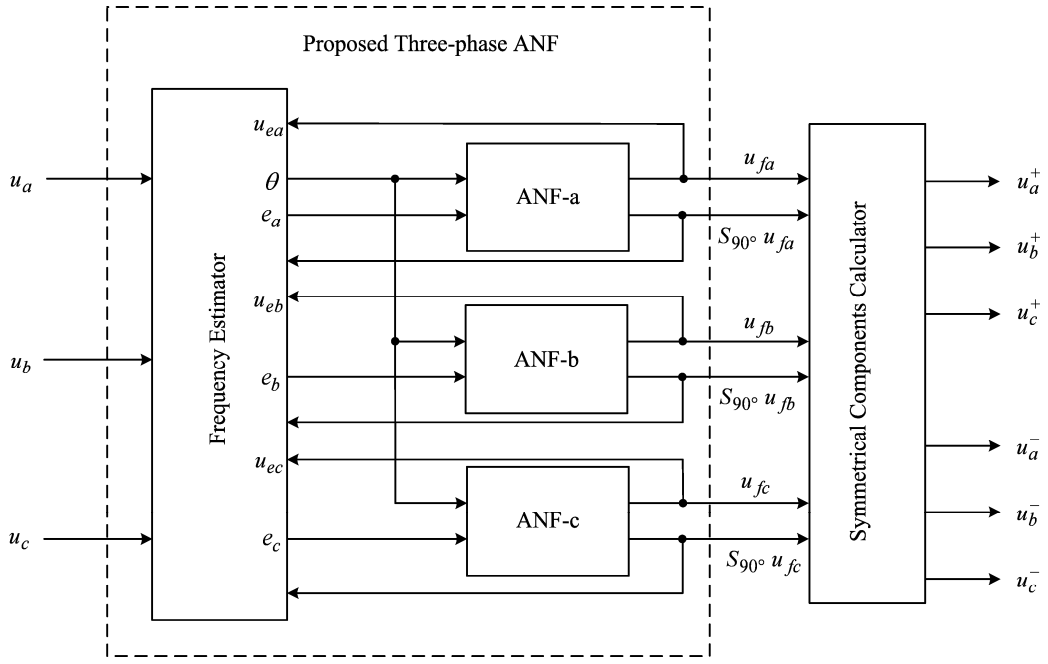

Figure 6.2 Proposed structure for three-phase systems [74].

A structural block diagram of the first stage of the proposed algorithm is shown in Fig. 6.2 in which the detailed implementation block diagram of the frequency estimator and the αth sub-filter are shown in Figs. 5.2 and 5.3 in the previous chapter. The second stage of the proposed algorithm is a linear transformation that is shown structurally in Fig. 6.1.

6.1.1 Comparison

The fast and accurate detection of the positive-sequence component of the utility voltage is a prerequisite for grid connected converters and is required to synchronize grid connected converters with the utility systems during the grid faults. This section is devoted to give a brief comparison between the proposed three-phase synchronization technique and the SRF-PLL when the input signal is unbalance.

Among the various solutions to extract the phase angle, the SRF-PLL (chapter 2) is used in almost all PLL techniques for three-phase systems. This scheme is extremely simple and provides a highly fast and accurate synchronization signal under ideal conditions where there is no voltage distortion/unbalance. The simplicity of this structure has encouraged some authors to propose new schemes based on this topology. Improved versions of SRF-PLL are presented to overcome distortion/unbalance problems. The PSF-PLL, SSI-PLL, DSOGI-PLL, and DSRF-PLL are among the newly developed solutions to improve SRF-PLL performance. These modified SRF-PLL techniques reported to have a better performance compared under unbalance situations. However, when the signal is distorted by harmonics, the bandwidth of these methods should be reduced, thus the time response is increased.

The basic configuration of SRF-PLL is shown in Fig. 6.3. In this section, the proposed method is compared with the SRF-PLL under unbalanced conditions. The parameters are adjusted to

achieve a settling time of 20ms for both methods. Note, the parameters of SRF-PLL are set based on the equations given in [11].

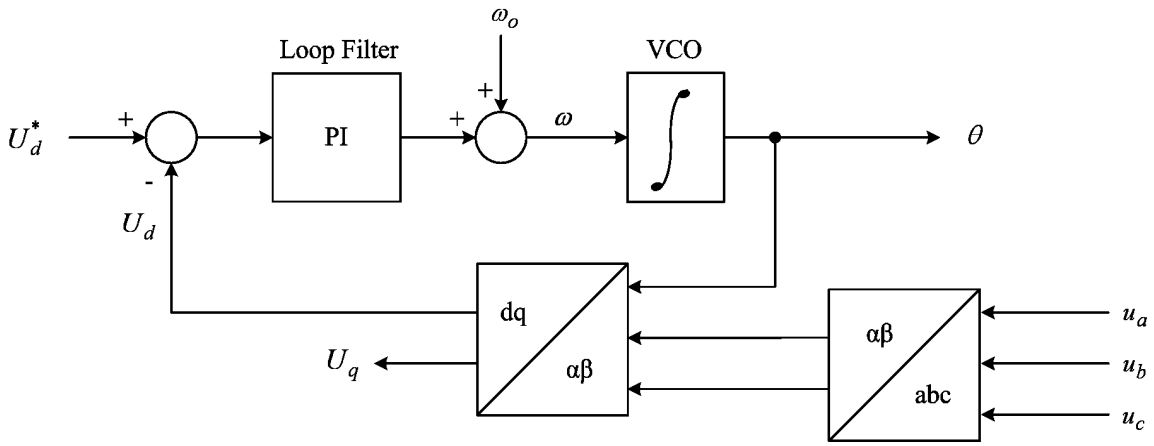

Figure 6.3 The SRF-PLL structure.

The three-phase programmable source provides a 3 Hz step change in the frequency of the three-phase signal, and 60ms later, adds a 0.1 p.u. negative sequence to this signal and its frequency is changed to 60 Hz, shown in Fig. 6.4. The tracking capability of the proposed and SRF-PLL methods are shown in Fig. 6.5. As it is expected, both methods provide a highly fast and accurate response during the normal conditions. However, as expected, the SRF-PLL method fails to deal with unbalance situation. Fig. 6.5 shows that the proposed technique delivers a highly fast and accurate frequency and thus synchronization signal under both balanced and unbalanced conditions.

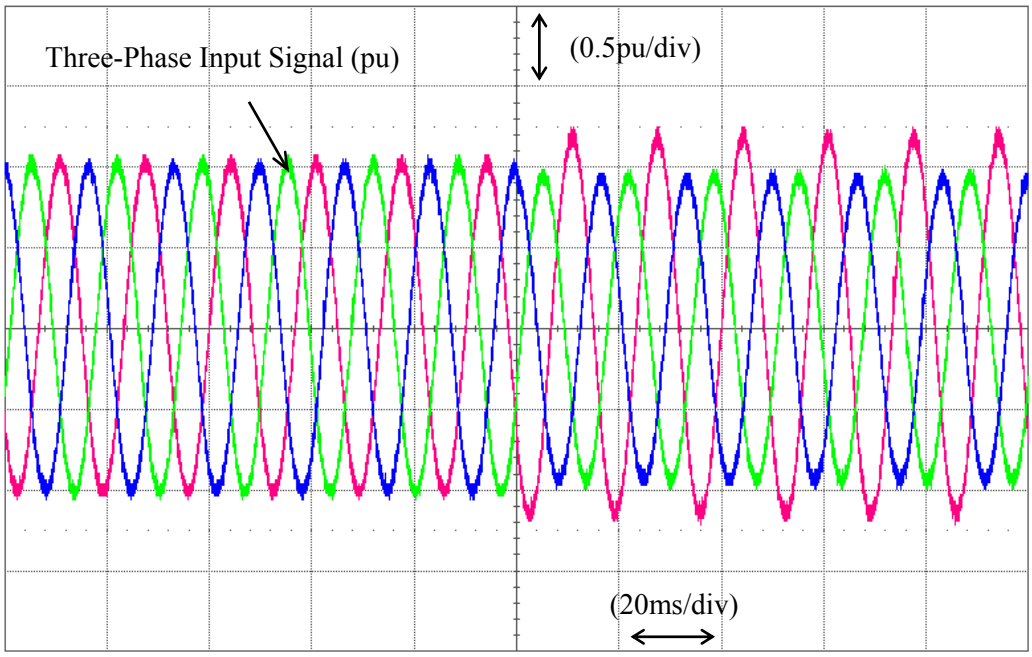

Figure 6.4 Experimental results; distorted three-phase input signal.

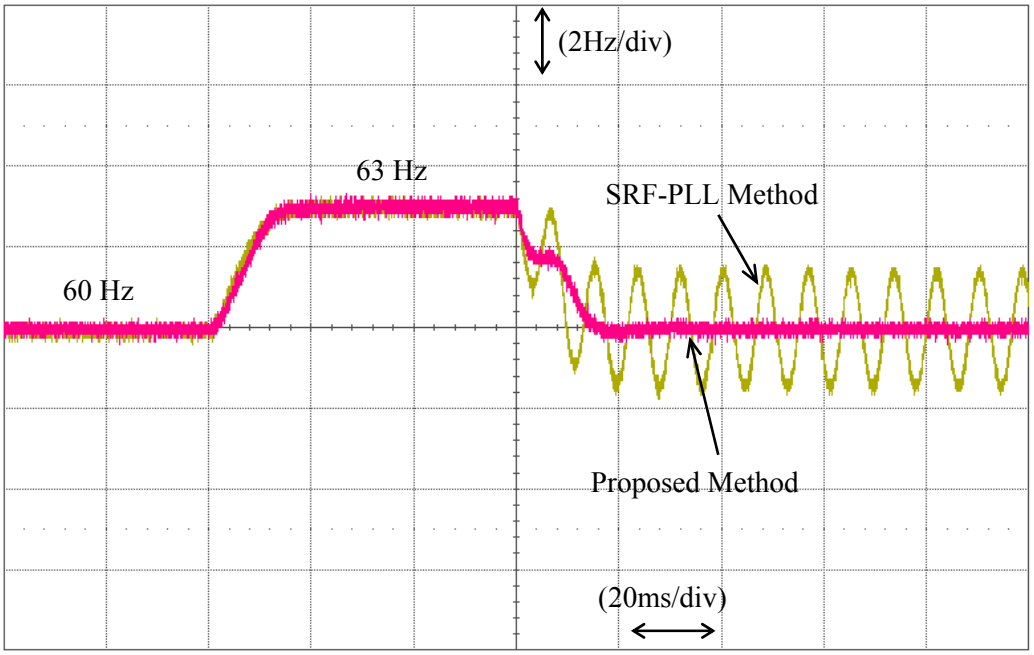

Figure 6.5 Experimental results; extracted frequency of the distorted input signal of Fig. 6.4 by SRF-PLL and the proposed method.

The prominent features of the proposed algorithm when compared with PLL-based algorithms are: i) avoiding the use of a VCO unit which leads to a simpler implementation, ii) avoiding the main shortcoming of the conventional SRF-PLL which is the generation of the double-frequency ripples in the presence of negative-sequence component, iii) measuring capability of sequence components under unbalanced system situations (will be shown in the next section), iv) frequency-adaptivity, structural robustness with respect to distortions as well as amplitude/frequency variations (will be shown in the next section), controllable behavior in terms of transient speed and steady-state accuracy are further features of the proposed system.

6.1.2 Performance Evaluation

This section evaluates the performance of the proposed three-phase based symmetrical components extractor. The parameters of the three-phase ANF are set to γ=18000 and ζ_α=0.707. The initial condition for the integrator that outputs the frequency, ω, is set to $2\pi 60$ rad/sec (the nominal power system frequency). The initial conditions for all other integrators are set to zero.

6.1.2.1 Unbalanced

The adaptability of the proposed system under unbalanced condition, which is a common test in distribution systems or grid connected converters, is demonstrated here. In this test, a three-phase programmable voltage source is used to produce a three phase distorted signal. Under normal conditions, the input to the system is a set of balanced three-phase sinusoidal voltages of 1.0 p.u. amplitude. Since the system is balanced, no negative- or zero-sequence components exist. Then, a step change (-0.2 p.u.) in the amplitudes (positive-sequence) of all three-phase voltages is applied and simultaneously 0.1 p.u. negative-sequence and 0.05 p.u. zero-sequence voltages are added to the input signal, Fig. 6.6.

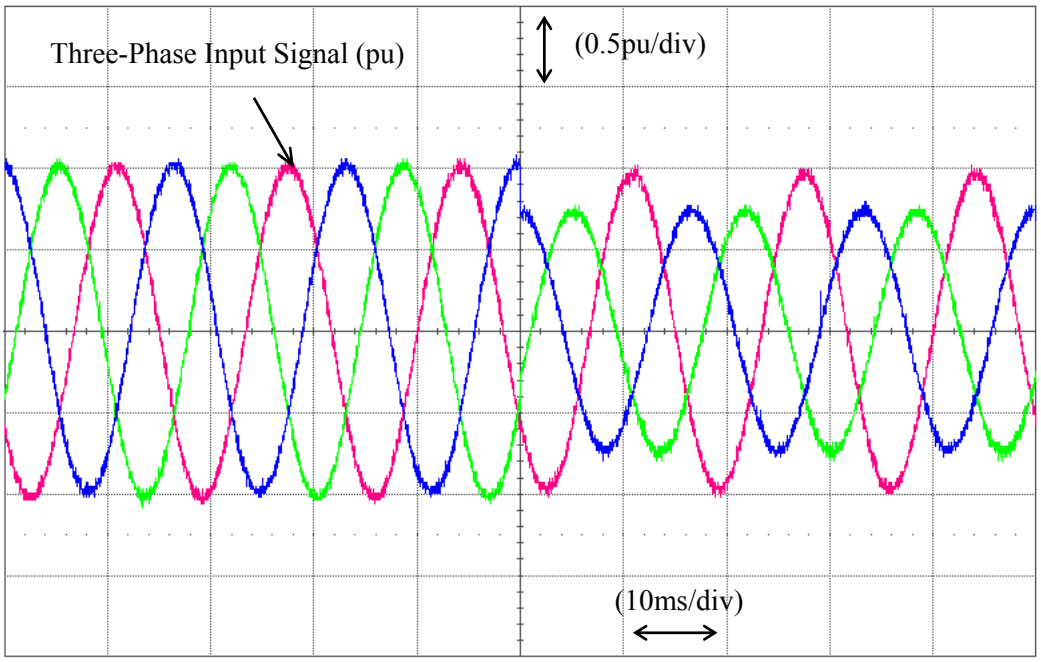

Figure 6.6 Experimental results; three phase distorted signal.

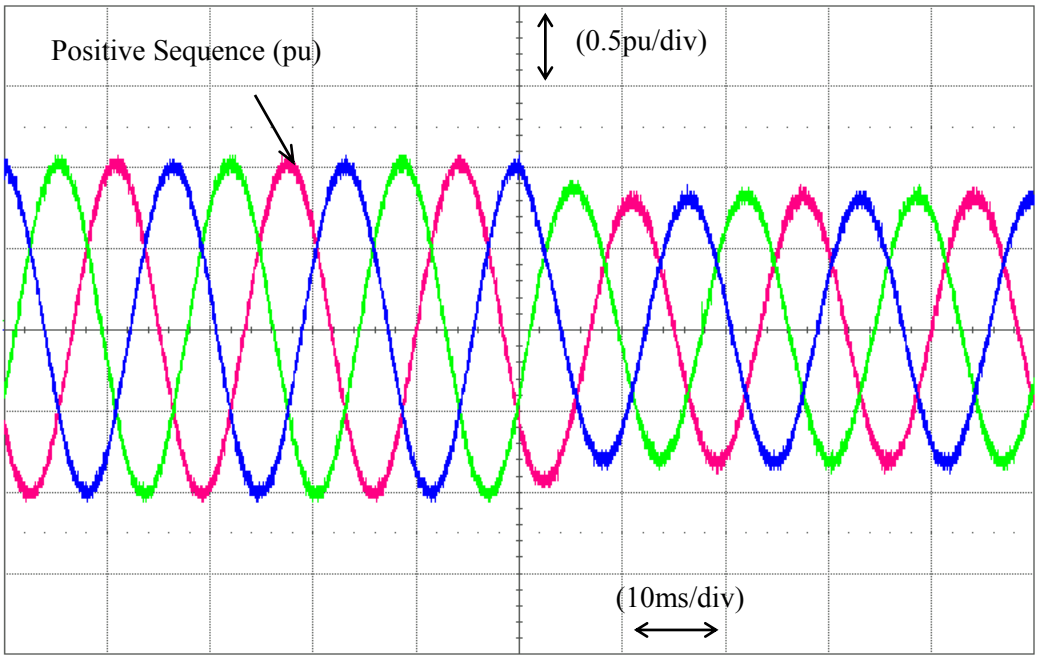

Figure 6.7 The proposed scheme extracts positive sequence components.

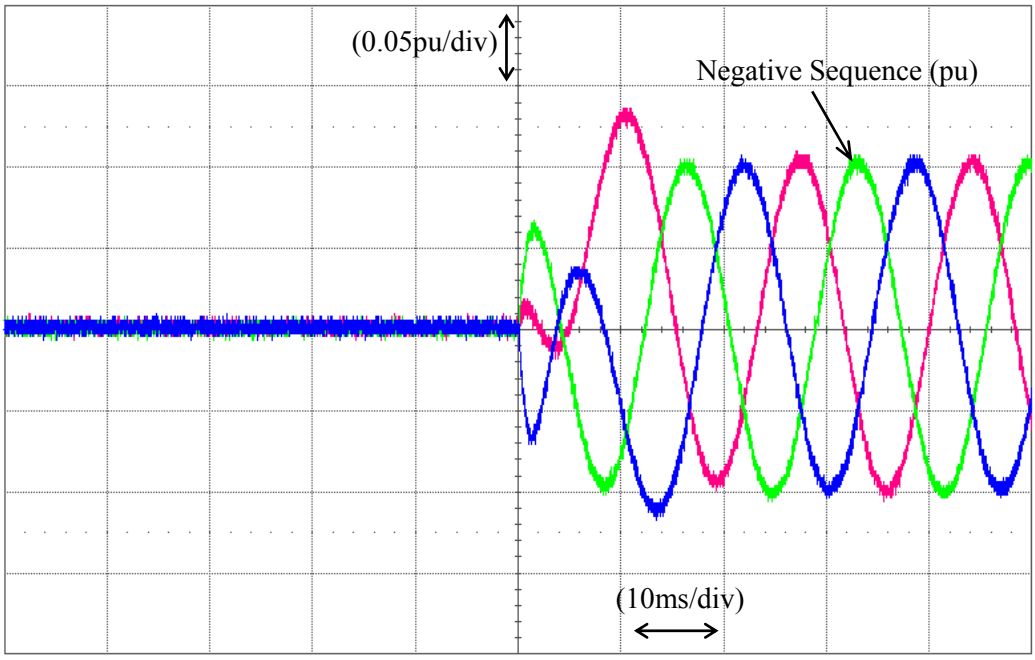

Figure 6.8 The proposed scheme extracts negative sequence components.

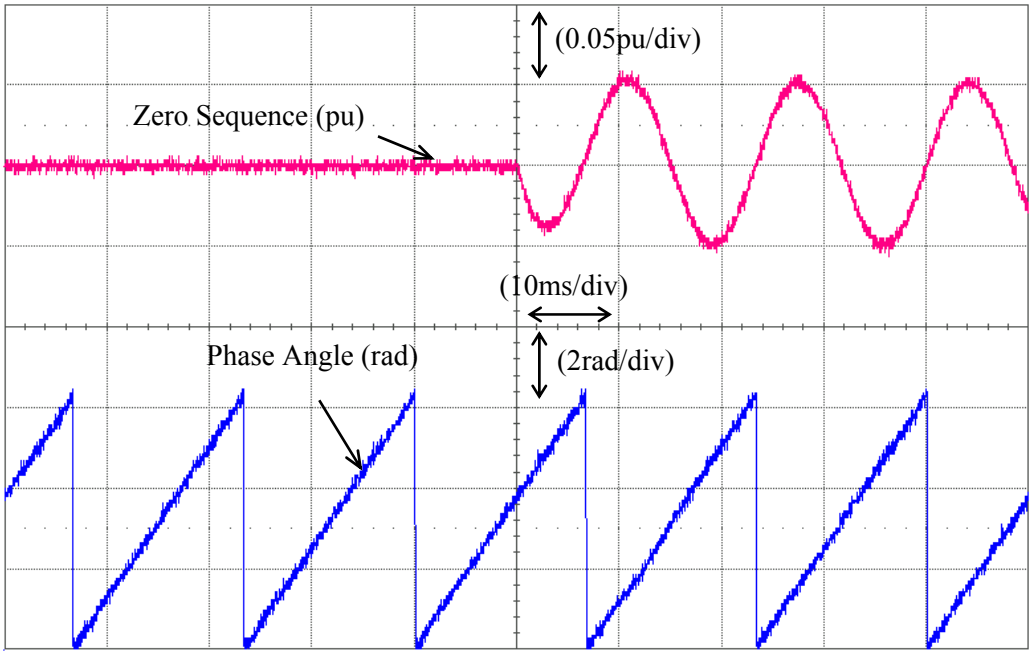

Figure 6.9 The proposed scheme extracts zero sequence component and phase angle of the positive sequence.

Figs. 6.7 to 6.9 show that the proposed structure tracks all variations, and extracts positive-, negative- and zero-sequence components. It also outputs the phase angle of the positive sequence component faithfully. Note that the extracted phase-angle of the positive-sequence component is used for synchronization.

6.1.2.2 Unbalanced and Harmonics

In this section, to reject the harmonics, the parameters of the proposed ANF are set in such a way that the settling time of the proposed technique is 50ms. The response of the proposed method and fast SRF-PLL are compared in Fig. 6.10, where 0.1 p.u. 5^{th} and 7^{th} harmonics are added to the balanced input signal. Although the proposed method is set to have a longer time response, but the extracted frequency is free of harmonics.

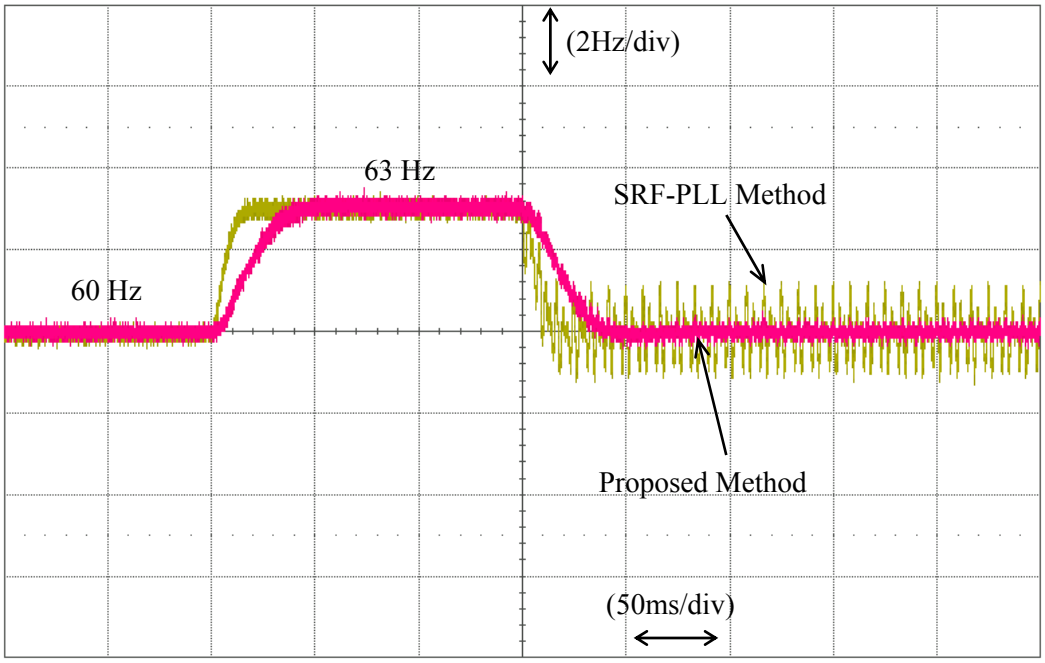

Figure 6.10 Frequency tracking capability of SRF-PLL and the proposed method when the input signal is distorted by harmonics.

Although this method with the time response (50ms) might not be used in the control path of the applications where a very fast synchronization technique is required, the time response (50ms) of the proposed method is well within the range of fast islanding detection [82]. Therefore, in continue the proposed method with 50ms time response is used to extract the instantaneous sequence components and their amplitudes, which can be used for islanding detection in DG systems. In addition, the adaptability of the symmetrical components' extractor, where the input signal is unbalanced and distorted by harmonics, is evaluated. For this test, under normal conditions, the input to the system is a set of balanced three-phase sinusoidal voltages of 1.0 p.u. amplitude. Since the system is balanced, no negative- or zero-sequence components exist. Then, 0.1 p.u. negative-sequence and 0.05 p.u. zero-sequence are added to the signals and the THD of the faulty signal is set to 5% (3.7% of 5^{th}, 3.1% of 7^{th} and 1% of 9^{th} harmonics), Fig. 6.11.

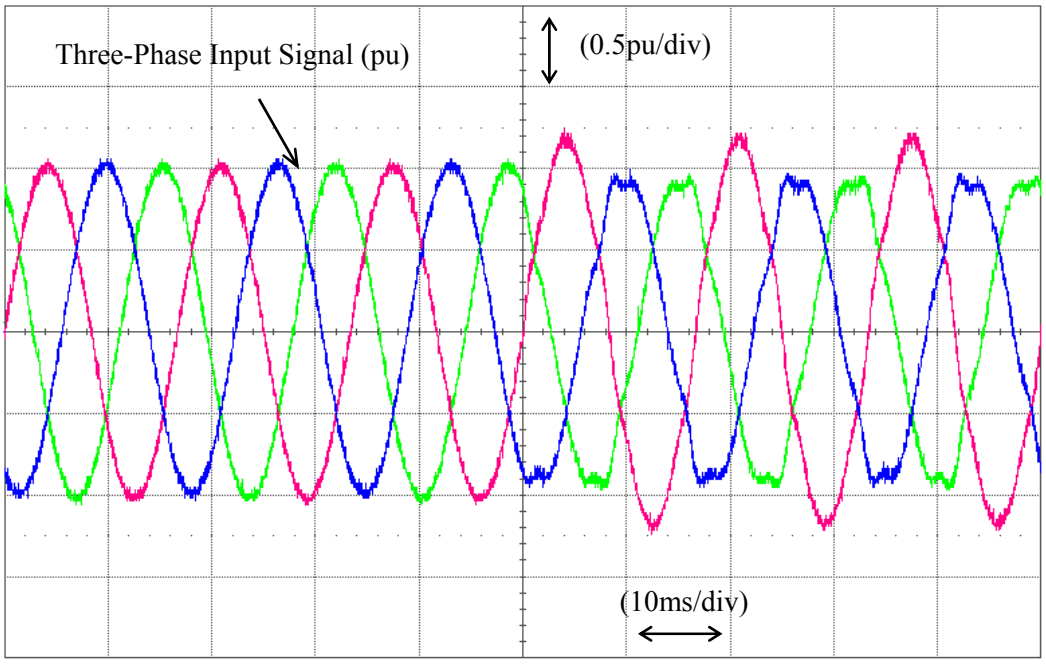

Figure 6.11 Experimental results; distorted signal by harmonics/unbalances.

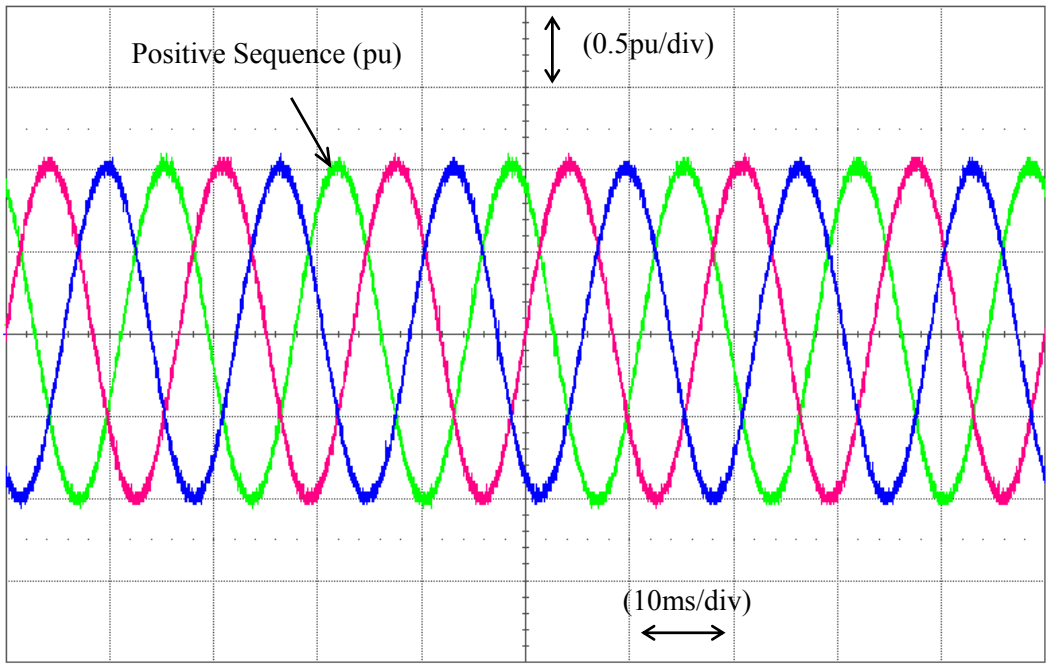

Figure 6.12 Extracted positive sequence components.

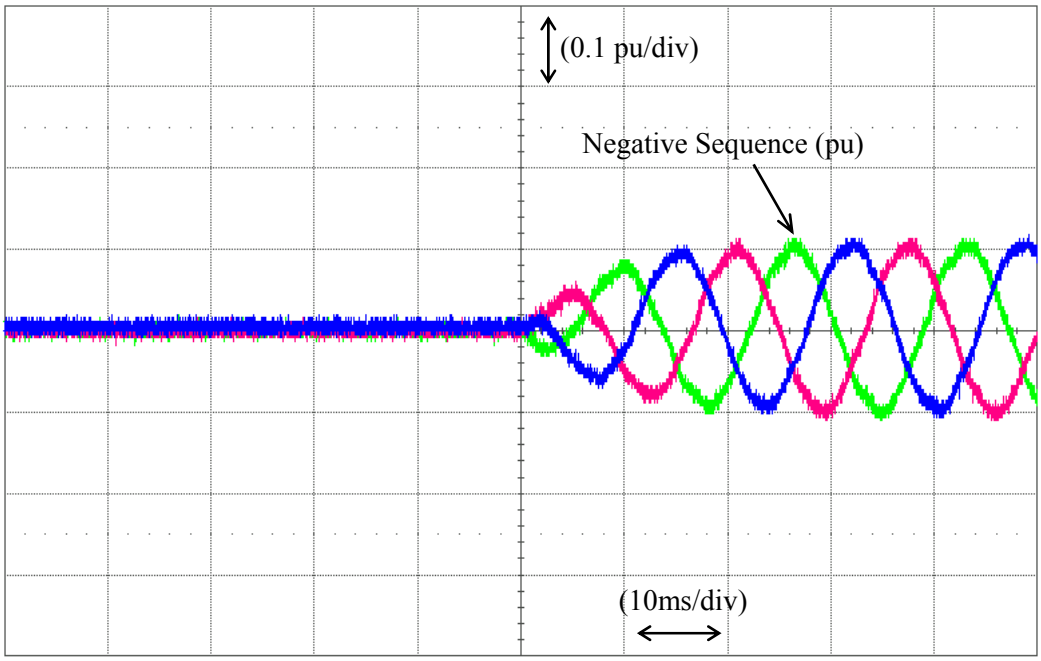

Figure 6.13 Extracted negative sequence components.

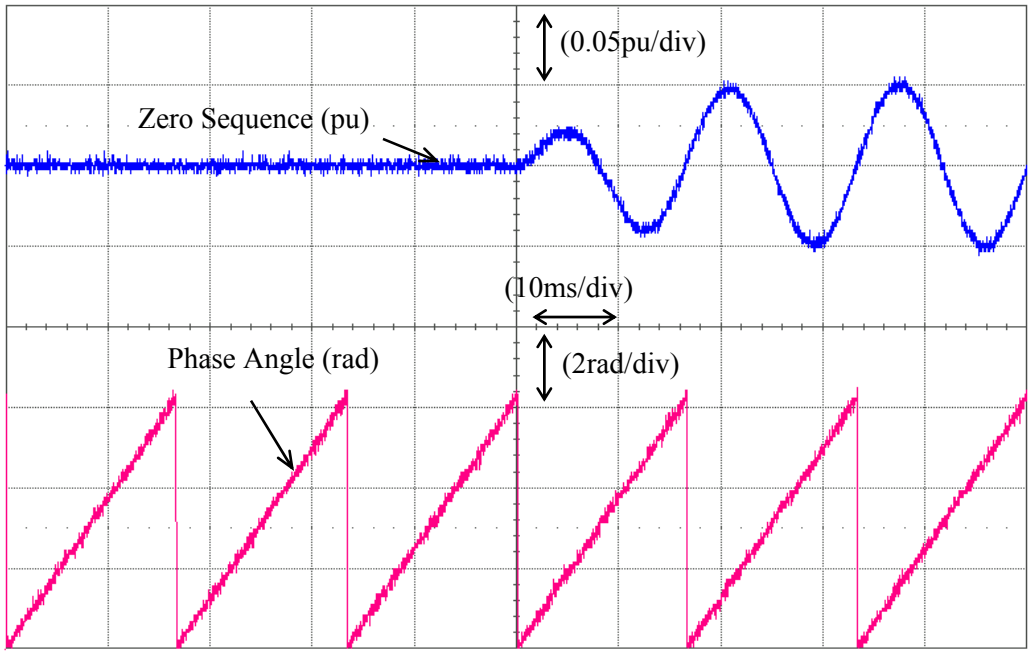

Figure 6.14 Extracted zero sequence component and phase angle of the positive sequence.

Figs. 6.12 to 6.14 show that the fast response and accurate performance of the proposed method are revealed even when the measured signal is simultaneously affected by harmonics and unbalances.

$A_\alpha = \left(\bar{\theta}^2 \bar{x}_\alpha{}^2 + \dot{\bar{x}}_\alpha{}^2\right)^{1/2}$ is the amplitude of the fundamental component of the α^{th} phase of the input signal. Note that both $\bar{\theta}\,\bar{x}_\alpha$ and $\dot{\bar{x}}_\alpha$ are available at the output of Fig. 6.2. Fig. 6.15 shows the amplitudes of the sequence components. Fig. 6.16 shows the magnified error of the extracted frequency. It shows that the proposed method successfully attenuates the harmonics impacts and extracted frequency has around 40 mHz distortion when the signal contains harmonics.

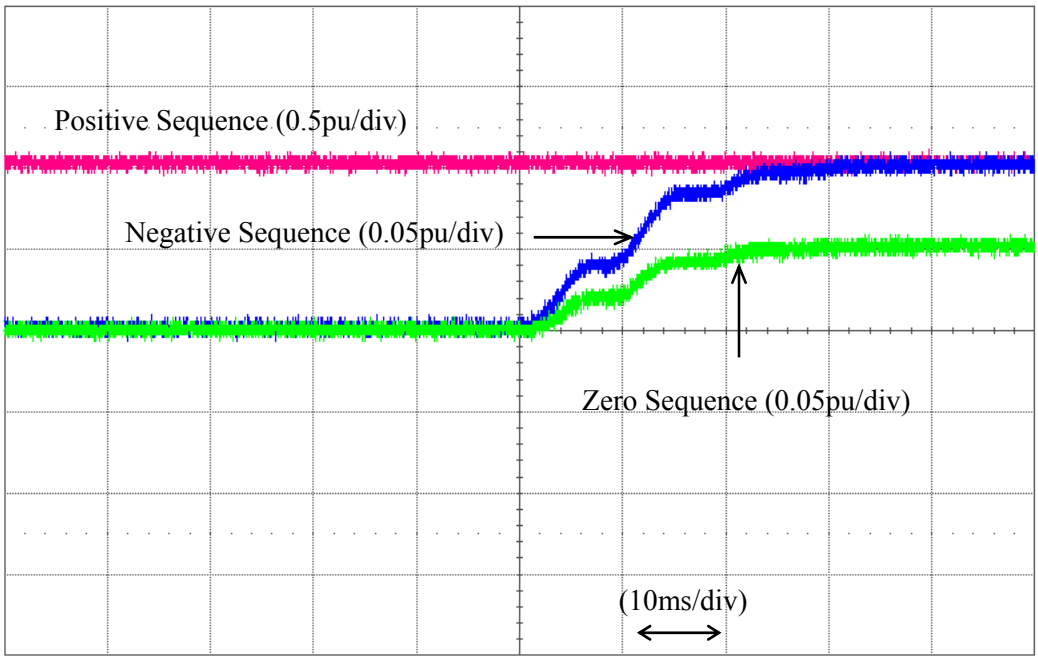

Figure 6.15 The proposed scheme extracts amplitudes of the sequence components.

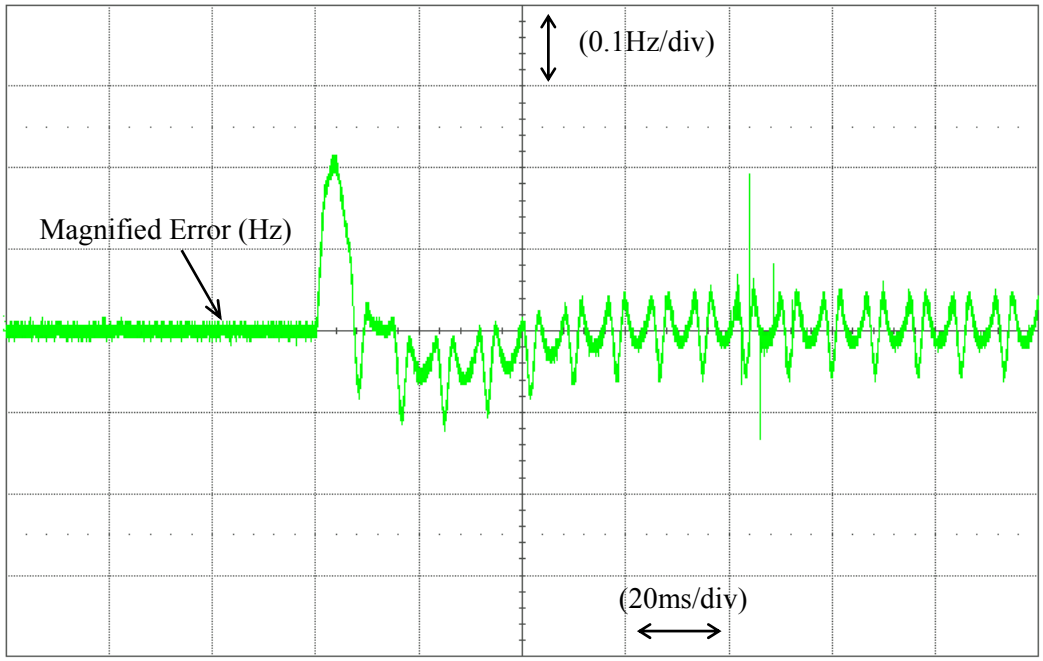

Figure 6.16 The magnified error of the extracted frequency.

6.1.2.3 Modified Structure for Faster Time Response

The time response and performance of the proposed method under harmonics conditions can be improved by making some modifications. Pre-filtering of the input signal and post-filtering of the estimated values (amplitude and frequency) can enhance the performance of the system. Band pass filtering of the three-phase input signal, adding a low pass filter just after the estimated frequency, or even a low pass filter in the frequency estimation loop could improve the performance of the algorithm in the presence of harmonics. These filters smooth the estimated variables at the expense of increasing the transient time of the system. For measurement applications, usually the accuracy of the extracted values is more important than the speed and thus the use of these filters are preferred.

It is shown in Section 6.1.2.2 that the proposed system successfully rejects the harmonics when its parameters are set in such a way that the time response of the proposed system is increased to 50ms. Even though this is fast enough for several applications, to make the proposed system faster while rejecting harmonics, the structure of the sub-filter in Fig. 6.2 is modified and replaced by the multi-block ANF [74], as shown in Fig 6.17. In this configuration the inputs $e_\alpha\,(\alpha = a,b,c)$ and θ are coming from the frequency estimator and the outputs $u_{e\alpha}\,(\alpha = a,b,c)$, which is equal to $u_{f\alpha}\,(\alpha = a,b,c)$ when the input signal is free of harmonics, and $S_{90^\circ} u_{f\alpha}\,(\alpha = a,b,c)$ are fed back to the frequency estimator of Fig. 6.2. Then, $u_{f\alpha}\,(\alpha = a,b,c)$ and $S_{90^\circ} u_{f\alpha}\,(\alpha = a,b,c)$ are connected to the linear transformation to calculate the symmetrical components. The multi-block ANF is proposed to allow an increase in the filter's bandwidth, and thus in the filter's convergence speed. The sub-filters in the multi-block structure remove low-frequency harmonics and output a signal for the main ANF that contains no low-order harmonics.

The number of eliminated harmonics depends directly on the number of sub-filters. The filter parameters can now be adjusted to increase the bandwidth of the filter, and achieve a much faster response with no harmonics at the estimated frequency. Since the proposed sub-filters are notch filters, their dynamics only appear around their notch frequency (harmonic frequencies), and they do not affect the dynamic of the main filter which is again a notch filter centered at the fundamental frequency. However, while removing low-order harmonics, the bandwidth of the main filter can be increased.

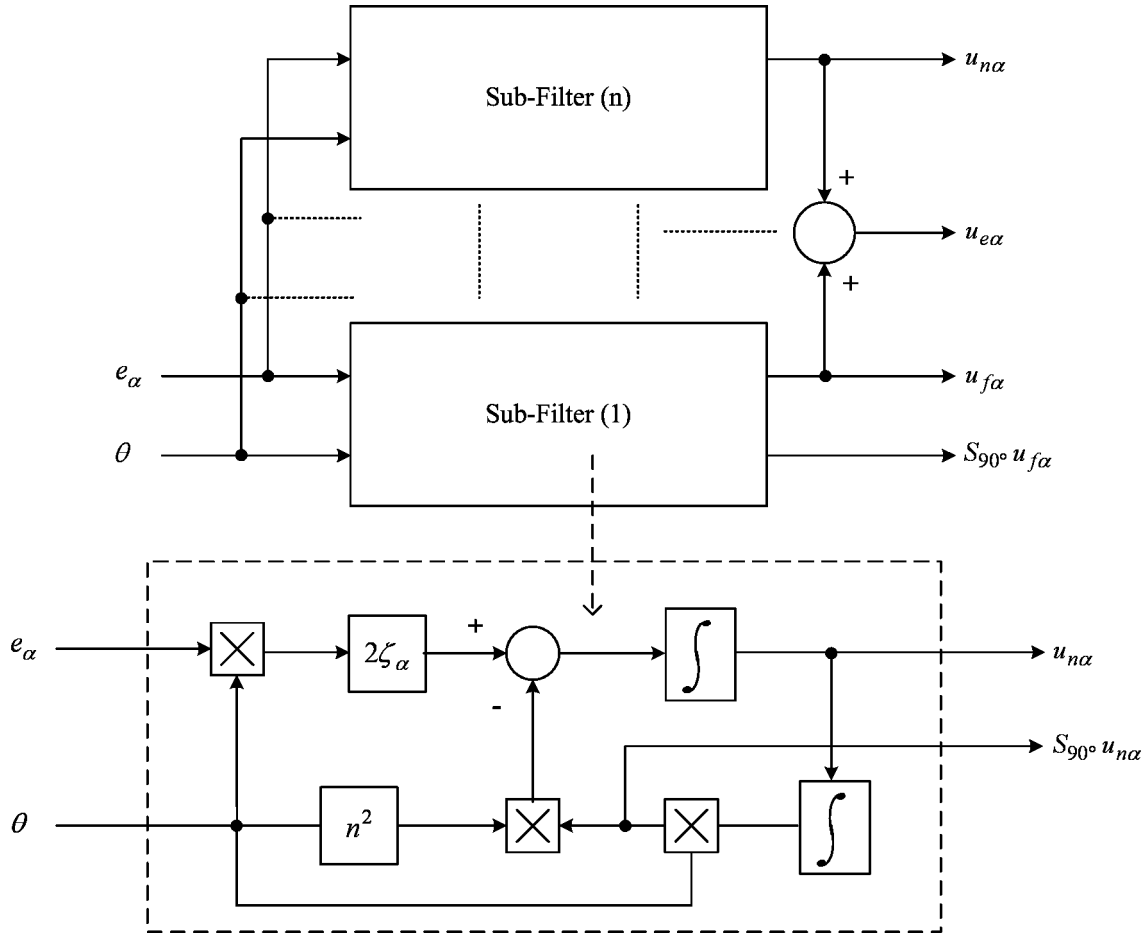

Figure 6.17 Modified structure for faster time response.

The input signal is assumed to be periodic, which is the case in many power electronics grid-connected converter applications. No further information about the input signal is required since the multi-block ANF with an appropriate number of units eliminates undesired low-order harmonics that are the closest ones to the fundamental. In other words, periodicity of the input signal is the only required condition, and the number of deleted harmonics does not depend on the magnitude, phase, or location of the harmonics. Higher order harmonics are naturally eliminated by the ANF.

In Fig. 6.18, the proposed method is compared with the SRF-PLL under harmonics conditions. The parameters are adjusted to achieve a settling time of 20ms for both methods. The three-phase programmable source provides a 3 Hz step change in the frequency of the three-phase signal, and 150ms later, its frequency is changed back to 60 Hz, and the THD of the faulty signal is set to 5%. The tracking capability of the proposed and SRF-PLL methods are shown in Fig. 6.18. As expected, both methods provide a highly fast and accurate response during ideal conditions. However, the SRF-PLL method fails to deal adequately with the harmonics situation when its controller's parameters are set to be fast. Fig. 6.18 shows that the proposed technique provides a highly fast and accurate extraction of the frequency and thus synchronization signal under both balanced and harmonics conditions.

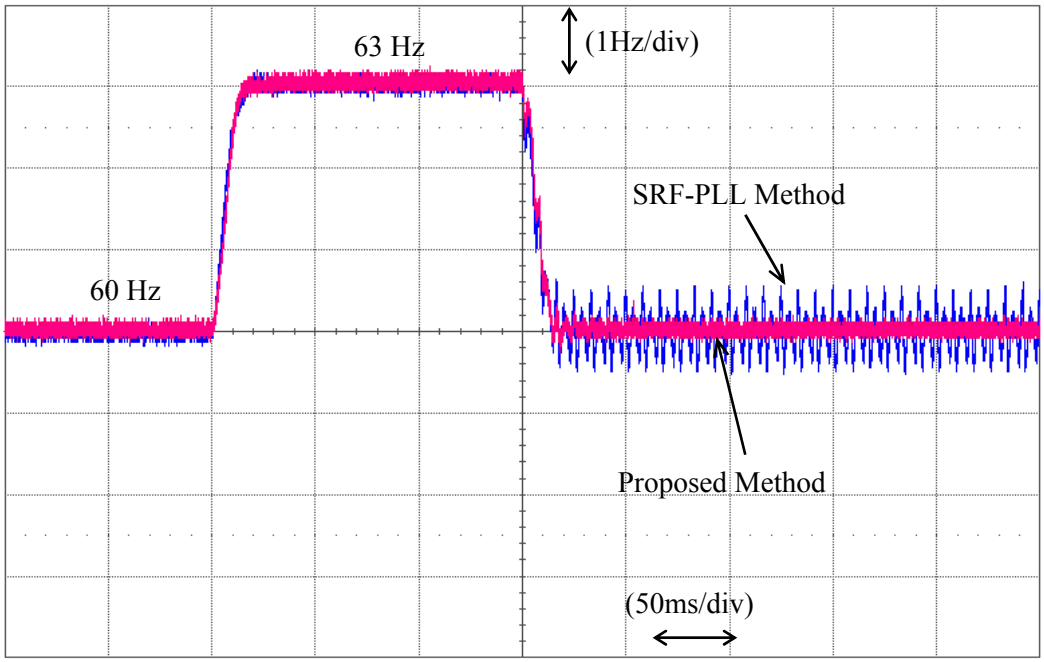

Figure 6.18 Experimental results; extracted frequency by the SRF-PLL and the proposed method.

Later on it will be shown that the modified version of the proposed method provides a highly fast and accurate extraction of the frequency and thus synchronization signal, and also sequence components of the measured signals under balanced/unbalanced/harmonics conditions.Moreover, it is shown in previous chapter that this configuration is able to extract a selective harmonic which can be employed for further harmonic analysis or elimination purposes.

In this section, the measured faulty signal in Fig. 6.12 is applied to symmetrical components' extractor based on Fig. 6.17. The ANF's parameters are adjusted to achieve a settling time of 20ms. Figs. 6.19 to 6.22 show that the fast response and accurate performance of the proposed method are revealed even when the measured signal is simultaneously affected by harmonics and unbalances.

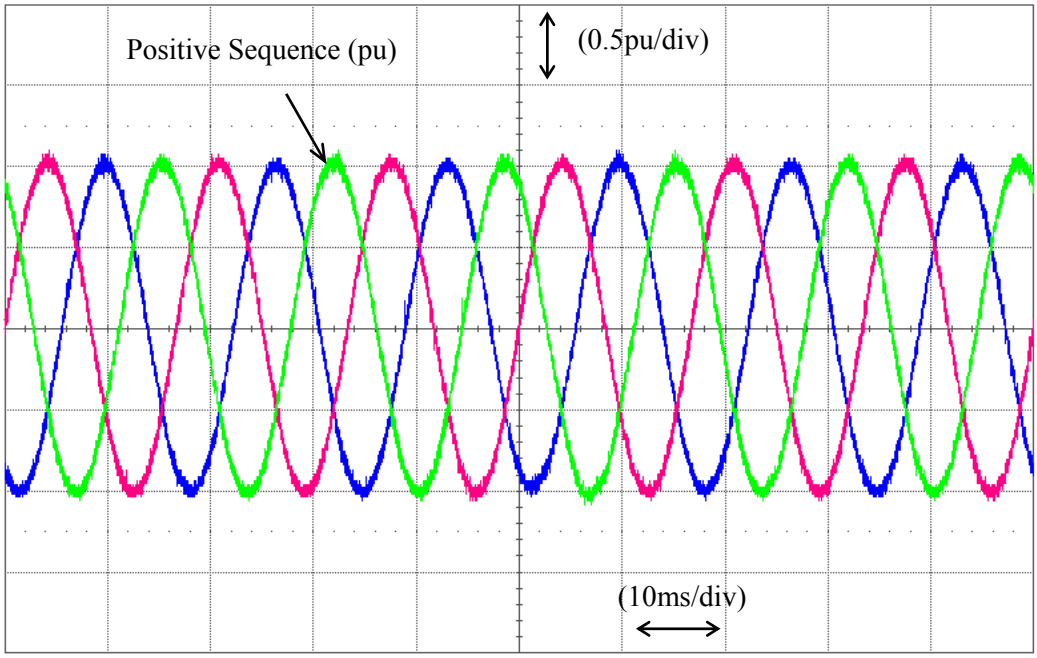

Figure 6.19 Extracted positive sequence components by the proposed modified scheme.

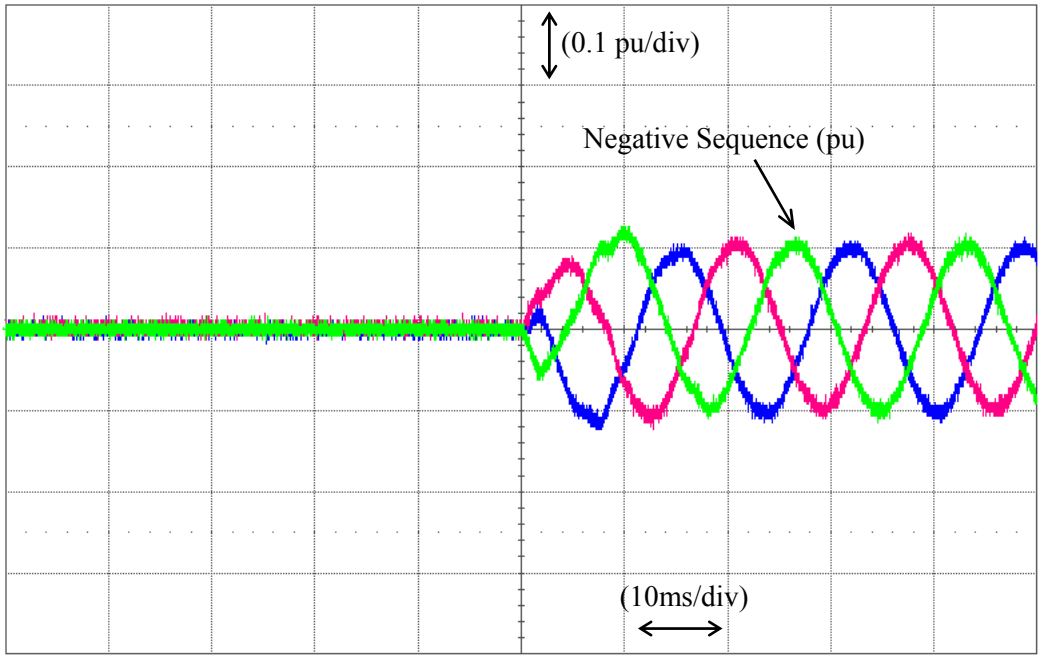

Figure 6.20 Extracted negative sequence components by the proposed modified scheme.

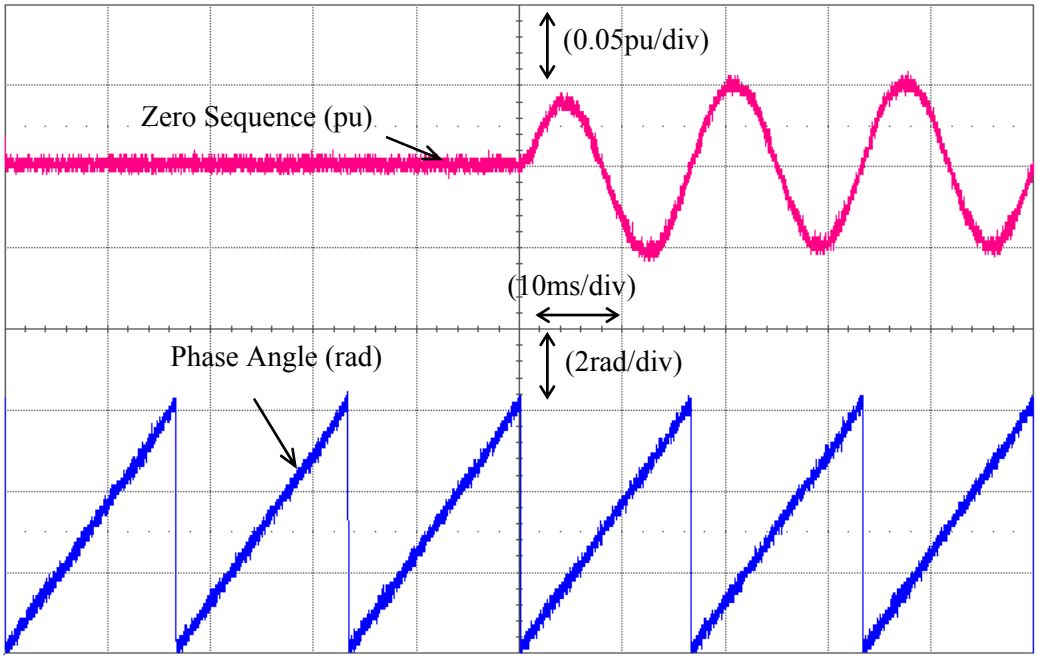

Figure 6.21 Extracted zero sequence component and phase angle of the positive sequence by the proposed modified scheme.

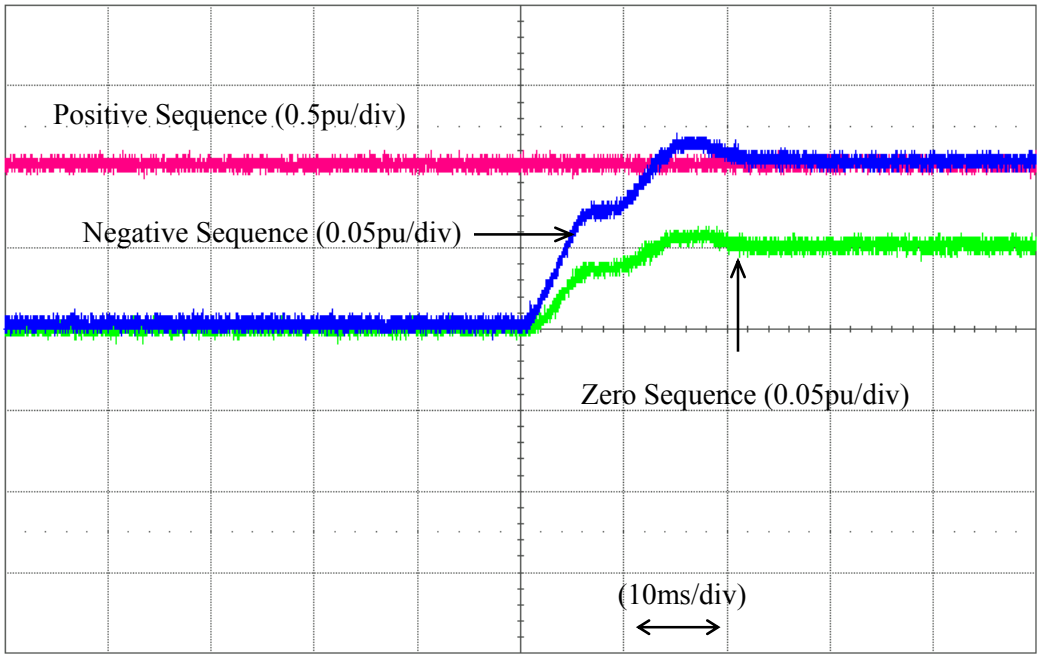

Figure 6.22 Extracted amplitudes of the sequence components by the proposed modified scheme.

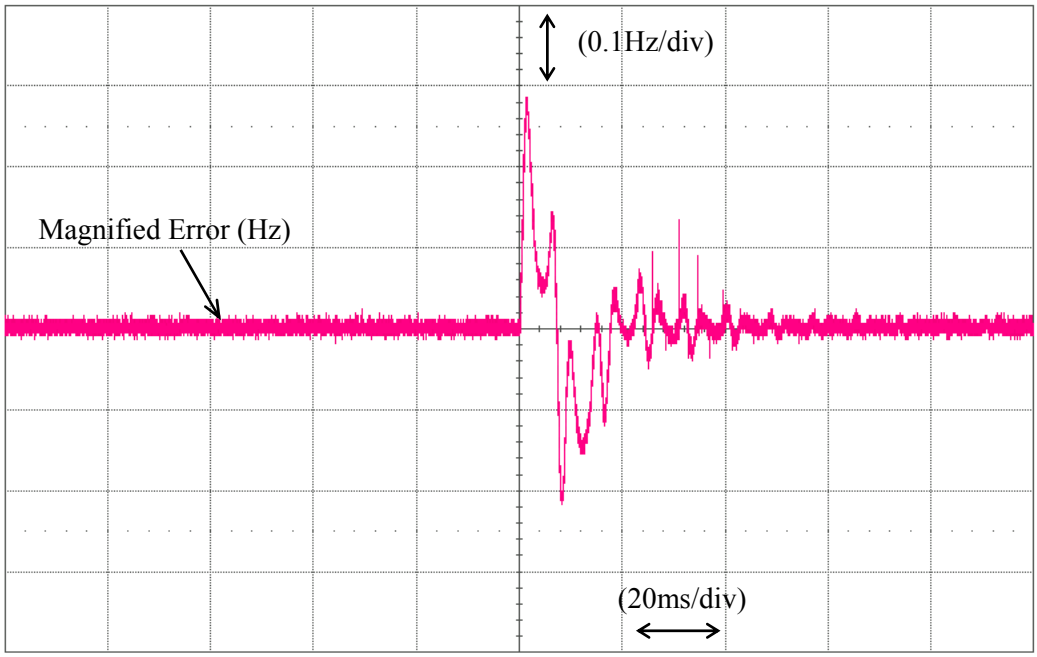

Figure 6.23 The magnified error of the extracted frequency.

Comparing Fig 6.23 and 6.16 reveals the proposed-method based on Fig. 6.17 is highly fast and accurate. The fast response and accurate performance of the proposed unit in extracting symmetrical components are also shown under faulty conditions. Results show that the proposed system needs less than one cycle to detect the fault and therefore extract the symmetrical components. As mentioned earlier, the fast and accurate detection of the positive-sequence component of the utility voltage is required in order to synchronize the converter-interfaced DG units with the utility systems and keep generation up during the grid faults. The proposed method detects a voltage-dip or any other faults in the utility network and extracts the positive sequence of the grid voltage, and therefore tracks the new phase angle of the grid voltage.

6.2 Conclusion

This chapter introduced a new three-phase based ANF method for the online estimation of symmetrical components. The performance of the proposed method was evaluated under power system disturbances, harmonics and other types of pollutions that exist in the grid signal. Moreover, its capability of decomposing three-phase quantities into symmetrical components, tracking the frequency variations, and providing means for power quality, protection, control and monitoring was verified. In addition, a modified version of the three-phase ANF based symmetrical components extractor was proposed and its capability to the fast extracting of sequence components in unbalanced three-phase systems was verified through the experimental work. The proposed scheme was compared with SRF-PLL technique and it was shown that the proposed method provides a fast and precise detection of a voltage-dip or any other faults in the utility network and extracts the positive sequence of the grid voltage. Therefore, it tracks the new phase angle of the grid voltage during the fault, which is required to synchronize the converter-interfaced DG units with the utility systems and keep generation up during the grid faults.

Chapter 7
Summary

7.1 Summary of Contributions

This thesis introduced a new grid synchronization, or more visibly a new "*power signal processor*" based on the concept of ANF that can potentially stimulate much interest in the field and provide improvement solutions grid-connected DG systems. The processor is simple and offers high degree of immunity to power system disturbances, harmonics and other types of pollutions that exist in the grid signal. The processor is capable of decomposing three-phase quantities into symmetrical components, extracting harmonics, tracking the frequency variations, and providing means for voltage regulation and reactive power control. In addition, this simple and powerful synchronization tool will simplify the control structure of grid-connected DG systems because it outputs all useful signal's information. The prominent and superior features of the proposed technique are: i) its simplicity that provides major advantage for its implementation within embedded controllers, ii) the lack of a need for a synchronizing tool like a PLL, iii) its capability to the measuring of positive and negative sequences in unbalanced three-phase systems, iv) simultaneous extraction of harmonics and all useful information embedded in a signal such as frequency, amplitude, and phase angle, (v) adjustable accuracy and speed of response. In addition, the non-linear structure of the proposed algorithm allows direct estimation

of the signal's frequency and its multiples with no use of linearization processes or other simplifying assumptions. The structural simplicity of the algorithm makes it desirable from the standpoint of digital implementation in software and hardware environments. Theoretical analysis is presented and some features of the proposed power signal processor are validated through simulation and experimental results.

The research on the proposed *"power signal processor"* has addressed the following outcomes and contributions:

1. An adaptive, simple and powerful ANF-based grid synchronization tool for grid-connected converters capable of single and multiple frequencies tracking/estimation
2. An advanced power signal processor to extract key power system information required especially in single-/three- phase converter-interfaced DG systems for real-time extraction of symmetrical components, harmonics and reactive currents components and selective harmonics.
3. Development of a three-phase adaptive, simple and powerful grid synchronization tool for grid-connected converters.
4. An advanced three-phase power signal processor to extract key power system information required especially in converter-interfaced DG systems for:
    a. accurate measuring of positive and negative sequences for unbalance system operation.
    b. real-time extraction and decomposition of harmonics

This new processor with some modification can perfectly perform almost every single signal processing function that might be required for control and safety purposes in DG systems. In addition, the new processor employs mathematical tools that streamline the control formulation and thus the system implementation.

7.2 Suggested Future Work

This dissertation has made major contributions to grid-connected converters by proposing a new "*Power Signal Processor*"; but, it has left many open areas to be investigated. Some future research works are presented here: (a) investigating new signal facilities such as island detecting capability, (b) FPGA Implementation and an application specific integrated circuit (ASIC) product development should be explored to provide a smaller, more reliable and cheaper synchronization tool, and (d) formulating optimum ANF parameters adjustment. In addition, the proposed power signal processor can be used in the control system of grid-connected converters as the main signal processor. This capability can be investigated in a wide range of applications such as converter-interfaced DG units, e.g. wind and photovoltaic, and in FACTS and Custom Power Controllers, e.g. APFs, UPFCs and STATCOMs. It is our hope that the proposed powerful tool could be used as a grid-side power processor in control of distributed generation systems for power quality and protection purposes in the near future.

7.3 Conclusion

This thesis presented a new synchronization method for grid-connected converters such as distributed generation system. The proposed ANF based synchronization technique does not require a synchronizing tool like a PLL. Adaptive nature of the proposed technique allows fast and precise tracking of the frequency and amplitude variations. The proposed approach is adapted to meet special interests including the real-time extraction and measurement of symmetrical components, harmonics and reactive components of a power signal of a time-varying characteristic. This is very beneficial for power quality and protection purposes. Symmetrical

components have conventionally been used to analyze unbalanced faults and unbalanced power systems. The proposed system can operate as an analysis tool (like DFT), as a synthesis tool (like PLL), or as a combination of both. Particularly, it can be employed as a signal processor in the control system of the fast growing technologies of distributed generation systems and renewable energy resources. The proposed system may also be used as the main processing part of the power quality measurement and monitoring systems which will provide them with more features due to its capabilities. The immediate advantages of the proposed system are: frequency-adaptivity, full account of unbalanced conditions, high degree of immunity to disturbances and harmonics, and structural robustness. The theoretical analysis is presented, and simulation and experimental results confirm the validity of the analytical work.

References

[1] F. Blaabjerg, R. Teodorescu, M. Liserre, and A. V. Timbus, "Overview of control and grid synchronization for distributed power generation systems," *IEEE Trans. Ind. Electron.*, vol. 53, no. 5, pp. 1398-1409, Oct. 2006.

[2] J. M. Carrasco, L. G. Franquelo, J. T. Bialasiewicz, E. Galvan, R. C. P. Guisado, M. A. Martin Prats, J. I. Leon, N. M. Alfonso, "Power electronic systems for grid integration of renewable energy sources: a survey" *IEEE Trans. Industrial Electronics,* vol. 53, no. 4, pp. 1002-1016, August. 2006.

[3] F. Blaabjerg, Z. Chen, and S.B. Kjaer, "Power electronics as efficient interface in dispersed power generation systems" *IEEE Trans. Power. Electron.*, vol. 19, no. 5,pp. 1184-94, Sep. 2004.

[4] S.B. Kjaer, J. K Pedersen, and F. Blaabjerg, "A review of single-phase grid-connected inverters for photovoltaic modules" *IEEE Trans. onIndustry Application.*, vol. 41, no. 5,pp. 1292-1306, Sep.-Oct. 2005.

[5] Y. Xue, L. Chang, S. B. Kjaer, J. Bordonau, T. Shimizu, "Topologies of single-phase inverters for small distributed power generators: an overview" *IEEE Trans. Power Electronics.*, vol. 19, no. 5,pp. 1305-1314, Sep. 2004.

[6] R. Teodorescu and F. Blaabjerg, "Flexible control of small wind turbines with grid failure detection operating in stand-alone and grid-connected mode," *IEEE Trans. Power Electron.*, vol. 19, no. 5, pp.1323–1332, Sep. 2004.

[7] Z. Chen, "Compensation schemes for a SCR converter in variable speed wind power systems," *IEEE Trans. Power Delivery*, vol. 19, pp. 813-821, Apr. 2004.

[8] Z. Chen and E. Spooner, "Grid power quality with variable-speed wind turbines," *IEEE Trans. Energy Conv.*, vol. 16, pp. 148-154, June 2001.

[9] M. Dai, M.N. Marwali, J.W. Jung, A. Keyhani, "Power Flow Control of a Single Distributed Generation Unit," *IEEE Trans. Power Electronics.*, vol. 23, no. 1, pp. 343-352, Jan. 2008.

[10] F. Gao and M.R. Iravani, "A Control Strategy for a Distributed Generation Unit in Grid-Connected and Autonomous Modes of Operation," *IEEE Trans. Power Delivery,* vol. 23, no. 2, pp. 850-859, April 2008.

[11] A. V. Timbus , M. Liserre , R. Teodorescu and F. Blaabjerg, "Synchronization methods for three phase distributed power generation systems. An overview and evaluation," *Proc. IEEE PESC*, 2005, pp. 2474-2481.

[12] J. Svensson, "Synchronisation methods for grid-connected voltage source converters," *Proc. Inst. Electr. Eng.—Gener. Transm. Distrib.*, vol. 148, no. 3, pp. 229–235, May 2001.

[13] M. Karimi-Ghartemani and M. Iravani, "A method for synchronization of power electronic converters in polluted and variable-frequency environments," *IEEE Trans. Power Syst.*, vol. 19, no. 3, pp. 1263–1270, Aug. 2004.

[14] L.R. Limongi, R. Bojoi, C. Pica, F. Profumo, A. Tenconi, "Analysis and Comparison of Phase Locked Loop Techniques for Grid Utility Applications" *Proc. IEEE Power Conversion Conference PCC*, 2007, pp. 674-681.

[15] R. M. Santos Filho, P. F. Seixas, P. C. Cortizo, L. A. B. Torres, and A. F. Souza, "Comparison of three single-phase PLL algorithms for UPS applications" *IEEE Trans. on Industrial Electronics*, Vol. 55, No. 8, pp. 2923-2932, August 2008.

[16] S. J. Lee, H. Kim, S. K. Sul, and F. Blaabjerg, "A novel control algorithm for static series compensators by use of PQR instantaneous power theory," *IEEE Trans. Power Electron.*, vol. 19, no. 3, pp. 814–827, May 2004.

[17] G. Saccomando and J. Svensson, "Transient operation of grid connected voltage source converter under unbalanced voltage conditions," in *Proc. IEEE IAS Annu. Meeting 2001*, vol. 4, pp. 2419-2424.

[18] H.Awad, J. Sevensson, and M. J. Bollen, "Tuning software phase-locked loop for series-connected converters," *IEEE Trans. Power Del.*, vol. 20, no. 1, pp. 300-308, Jan. 2005.

[19] G. C. Hsieh and J. C. Hung, "Phase-locked loop techniques—A survey," *IEEE Trans. Ind. Electron.*, vol. 43, pp. 609-615, Dec. 1996.

[20] M.A. Perez, J.R. Espinoza, L.A. Moran, M.A. Torres, E.A. Araya, "A Robust Phase-Locked Loop Algorithm to Synchronize Static-Power Converters With Polluted AC Systems," *IEEE Trans. Power Electron.*, vol. 55, no. 5, pp. 21852192, May 2008.

[21] M. Karimi-Ghartemani and M. R. Iravani "A nonlinear adaptive filter for online signal analysis in power system: Applications," *IEEE Trans. Power Del.*, vol. 17, pp. 617, Apr. 2002.

[22] H. Karimi, M. Karimi-Ghartemani and M. R. Iravani, "Estimation of frequency and its rate of change for applications in power systems," *IEEE Trans. Power Del.*, vol. 19, no. 2, pp. 472-480, Apr. 2004.

[23] N. Arruda, B. J. C. Filho , S. M. Silva , S. R. Silva and A. S. A. C. Diniz "Wide bandwidth single and three-phase PLL structures for grid-tied PV systems," *Proc. 28th IEEE Photovoltaic Spec. Conf.*, 2000, pp. 1660-1663.

[24] L. N. Arruda, S. M. Silva and B. J. C. Filho "PLL structures for utility connected systems," *36th Conf. Rec. IEEE IAS Annu. Meeting*, vol. 4, Sep. 2001, pp. 2655-2660.

[25] S. M. Silva, B. M. Lopes , B. J. C. Filho , R. P. Campana and W. C. Boaventura "Performance evaluation of PLL algorithms for single-phase grid-connected systems," *39th Conf. Rec. IEEE IAS Annu. Meeting*, vol. 4, Aug. 2004, pp. 2259-2263.

[26] M. Ciobotaru, R. Teodorescu and F. Blaabjerg "Improved PLL structures for single-phase grid inverters," *Proc. Int. Conf. PELINCEC*, Oct. 2005.

[27] M. Ciobotaru, R. Teodorescu and F. Blaabjerg "A new single-phase PLL structure based on second order generalized integrator," *Proc. 37th IEEE PESC*, Jun. 2006, pp. 1511-1516.

[28] S. Shinnaka "A Robust Single-Phase PLL System With Stable and Fast Tracking," *IEEE Trans. Industry Applications*, vol. 44, no. 2, pp. 624-633, March/April 2008.

[29] V. Kaura and V. Blasko, "Operation of phase loop system under distorted utility conditions," *IEEE Trans. Ind. Appl.*, vol. 33, no. 1, pp. 58–63, 1997.

[30] K. Chung, "A phase tracking system for three phase utility interface inverters," *IEEE Trans. Power Electron.*, vol. 15, no. 3, pp. 431–438, May 2000.

[31] S. K. Chung, "Phase-locked loop for grid-connected three-phase power conversion systems," *Proc. Inst. Elect. Eng., Elect. Power Applicat.*, vol. 147, no. 3, pp. 213-219, May 2000.

[32] X. Yuan, W. Merk, H. Stemmler and J. Allmeling "Stationary frame integrators for current control of active power filters with zero steady-state error for current harmonics of concern under unbalanced and distorted operating conditions", *IEEE Transactions on Industry Applications,* Vol. 38, n. 2, March-April 2002 pp. 523 - 532.

[33] R. I. Bojoi, G. Griva, V. Bostan, M. Guerriero, F. Farina and F. Profumo "Current control strategy for power conditioners using sinusoidal signal integrators in synchronous reference frame", *IEEE Trans. Power Electron.,* Vol. 20, n. 6, Nov. 2005 pp. 1402 - 1412.

[34] P. Rodriguez, R. Teodorescu, I. Candela, A. V. Timbus, M. Liserre, F. Blaabjerg "New positive-sequence voltage detector for grid synchronization of power converters under faulty grid conditions", *Conf. Rec. PESC'06,* 18-22 June 2006 pp. 1 - 7.

[35] P. Rodríguez, A. Luna, M. Ciobotaru, R. Teodorescu, and F. Blaabjerg, "Advanced grid synchronization system for power converters under unbalanced and distorted operating conditions," *in Proc. IECON,* pp. 5173–5178, 2006.

[36] P. Rodriguez, A. V. Timbus, R. Teodorescu, M. Liserre, F. Blaabjerg, "Flexible Active Power Control of Distributed Power Generation Systems During Grid Faults" *IEEE Trans. Power. Electron.,* vol. 57, no. 5,pp. 2583-2592, Oct. 2007.

[37] A. Yazdani, R. Iravani, "A unified dynamic model and control for the voltage source converter under unbalanced grid conditions," *IEEE Trans. Power Delivery,* vol. 21, no. 3, pp. 1620-1629, July 2006.

[38] P. Rodriguez, J. Pou, J. Bergas, I. Candela, R. Burgos, and D. Boroyevich, "Decoupled double synchronous reference frame PLL for power converters control," *IEEE Trans. Power Electron.*, vol. 22, no. 2, pp. 584-592, March 2007.

[39] D. Jovic, "Phase-locked loop system for FACTS," *IEEE Trans. Power Sys.*, vol. 18, no. 3, pp. 1116-1124, Aug. 2003.

[40] S.-J. Lee, J.-K. Kang, and S.-K. Sul, "A new phase detecting method for power conversion systems considering distorted conditions in power system," *in Proc. Industry Applications Conf., 34th IAS Annu. Meeting,* 1999, vol. 4, pp. 2167-2172.

[41] G. M Lee, D. C. Lee J. K. Seok , "Control of series active power filters compensating for source voltage unbalance and current harmonics," *IEEE Trans. Ind. Electr.*, vol. 51, no. 1, pp. 132-139, Feb. 2004.

[42] M. R. Iravani and M. Karimi-Ghartemani, "Online estimation of steady state and instantaneous symmetrical components," *Proc. Inst. Elect. Eng.*, vol. 150, no. 5, pp. 616-622, Sep. 2003.

[43] H.-S. Song and K. Nam, "Instantaneous phase-angle estimation algorithm under unbalanced voltage-sag conditions," in *Proc. Inst. Elect. Eng. Generation, Transmission, and Distribution*, vol. 147, no. 6, 2000, pp. 409-415.

[44] L. Asiminoaei, F. Blaabjerg, and S. Hansen, "Detection is key—Harmonic detection methods for active power filter applications," *IEEE Ind. Appl. Mag.*, vol. 13, no. 4, pp. 22–33, Jul./Aug. 2007.

[45] V.M. Moreno, M. Liserre, A. Pigazo, and A. Dell'Aquila, "A Comparative Analysis of Real-Time Algorithms for Power Signal Decomposition in Multiple Synchronous Reference Frames" *IEEE Transactions on Power Electronics*, Volume: 22, Issue: 4, Page(s): 1280-1289, July 2007.

[46] H Akagi, "Active harmonic filters," *Proceedings of IEEE.*, vol. 93, no. 12, pp. 2128-2141, Dec. 2005.

[47] W. M.Grady, M. J.Samotyj, and A. H.Noyola, "Survey of active power line conditioning methodologies," *IEEE Trans. Power Delivery*, vol. 5, pp. 1536-1542, 1990.

[48] B. Singh, K. Al-Haddad, and A. Chandra, "A review of active filters for power quality improvement," *IEEE Trans. Ind. Electron.*, vol. 46, no. 5, pp. 960–971, Oct. 1999.

[49] M. El-Habrouk, M. K. Darwish, and P. Mehta, "Active power filters: a review," *IEE Proc.-Electr. Power Appl.*, vol. 147, no. 5, pp. 403-413, September 2000.

[50] J. M. M Ortega, M. P. Steve, M. P. Payan, A. G. Exposito, and L. G. Franquelo, "Reference current computation method for active power filter: accuracy assessment in the frequency domain," *IEEE Trans. Power Electron.*, vol. 20, no. 2, pp. 446-456, March 2005.

[51] M. EI-Habrouk and M. K. Darwish, "Design and implementation of a modified Fourier analysis harmonic current computation technique for power active filters using DSP's," *Proc. Inst. Elect. Eng.—Elect. Power Appl.*, vol. 148, no. 1, pp. 21-28, Jan. 2001.

[52] H. Akagi, Y. Kanazawa, and A. Nabae, "Instantaneous reactive power compensators comprising switching devices without energy storage components," *IEEE Trans. Ind. Appl.*, vol. 20, pp. 625-630, May/June 1984.

[53] M. J. Newman, D. N. Zmood, and D. G. Holmes, "Stationary frame harmonic reference generation for active filters," *IEEE Trans. Ind. Applicat*., vol. 38, no. 6, pp. 1591–1599, Nov./Dec. 2002.

[54] S. Buso, L. Malesani, and P. Mattavelli, "Comparison of current control techniques for active filter applications," *IEEE Trans. Ind. Electron.*, vol.45, no. 5, pp. 722–729, Oct. 1998.

[55] J. Allmeling, "A control structure for fast harmonics compensation an active filters," *IEEE Trans.Power Electron.*, vol. 19 no. 2, pp. 508-512, March 2004.

[56] P. Mattavelli, "A close-loop selective harmonic compensation for active filters," *IEEE Trans. Ind. Appl.*, vol. 37, no. 1, pp. 81-89, Jan./Feb. 2001.

[57] V. Blasko, "A novel method for selective harmonic elimination in power electronic equipment," *IEEE Trans. Power Electron.*, vol. 22, no. 1, pp. 223-228, Jan. 2007.

[58] S. H. Seok and K. Nam, "Dual current control scheme for PWM converter under unbalanced input voltage conditions," *IEEE Trans. Ind. Electron.*, vol. 46, pp. 953–959, Oct. 1999.

[59] S. Tepper, J. Dixon, G. Venegas, and L. Moran, "A simple frequency independent method for calculating the reactive and harmonic current in a nonlinear load," *IEEE Trans. Ind. Electron.*, vol. 43, pp. 647-654, Dec. 1996.

[60] J. W. Dixon, J. J. Garcia, and L. A. Moran, "Control system for three-phase active power filter which simultaneously compensates power factor and unbalanced loads," *IEEE Trans. Ind. Electron.*, vol. 42, pp. 636-641, Dec. 1995.

[61] M. Karimi-Ghartemani, H. Mokhtari, R. Iravani, and M. Sedighy, "A signal processing system for extraction of harmonics and reactive currents of single phase systems," *IEEE Trans. Power Del.*, vol. 19, no. 3, pp. 979-986, July 2004.

[62] S. Lou and Z. Hou, "An adaptive detecting method for harmonic and reactive currents," *IEEE Trans. Ind. Electron*., vol. 42, pp. 85-89, Feb. 1995.

[63] H. Karimi, M. Karimi-Ghartemani, R. Iravani and A. Bakhshai, "An adaptive filter for synchronous extraction of harmonics and distortions," *IEEE Trans. Power Delivery*, vol. 18, no. 4, pp. 1350-1353, Oct. 2003.

[64] M. Mojiri and A. Bakhshai, "An adaptive notch filter for frequency estimation of a periodic signal," *IEEE Trans. Automat. Control*, vol. 49, no. 2, pp. 314–318, Feb. 2004.

[65] M. Mojiri, M. Karimi-Ghartemani and A. Bakhshai, "Time domain signal analysis using adaptive notch filter," *IEEE Trans. Signal Processing*, vol. 55, no. 1, pp. 85-93, Jan 2007.

[66] M. Mojiri and A. Bakhshai, "Estimation of n frequencies using adaptive notch filter," *IEEE Trans. Circuit and Systems II: Express Briefs*, vol. 54, no. 4, pp. 338-342, April 2007.

[67] M. Mojiri, M. Karimi-Ghartemani and A. Bakhshai, "Estimation of Power System Frequency Using Adaptive Notch Filter," *IEEE Transactions on Instrumentation and Measurement,* Vol. 56, No. 6, Dec. 2007, pp. 2470-2477.

[68] D. Yazdani, A. Bakhshai, G. Joos, and M. Mojiri, "A nonlinear adaptive synchronization technique for grid-connected distributed energy sources," *IEEE Trans. Power Electron.,* Vol. 23, no. 4, pp. 2181-2186, July 2008.

[69] D. Yazdani, A. Bakhshai, G. Joos, and M. Mojiri, "A Nonlinear Adaptive Synchronization Technique for Single-Phase Grid-Connected Converters"*, IEEE Power Electronics Specialists Conference, PESC 2008,* pp. 4076-4079, 2008.

[70] D. Yazdani, A. Bakhshai, G. Joos, and M. Mojiri, "A Single-phase Adaptive Synchronization Tool for Grid-Connected Converters", *IEEE IECON 2008.*

[71] D. Yazdani, A. Bakhshai, G. Joos, and M. Mojiri,"Adaptive Notch Filtering Approach for Harmonic and Reactive Current Extraction in Active Power Filters", *IEEE IECON 2008.*

[72] D. Yazdani, A. Bakhshai, G. Joos, and M. Mojiri, "A Real-Time Selective Harmonic Extraction Approach Based on Adaptive Notch Filtering", *IEEE International Symposium on Industrial Electronics,* ISIE 2008, pp. 226-230..

[73] D. Yazdani, A. Bakhshai, G. Joos, and M. Mojiri, "A Real-Time Sequence Components Decomposition for Transient Analysis in Grid-connected Distributed Generation Systems", *IEEE International Symposium on Industrial Electronics,* ISIE 2008, pp.1651-1656.

[74] D. Yazdani, M. Mojiri, A. Bakhshai, and G. Joos, "A Fast and Accurate Synchronization Technique for Extraction of Symmetrical Components," Accepted for Publication in *IEEE Transaction on Power Electronics*.

[75] A. V. Timbus , M. Liserre , F. Blaabjerg , R. Teodorescu and P. Rodriguez "PLL algorithm for power generation systems robust to grid faults," *Proc. IEEE PESC*, 2006, pp. 1360-1366.

[76] G. Saccomando, J. Svensson, and A. Sannino, "Improving voltage disturbance rejection for variable-speed wind turbines," *IEEE Trans. Energy Convers.*, vol. 17, no. 3, pp. 422-428, Sep. 2002.

[77] A. Sannino, M. H. J. Bollen and J. Svensson "Voltage tolerance testing of three-phase voltage source converters," *IEEE Trans. Power Del.*, vol. 20, pp. 1633, Apr. 2005.

[78] A. Von Jouanne and B. Benerjee "Assessment of voltage unbalance," *IEEE Trans. Power Del.*, vol. 16, pp. 782, Oct. 2001.

[79] M. H. J. Bollen, "Algorithms for characterizing measured three-phase unbalanced voltage dips," *IEEE Trans. Power Delivery*, vol. 18, pp. 937- 944, Jul. 2003.

[80] G. C. Paap, "Symmetrical components in the time domain and their application to power network calculations," *IEEE Trans. Power Sys*., vol. 15, no. 2, pp. 522-528, May 2000.

[81] M. Karimi-Ghartemani, H. Karimi, "Processing of Symmetrical Components in Time-Domain" *IEEE Trans. Power Sys.*, vol. 22, no. 2, pp. 572-579, May 2007.

[82] H. Karimi, A. Yazdani, and R. Iravani, "Negative-sequence current injection for fast islanding detection of a distributed resource unit," *IEEE Trans. Power Electronics,* vol. 23, no. 1, pp. 298-307, Jan. 2008.

[83] B. Riedle and P. Kokotovic, "Integral manifolds of slow adaptation," *IEEE Trans. Automat. Contr.*, vol. 31, no. 4, pp. 316-324, April 1986.

[84] T. Kailath, *Linear Systems,* Englewood Cliffs, NJ: Prentice-Hall, 1980.

[85] B. Farhang-Boroujeny, *Adaptive Filters Theory and Applications*, John Wiley&Sons, 1998.

[86] J. K. Hale, *Ordinary Differential Equations*, John Wiley and Sons, 1969.

[87] S. Sastry and M. Bodson, *Adaptive Control: Stability, Convergence and Robustness*, Englewood Cliffs, NJ: Prentice-Hall, 1989.

Appendix A

Stability Analysis

This section outlines the detailed local stability analysis of the proposed method which is mathematically represented by the dynamical system of (5.1) and (5.2).

Define the state vector $\chi = \begin{pmatrix} x^t & \dot{x}^t \end{pmatrix}^t$ where $x = \begin{pmatrix} x_a & x_b & x_c \end{pmatrix}^t$ and observe θ as an *adjustable parameter*. Then, the equations set (5.1) and (5.2) can be represented by the following nonlinear dynamic system

$$\dot{\chi} = A(\theta)\chi + B(\theta)u(t) \quad , \chi \in \Re^6, u \in \Re^3 \tag{A.1}$$

$$\dot{\theta} = \gamma f(t, \theta, \chi) \quad , \theta \in \Re \tag{A.2}$$

In (A.1), $A(\theta)$ and $B(\theta)$ are

$$A(\theta) = \begin{pmatrix} 0 & I \\ -\theta^2 I & -2\theta\zeta \end{pmatrix}, B(\theta) = \begin{pmatrix} 0 \\ 2\theta\zeta \end{pmatrix} \tag{A.3}$$

in which the diagonal matrix ζ is defined as,

$$\zeta = diag(\zeta_a \quad \zeta_b \quad \zeta_c) \tag{A.4}$$

Moreover, the function $f(t, \theta, \chi)$ in (A.2) is given by,

$$f(t, \theta, \chi) = -\theta \sum_{\alpha = a,b,c} x_\alpha (u_\alpha - \dot{x}_\alpha) \tag{A.5}$$

(A.1) and (A.2) are in a standard form suitable for the application of integral manifold of slow adaptation concept [83]. When the adaptation gain γ is small, the estimated frequency, θ, tends

to evolve slowly compared to the filter states χ. As shown in [83], this concept of slow adaptation can be made precise by proving that it occurs on an integral manifold of (A.1) and (A.2). An integral manifold is, by definition, a time varying $1-$dimensional (1-D) surface $M_\gamma = \{(t,\theta,\chi) : \chi = h_\gamma(t,\theta)\}$ such that

$$(\chi(t_o),\theta(t_o)) \in M_\gamma \Rightarrow (\chi(t),\theta(t)) \in M_\gamma, \quad \forall t \geq t_o \tag{A.6}$$

If a manifold M_γ exists for each value of γ in the interval $[0,\gamma_o]$, then we shall say that a $\gamma-$family of slow manifolds exists. The simplest member of these integral manifolds is the "frozen parameter" integral manifold M_o defined by $\gamma = 0$ [83]. M_o represents the well-known steady state response of the linear time-invariant system (A.1). Note that if $\gamma = 0$, θ is constant (freezed).

Proposition 1. Let $\chi^o(t,\theta)$ be the steady state response with frozen θ of the linear time invariant system (A.1). Then, its components are given by,

$$x_\alpha^o(t,\theta) = B_\alpha \sin\phi_\alpha(t) \tag{A.7}$$

$$\dot{x}_\alpha^o(t,\theta) = \omega_o B_\alpha \cos\phi_\alpha(t)$$

for $\alpha = a,b,c$, where,

$$B_\alpha = A_\alpha \left| G_\alpha(j\omega_o,\theta) \right| \ , \ \phi_\alpha(t) = \omega_o t + \delta_\alpha + \angle G_\alpha(j\omega_o,\theta) \tag{A.8}$$

and

$$G_\alpha(s,\theta) = \frac{2\zeta_\alpha \theta}{s^2 + 2\zeta_\alpha \theta s + \theta^2} \tag{A.9}$$

Proof. Taking the Laplace transform of both sides of (A.1), and ignoring the initial conditions, yields

$$X(s,\theta) = (sI - A(\theta))^{-1} B(\theta) U(s)$$

$$= \begin{pmatrix} sI & -I \\ \theta^2 I & sI + 2\theta\zeta \end{pmatrix}^{-1} \begin{pmatrix} 0 \\ 2\theta\zeta \end{pmatrix} U(s) \tag{A.10}$$

Applying the matrix inversion formulas of [84, Appendix A.22], (A.10) transforms to

$$X(s,\theta) = \begin{pmatrix} \left(s^2 I + 2\theta s\zeta + \theta^2 I\right)^{-1} & 2\theta\zeta \\ s\left(s^2 I + 2\,\theta s\zeta + \theta^2 I\right)^{-1} & 2\theta\zeta \end{pmatrix} U(s) \tag{A.11}$$

Noting that $\left(s^2 I + 2\theta s\zeta + \theta^2 I\right)$ is a diagonal matrix. By means of these notations, the transfer function $G_\alpha(s,\theta)$ from $U_\alpha(s)$ to $X_\alpha(s,\theta)$ is given by (A.9).

As, $G_\alpha(s,\theta)$ is a stable transfer function, when forced by the input signal $u(t)$ given by (5.3), $x_\alpha(t,\theta)$ will tend to yield a steady state response. Therefore, the steady state response with frozen θ of (A.1) is given by (A.7).

Remark 1. Since $G_\alpha(s,\theta)$ is a stable transfer function, any transient response resulted from the input signal and/or the initial conditions decays to zero. Therefore, these terms have no effect on the steady state response and can be ignored.

Proposition 2. There exists $\gamma_o > 0$ such that for each $\gamma \in [0, \gamma_o]$, (A.1) and (A.2) have a uniquely defined integral manifold $M_\gamma = \{(t,\ \theta,\ \chi):\ \chi = h_\gamma(t,\theta)\}$ which arbitrarily approaches the frozen parameter integral manifold M_o as $\gamma \to 0$. Moreover, on the manifold M_γ, the θ

update law is asymptotically stable in the sense that $\theta \to \omega_o$ as $t \to \infty$.

Proof. Introducing the deviation of χ from $\chi^o(t,\theta)$ as a new state variable

$$z = \chi - \chi^o(t,\theta) \tag{A.12}$$

we rewrite (A.1) and (A.2) in the form of

$$\dot{z} = A(\theta)z - \gamma\, \chi^o_\theta(t,\theta) F(t,\theta,z) \tag{A.13}$$

$$\dot{\theta} = \gamma\, f\left(t,\ \theta,\ \chi^o(t,\theta) + z\right) \equiv \gamma\, F(t,\ \theta,\ z) \tag{A.14}$$

where $\chi^o_\theta(t,\theta) = \partial\chi^o(t,\theta)/\partial\theta$ is the sensitivity vector.

Obviously, the characteristic polynomial of $A(\theta)$ is given by $\prod_{\alpha=a,b,c}\left(s^2 + 2\,\theta\zeta_\alpha\, s + \theta^2\right)$, which is a stable polynomial. Therefore, the following assumption is satisfied by (A.13).

Assumption 1. The frozen θ unforced system, $\dot{z} = A(\theta)z$, is exponentially stable. Also, since $|G_\alpha(j\omega_o,\theta)|$ and $\angle G_\alpha(j\omega_o,\theta)$ are continuous functions of θ, and since $u(t)$ is a periodic signal, the following assumptions are satisfied by (A.13) and (A.14).

Assumption 2. $\chi^o(t,\theta)$, $\chi^o_\theta(t,\theta)$ are bounded and the latter is Lipschitzian in θ.

Assumption 3. $F(t,\theta,z)$ is continuous on a compact set, hence it is bounded and Lipschitzian in θ and z on the compact set.

Using these assumptions, the existence of an $\gamma-$family of slow manifolds M_γ for sufficiently small γ is guaranteed by [83, Th.3.1].

Proceeding as done in [64]-[65], it is possible to show that the integral manifold M_γ can be formulated as

$$h_\gamma(t,\theta) = \chi^o(t,\theta) + \gamma\, h_1(t,\theta) + \gamma^2\, h_2(t,\theta) + \ldots \tag{A.15}$$

The expressions for $h_1, h_2, \ldots$ are complicated and there is no need to compute them. However, note that $h_\gamma(t,\theta) \to \chi^o(t,\theta)$ as $\gamma \to 0$, thus M_γ approaches M_o as $\gamma \to 0$. Also, $u(t)$ is a periodic signal, therefore $h_\gamma(t,\theta))$ is a periodic function in t [83-86].

The stability of the θ update law can be shown as an application of the averaging theory of [86,] and [87, Th.4.4.3]. Note that $\gamma = 0$ implies $h_\gamma(t,\theta) = \chi^o(t,\theta)$ and $z = 0$ and the θ update law reduces to

$$\dot{\theta} = \gamma f\left(t, \theta, \chi^o(t,\theta)\right) \tag{A.16}$$

Its averaged system is

$$\begin{aligned}\dot{\theta}_{av} &= -\gamma\ avg\left[f\left(t, \theta_{av}, \chi^o(t, \theta_{av})\right)\right] \\ &= -\gamma\, avg\left[\theta_{av} \sum_{\alpha=a,b,c} x_\alpha^o(t, \theta_{av})\left(u_\alpha(t) - \dot{x}_\alpha^o(t,\theta_{av})\right)\right]\end{aligned} \tag{A.17}$$

where '*av*' stands for the averaged values, and $avg[f(t,x)] = \frac{1}{T_o}\int_o^{T_o} f(\tau,x)d\tau$ ($T_o = 2\pi/\omega_o$).

Using the equations set of (5.5), the averaged system of (A.17) is given by,

$$\dot{\theta}_{av} = -\gamma\, avg\left[\sum_{\alpha=a,b,c} \frac{1}{2\zeta_\alpha} x_\alpha^o(t, \theta_{av})\left(\ddot{x}_\alpha^o(t, \theta_{av}) + \theta^2\, x_\alpha^o(t, \theta_{av})\right)\right]$$

Using (A.7), the averaged system can be expressed as

$$\dot{\theta}_{av} = -\gamma\, avg\left[\left(\theta_{av}^2 - \omega_o^2\right) \sum_{\alpha=a,b,c} \frac{1}{2\zeta_\alpha}\, {x_\alpha^o}^2(t, \theta_{av})\right] \tag{A.18}$$

$$\dot{\theta}_{av} = -\gamma\left(\theta_{av}^2 - \omega_o^2\right) \sum_{\alpha=a,b,c} \frac{1}{4\zeta_\alpha}\, A_\alpha^2\, \left|G_\alpha(j\omega_o, \theta_{av})\right|^2 \tag{A.19}$$

The averaged system (A.19) has an isolated equilibrium point at $\theta_{av} = \omega_o$.

The linearized system around this equilibrium point with the dynamics of

$$\dot{\theta}_{av} = -\frac{\gamma}{2\,\omega_o} \sum_{\alpha=a,b,c} \frac{A_\alpha^2}{\zeta_\alpha} \left(\theta_{av} - \omega_o \right) \tag{A.20}$$

is asymptotically stable. This results in the dynamics represented by (A.19) is locally and asymptotically stable. Hence, based on the averaging theory, (A.14) and equivalently (A.2) are locally asymptotically stable. This means that the θ update law is locally asymptotically stable which concludes local stability analysis.

Remark 2. The attractiveness feature of the integral manifold M_γ can be proved by using [84, Th.5.1] and based on the assumptions 1, 2 and 3 stated before.

Remark 3. It is worthwhile noting that as θ tends to ω_o, we have

$$G_\alpha \left(j\omega_o, \theta \right) = \frac{1}{j\omega_o} \tag{A.21}$$

and $x_\alpha^o \left(t, \theta \right)$ in (A.7) tends to $-A_\alpha \cos\left(\omega_o t + \delta_\alpha \right) / \omega_o$. This implies that the frozen parameter integral manifold M_o contains the desired quasi periodic orbit.